Hydrology of a Moderate–Rich Fen Watershed Prior to, and Following Wildfire in the Western Boreal Plain, Northern Alberta, Canada,

by

Matthew Charles Elmes

A thesis
presented to the University of Waterloo
in fulfillment of the
thesis requirement for the degree of
Doctor of Philosophy
in
Geography

Waterloo, Ontario, Canada, 2018

Examining Committee

The following served on the Examining Committee for this thesis. The decision of the Examining Committee is by majority vote.

Supervisor: Dr. Jonathan Price, Professor, Department of Geography and Environmental Management, University of Waterloo, Canada.

Internal Member: Dr. Richard Petrone, Professor, Department of Geography and Environmental Management, University of Waterloo, Canada.

Internal Member: Dr. Maria Strack, Professor, Department of Geography and Environmental Management, University of Waterloo, Canada.

Internal–External Member: Dr. Kevin Devito, Professor, Biological Sciences, University of Alberta. Adjunct status through Department of Geography and Environmental Management, University of Waterloo, Canada.

External Examiner: Dr. Jim Buttle, Professor, School of the Environment, Trent University.

Author's Declaration

This thesis consists of data and writing all of which I was the primary author: see "Statement of Contributions" included in the thesis.

This is a true copy of the thesis, including any required final revisions, as accepted by my examiners.

I understand that my thesis may be made electronically available to the public.

Statement of contributions

This thesis has been structured in accordance with the manuscript option. Chapter two has been submitted to a peer–review journal. Chapter three has been published in Natural Hazards and Earth System Sciences. Chapters 4 and 5 have been prepared for submission but have not yet been submitted.

Dr. J. Price was the advisor for this thesis, and helped with the research design and provided feedback on the analysis. M. Elmes was the first author on all of the chapters within this thesis, and wrote the initial draft of each chapter. As the thesis advisor, Dr. Price reviewed all of the chapters within this thesis and provided comments and suggestions where needed.

Chapter two is submitted as:

Elmes MC, Price JS. Hydrologic function of a moderate–rich fen watershed in the Athabasca Oil Sands Region of the Western Boreal Plain, northern Alberta. Submitted to: *Journal of Hydrology*.

M. Elmes completed the data analysis, generated the original ideas of the conceptual model, and wrote the first draft of the manuscript, which was then edited and adapted by J. Price.

Chapter three has been published as:

Elmes MC, Thompson DK, Sherwood JH, Price JS. 2018. Hydrometeorological conditions preceding wildfire, and the subsequent burning of a fen watershed in Fort McMurray, Alberta, Canada. *Natural Hazards and Earth System Sciences*, **18**: 157–170, DOI:10.5194/nhess-18-157-2018.

M. Elmes completed the data analysis and writing for this manuscript. D. Thompson provided important suggestions on analyses and interpretation prior to the writing of the first manuscript. J. Price and J. Sherwood provided important comments and suggestions with respect to data analyses and interpretation. All four co–authors (including myself) provided editorial revisions. Comments from a government colleague of D. Thompson (Tom Schiks) were also incorporated into an earlier draft of the manuscript.

Chapter four has been prepared (but not yet submitted) as:

Elmes MC, Price JS. The hydrologic role of fen margins in the low–relief Western Boreal Plain, northern Alberta, Canada, prior to, and following wildfire. To be submitted to: *Journal of Hydrology*.

M. Elmes completed the data analysis and wrote the first draft of the manuscript, which were then edited and adapted by J. Price.

Chapter five has been prepared (but not yet submitted) as:

Elmes MC, Thompson DK, Price JS. Changes to the hydrophysical properties of upland and riparian soils in a burned fen watershed in the Athabasca Oil Sands Region, northern Alberta, Canada. To be submitted to: *Catena*.

M. Elmes completed the data analysis and writing for this manuscript. D. Thompson provided important suggestions on analyses as well as data interpretation prior to the writing of the first draft of the manuscript. J. Price provided important comments and suggestions with respect to data interpretation, and all co–authors (including myself) provided editorial revisions.

By signing below, I indicate that I am in agreement with the evaluation of the roles and contributions of the various authors expressed above.

J. Price

D. Thompson

J. Sherwood

Abstract

Peatlands are a dominant land feature in the Athabasca Oil Sands Region (AOSR) of the Western Boreal Plain (WBP), northern Alberta, Canada, comprising >50% of the total land area, many of which are moderate–rich fens. The carbon stocks of moderate–rich fens in the WBP are susceptible to degradation through anthropogenic– and climate–related factors; yet, few studies have aimed to understand their hydrologic function. In addition, low relief and subtle topographic gradients allow for the expanse of peatland development along the margins between fen and upland. Few studies have explored the hydrologic role of fen margins, despite their typically lower water tables and therefore increased susceptibility to drying. This seven–year (2011–17) study explores the hydrologic function of fen and margin areas in a moderate–rich fen watershed, and how this function changes following wildfire.

The study site (Poplar Fen; 56°56′N; 111°32′W) is located in a meltwater channel belt characterized by relatively thin outwash sand and gravel (mean thickness = 6 m) underlying the peat. The watershed is underlain by a thick (~16 m) and shallow (~7 m below ground surface) aquitard, restricting hydrological connectivity between the fen and underlying regional aquifers. Vertical hydraulic gradients between peat and the underlying outwash aquifer and horizontal hydraulic gradients between fen and upland varied in correspondence with diurnal and seasonal precipitation trends. Groundwater discharge to the fen was enhanced during wet periods characterized by high rainfall. Conversely, flow reversals (groundwater recharge; fen to underlying aquifer and upland), and subsequently, enhanced fen water table drawdown persisted during extended dry periods. Results suggest the dominance of a local flow–system influencing the recharge/discharge patterns at Poplar Fen, with hydraulic head in the underlying outwash aquifer highly susceptible to fluctuations in the presence and absence of precipitation–driven recharge from adjacent uplands.

Contrary to fen areas, which received groundwater discharge from the underlying outwash aquifer during wet periods, and were prone to vertical flow reversals during dry periods, margins acted as permanent vertical recharge zones, providing groundwater to the underlying outwash aquifer. Furthermore, margins acted as large facilitators of lateral groundwater flow between upland and fen, and high pH and base cation concentrations allowed for the unique assemblage of

upland and fen vegetation communities. Therefore, margins act as distinct ecohydrological units, which influence the hydrologic function of Poplar Fen watershed.

In May of 2016, Poplar Fen was impacted by the ~590 000 ha Horse River wildfire, which spread into the city of Fort McMurray and subsequently advanced across the boreal mosaic of mixedwood uplands and peatlands. The destructive nature of the fire motivated the investigation of the hydrometeorological conditions that preceded the fire. Field hydrometeorological data from Poplar Fen between 2015–2016 confirmed the presence of cumulative moisture deficits prior to the fire. The susceptibility of fen and upland areas to water table and soil moisture decline over rain–free periods (including winter) was enhanced by the reliance on supply from the localized flow systems which originate in adjacent topographic highs. Subtle changes in topographic position were also found to influence groundwater connectivity, leading to greater organic soil consumption by fire in wetland margins and at high elevations. It was ultimately the accumulated moisture deficits, dating back to the summer of 2015, which led to the dry conditions that preceded the fire.

To address the potential changes in the hydrologic function of the uplands at Poplar Fen, differences in water repellency and hydrophysical properties were measured for burned and unburned upland duff and mineral soils. Samples were taken in the fall of 2017, the year after the watershed had burned (May 2016). Study locations included burned and unburned jack pine–dominated brunisol, and black spruce–dominated riparian uplands. Results illustrated significantly lower water repellency and higher infiltration on burned uplands at both upland types. This was due primarily to the destruction of naturally occurring hydrophobic substances by the fire. Furthermore, no significant differences were detected in duff moisture retention in brunisol uplands; however, burned duff samples had significantly lower water retention in riparian uplands. It is postulated that the lower water retention in riparian uplands was due to the greater organic layer thickness there, thus greater fuel load and potential for exceeding the temperature threshold of repellency destruction. Following retention, all soil cores exhibited high hysteresis, with differences in volumetric moisture content averaging 0.38 and 0.34 $m^3\ m^{-3}$ at –10 cm pressure for brunisol and riparian uplands, respectively. A net gain in upland water table recharge is anticipated at Poplar Fen following wildfire, which will help in sustaining recharge to the local flow systems

which discharge to lower–lying fen areas and prevent water table drawdown, thus accelerating the fen moss recovery process.

In conclusion, Poplar Fen, and watersheds with a similar hydrogeologic setting, will become increasingly susceptible to drying in the future due to anticipated changing climate scenarios. This will likely lead to enhanced water table drawdown, peat oxidation and subsequent decomposition, as well as seral succession to a more ombrogenous peatland system, rendering them more vulnerable to wildfire. However, base–rich fens are typically understudied in the WBP. It is recommended that similar hydrological methods are applied to other base–rich systems (including extreme–rich fens) throughout the WBP, which will improve our understanding of how these systems will respond to disturbance. Poplar Fen may also serve as an appropriate analogue for oil sands reclamation. Results from this thesis suggest that the hydrologic function of natural fen systems (i.e. moderate–rich fens) in the AOSR can be replicated. However, considering the susceptibility of this system to drying over regional climate cycles, fen reclamation should focus on specific engineering of the landscape to provide the necessary hydrological conditions for minimizing fen recharge conditions, water loss, and susceptibility to carbon degradation from enhanced decomposition and/or wildfire.

Acknowledgements

A four–year doctoral degree is filled with several ups and downs. And because of this I have a great deal of people to thank for helping me throughout and making this experience as enjoyable as possible. First, I would like to express my gratitude to my advisor, Dr. Jonathan Price, for taking a chance with a recent M.Sc. graduate with a limited background in peatlands. The amount of knowledge I have gained, and the level passion I have developed for peatland hydrology, would not have been the same without your supervision. You have challenged me a great deal over these past few years, and instilled a level of standard that I will apply to my future research endeavors. I would like to express my appreciation to my committee members, Dr. Rich Petrone, Dr. David Cooper, and Dr. Kevin Devito, for their guidance in the early stages of my research, and to external examiner Dr. Jim Buttle for his insights during my defense. An extra thank you to Dr. Rich Petrone is in order, as a professor, and as a colleague, for helping enhance my knowledge and interest in hydrometeorology. I also extend a big thank you to Dr. Daniel Thompson, for providing his expertise in fire science when my study site burned.

To all of my friends and colleagues in the Wetlands Hydrology lab, as well as the Hydrometeorology Research Group, thank you for your support and input over these past four years. I have learned a lot from you. Special thanks to Eric Kessel, James Sherwood, Behrad Gharedaghloo, Corey Wells, Tasha–Leigh Van Huizen, Scott Ketcheson, and Colin McCarter. To my colleague, groomsman, and best pal George Sutherland, thank you for all our hydromet talks, your field assistance, and the endless laughter and good times we have had over the past seven years.

Last, but certainly not least, I thank all of my family, whether related by blood, or through marriage. You have all been an important source of love and support. To the love of my life, my best friend, and the inspiration for my determination, thank you Saliy, for always believing in me. You have always inspired me to strive to be my best, and this thesis is a testament to our love and devotion. I am indebted to you always. And to my baby boy Yusef, thank you for being your perfect self, and for giving me yet another reason to be my best.

Dedication

To my four best friends: my loving wife Saliy, my son Yusef, and my cats, Jack and Raine.

Table of Contents

Examining Committee ii

Author's Declaration iii

Statement of contributions iv

Abstract vi

Acknowledgements ix

Dedication x

Table of Contents xi

List of Figures xiv

List of Tables xvii

1 Introduction 1

1.1 Objectives 2

1.2 Organization of thesis 3

2 Hydrologic function of a moderate–rich fen watershed in the Athabasca Oil Sands Region of the Western Boreal Plain, northern Alberta 4

2.1 Introduction 4

2.2 Site Description and regional hydrogeologic setting 6

2.3. Methodology 9

2.4. Results 12

2.4.1 Lithology 12

2.4.2 Hydraulic Conductivity 13

2.4.3 Hydrology 15

2.4.4 Water chemistry 19

2.5 Discussion 21

2.5.1 Hydrogeologic Setting of Poplar Fen Watershed 21

2.6 Conclusions 28

2.7 Acknowledgements 28

3 Hydrometeorological conditions preceding wildfire, and the subsequent burning of a fen watershed in Fort McMurray, Alberta, Canada 29

3.1 Introduction 29

3.2 Study Site 31

3.3 Methodology 33

3.3.1 Historical data collection 33

3.3.2 Field data collection 33

3.3.3 Drought Code 35

3.3.4 Burn depth and fuel consumption 37

3.4 Results 37

3.4.1 Hydrometeorology 37

3.4.2 Hydrology ... 40
3.4.3 Drought Code ... 43
3.4.4 Burn depth and fuel consumption ... 44
3.5 Discussion ... **45**
3.5.1 Pre–fire meteorology ... 45
3.5.2 Pre–fire hydrology ... 46
3.5.3 Assessing the hydrometeorological conditions preceding the Horse River wildfire and burning of Poplar Fen ... 48
3.5.4 Differences in burn severity within Poplar Fen ... 48
3.5.5 Soil moisture: an early indicator of spring wildfire danger ... 49
3.4 Conclusions ... **50**
3.5 Acknowledgements ... **51**

4 The hydrologic role of fen margins in the low–relief Western Boreal Plain, northern Alberta, Canada, prior to, and following, wildfire ... **52**
4.1 Introduction ... **52**
4.2 Study Site ... **55**
4.3 Methodology ... **56**
4.3.1 Ecology ... 56
4.3.2 Hydrology and physical characteristics ... 56
4.3.3 Geochemistry ... 59
4.4 Results ... **59**
4.4.1 Vegetation Composition ... 59
4.4.2 Topography and peat physical properties ... 61
4.4.3 Hydrological comparison of fen and margin areas, pre–fire ... 63
4.4.4 Hydrological comparison of fen and margin areas, post–fire ... 67
4.4.5 Geochemistry ... 69
4.5 Discussion ... **70**
4.5.1 Margins as distinct ecological and hydrological units ... 70
4.6 Conclusions ... **74**
4.7 Acknowledgements ... **75**

5 Changes to the hydrophysical properties of upland and riparian soils in a burned fen watershed in the Athabasca Oil Sands Region, northern Alberta, Canada ... **76**
5.1 Introduction ... **76**
5.2 Methodology ... **78**
5.2.1 Study site and research design ... 78
5.2.2 Water droplet penetration time and molarity of ethanol droplet tests ... 81
5.2.3 Grain size analysis ... 82
5.2.4 Infiltration tests ... 82
5.2.5 Moisture retention ... 82
5.2.6 Field Hydrological Data ... 83
5.2.7 Numerical Analyses ... 84
5.3 Results ... **84**
5.3.1 Grain Size ... 84
5.3.2 Water Repellency ... 86
5.3.3 Organic layer bulk density ... 87
5.3.4 Infiltration ... 88
5.3.5 Moisture Retention ... 88

5.4 Discussion **90**
5.4.1 Changes to water–repellency following wildfire 90
5.4.2 Changes to infiltration rates following wildfire 92
5.4.3 Changes to moisture retention and wettability following wildfire 93
5.4.4 Implications for the hydrologic functioning of Poplar Fen 93
5.5 Conclusions **95**
5.6 Acknowledgments **96**

6 Summary and conclusions **97**
6.1 Recommendations for fen reclamation **99**

7 References **100**

A.1 Appendix 1: Average community composition, reported as absolute cover (%), for vegetation plots measured along WT2 (left) and ET4 (right) (refer to Fig. 1 and 2). **113**

A.2 Appendix 2: Interception loss for burned and unburned brunisol upland locations measured in the summer of 2016. ..... **114**

List of Figures

Figure 2–1. (**a**) Map showing the regional setting of the study area, and (**b**) map of Poplar Fen study site, including transect locations and instrumentation. The channel fen extends south of the watershed boundary, but has a hydraulic gradient towards the south.

Figure 2–2. Field lithology drill logs of transects A–A' and B–B' at Poplar Fen watershed (see Figure 2–1 for locations).

Figure 2–3. Laboratory (0–0.6 m) and field estimates (0.6–1.5 m) of saturated horizontal hydraulic conductivities for channel fen and West wetland peat and underlying mineral sediments.

Figure 2–4. Average hydrological results for NT1–NT3 (see Fig. 2–1) from 2011–2015, including (**a**) channel fen water table with daily regional precipitation illustrated, (**b**) change in hydraulic head since last measurement in outwash piezometers underlying channel fen areas, (**c**) average vertical hydraulic gradients between channel fen peat and underlying mineral substrate (open and black circles) and corresponding average vertical groundwater fluxes (grey circles), and (**d**) average horizontal hydraulic gradients between upland and channel fen (open and black circles) and corresponding average horizontal groundwater fluxes (grey circles). Note that due to the log scale, negative discharge values are not shown on (**d**). Also included are vertical (**c**) and horizontal (**d**) hydraulic gradients for newly installed 2015 nests (black circles). Positive gradients and fluxes represent flow towards the fen. Note that calculated discharge in (**c**) and (**d**) in 2015 correspond only to gradients measured at NT1–NT3 and not the newly installed nests.

Figure 2–5. a) Comparison of water table position, b) vertical hydraulic gradients between wetland water table and underlying mineral, and c) horizontal gradients between wetland water table and upland to the west (hashed lines) and east (solid lines) of the West and East wetland areas (see Fig. 2–1).

Figure 2–6. Average pH, electrical conductivity (EC), and concentrations of major cations (Na^+, Ca^{2+}, and Mg^{2+}) and Cl^- for samples obtained from channel fen, upland, and West and East wetland wells, as well as underlying mineral piezometers from channel fen and West wetland nests obtained throughout 2015.

Figure 2–7. Isotopic signatures $\delta^{18}O$ and δD for precipitation obtained ~5 km from Poplar Fen (used to produce LMWL), and for water samples obtained at channel fen, West and East wetlands, and upland water table wells and underlying outwash piezometers (see legend for colour scheme), at Poplar Fen in August, 2014 (circles), June, 2015 (squares), and July, 2015 (triangles). Additional water lines were plotted, including the GMWL, as well as water lines of regional Alberta Basin formation water samples reported in Connolly et al., 1990 (CFWL) and Hitchon and Friedman, 1969 (HFFWL), adapted from Lemay, 2002.

Figure 2–8. Conceptual model of fen landscape connectivity at Poplar Fen for moderate–rich channel fen, poor–fen, and spruce swamp systems, comprising lithological information from cross–section A–A' (Fig. 2–2) during typical wet and dry conditions observed between 2011–15. Due to insufficient hydrological information below 2.0 m, equipotential and flow lines are idealized.

Figure 3–1. Map of the Poplar Fen watershed (**a**; 56°56′ N, 111°32′ W). The entire area was burned with the exception of areas highlighted in light grey. Included is an inset of northeastern boreal Alberta (**b**) showing the burned area during years of high spring fire frequency, including 1998 (purple), 2002 (green), 2011 (cyan), and 2016 (red).

Figure 3–2. Moisture probe profiles in upland duff and fen margin peat.

Figure 3–3. Measured accumulation and ablation of SWE at Gordon Lake snow pillow (**a**), and interpolated cumulative early spring rainfall from 1996 and 2016 at Poplar Fen (**b**). Coloured lines in graph (**b**) correspond to years of high burned area in the spring, including 1997–1998 (726 968 ha), 2001–2002 (496 515 ha), 2010–2011 (806 055 ha), and 2015–2016 (663 529 ha) (Natural Resources Canada, 2017).

Figure 3–4. Daily records of (**a**) maximum air temperature (with 20–year average), (**b**) average daily relative humidity, and (**c**) average daily wind speed at Mildred Lake climate station from 5 October 2015 to 17 May 2016, and (**d**) measured area–weighted SWE for Poplar Fen in 2016.

Figure 3–5. Logged (lines) and manually ("x" symbols) recorded water table position at NW fen (black) and NW margin (grey) (see Fig. 3–1), from 2011 to 2016, with field–measured rainfall (P), and total winter precipitation (WP) interpolated for the Poplar Fen area.

Figure 3–6. Average (SE) water table (black circles) and vertical hydraulic gradient (grey circle) between the water table and underlying mineral substrate for lower and upper fen, and margin areas, along with logged (line) and manually recorded ("x" symbol) water table (blue) and hydraulic head (red) for lower and upper fen areas in 2015. A negative hydraulic represents a loss of water from the fen to the underlying mineral substrates. Rainfall is also illustrated.

Figure 3–7. Volumetric water content ($m^3\ m^{-3}$) for upland duff and margin peat from 2 June 2015 to 2 May 2016, including with average 2016 snowmelt recharge (mm) for upland and margin, and Drought Code from May to October 2015.

Figure 4–1. Map of Poplar watershed with location of fen upland transects.

Figure 4–2. Cross–sections of transects WT2 and ET4 with locations of vegetation survey plots (red dots).

Figure 4–3. Physical properties of peat cores obtained WT2 and ET4 (see Fig. 4–1 and 4–2), including (**a**) bulk density, (**b**) specific yield, (**c**) horizontal K_{sat}, and (**d**) vertical K_{sat}.

Figure 4–4. Lab (open symbols) and field (closed symbols) measured saturated horizontal hydraulic conductivity in fen (circles) and margin (triangles) of Poplar Fen, along with changes in the weighted arithmetic mean K_{sat} of fen (black line) and margin (grey line) peat with change in water table position.

Figure 4–5. Average hydrological results for NT1–NT3 (see Fig. 4–1) from 2011–2015, and for salvaged nests along NT1 and WT and ET transects from 2016–2017, including (**a**) extrapolated

(lines) and/or manually (circles) recorded fen (black) and margin (grey) water table position and daily regional precipitation, (**b**) average horizontal hydraulic gradient between upland and margin (grey) and margin and fen (black), and (**c**) average vertical hydraulic gradients between peat and underlying mineral substrate in fen (black) and margin (grey) areas. Note that positive gradients signify a gain in groundwater from underlying mineral substrate or upland to peat.

Figure 4–6. Average area–weighted groundwater fluxes over the instrumental record, for NT1–NT3 from 2011–2015, and all salvaged nests from 2016–2017, including lateral fluxes between upland and margin (solid grey), margin and fen (solid black), and vertical fluxes between margin (dashed grey) and fen (dashed black) peat and underlying mineral substrate. Note that a positive horizontal flux represents a gain to the lower surface elevation, and a negative vertical flux represents a loss from margin peat to underlying mineral substrate.

Figure 4–7. Comparisons of vertical hydraulic gradients and groundwater fluxes between nests located at upper, lower, and toe slopes, over the 2015 field season (See fig. 4–1).

Figure 4–8. Photos of taken at several transect locations two months following the wildfire (refer to Fig. 4–1).

Figure 4–9. Average pH, electrical conductivity (EC), and concentrations of major cations (Na^+, Ca^{2+}, and Mg^{2+}) and anions (Cl^- and SO_4^{2-}) for samples from fen and margin wells and underlying mineral piezometers, as well as upland wells, obtained throughout 2015 at Poplar Fen.

Figure 5–1. Map of the Poplar Fen watershed (**a**); 56°56′ N, 111°32′ W), with unburned areas highlighted in light grey. Included is an inset of the AOSR (**b**) showing total burned area from 1998–2017 (dark grey).

Figure. 5–2 Relative proportions of sand, silt, and clay for burned and unburned brunisol and riparian upland soil samples obtained at Poplar Fen. Samples are overlying a soil texture triangle with the 12 basic texture classes outlined by the USDA (Soil Science Division Staff, 2017).

Figure. 5–3. Relative frequency of (a) WDPT and (b) MED results for surface (n = 24 at each location) and below ground surface (n = 40 for each depth interval at each location). Asterisks denote depth intervals where significant differences were detected between burned and unburned samples.

Figure 5–4. Notched boxplots of infiltration rate in burned and unburned brunisol and riparian upland locations.

Figure 5–5. Measured soil–water retention, $\theta(\psi)$, for burned and unburned, brunisol and riparian, duff and mineral cores, along with average hysteresis (dash lines). All retention curves are plotted individually (see faint lines) and average retention and hysteresis curves are also plotted (bold lines).

Figure 5–6. Measured ground heat flux (Q_G) and near surface (0–3 cm b.g.s.) volumetric moisture content in burned and unburned brunisol upland locations at Poplar Fen during the summer of 2016 following the fire (May. 17).

List of Tables

Table 2–1. Summary of estimated vertical and horizontal groundwater fluxes averaged (weighted) annually for 2011–2015 field seasons, along with average daily precipitation over the same time period. Note: a negative gradient and flux represents a loss of water from the fen.

Table 3–1. Summary of scenarios used for calculating a starting DC for 19 April 2016.

Table 3–2. Total hydrological year rainfall and snowfall from 1996 to 2016, interpolated for the Poplar Fen area.

Table 3–3. The 19 April 2016 startup and final 17 May DCs for Poplar Fen using four different scenarios.

Table 3–4. Average (±SE) surface change and fuel consumption in upland, margin, and fen at Poplar Fen.

Table 4–1. Summary of average daily hydrological results from 2011–2017, including rainfall, fen and margin water table position, horizontal and vertical hydraulic gradients, and corresponding average area–weighted groundwater fluxes (mm d^{-1}) for each hydraulic gradient.

1 Introduction

Within the Western Boreal Plain (WBP), Alberta, Canada, wetlands comprise roughly 50% of the landscape, with a relatively large proportion classified as peatlands (Vitt et al., 1996). Peatland function in the WBP is controlled by a set of hydrological and geochemical factors that establish a gradient in peatland type based on peat porewater chemistry and plant indicator species (Vitt et al., 1995). Peatlands in the WBP therefore follow a gradient from bogs, to poor, moderate–rich, and extreme–rich fens (Chee and Vitt, 1989; Vitt et al., 1995).

Patterns in the distribution of the various peatland types in the WBP are due to a range of landscape– and climate–related variables that are unique to the region. For example, peatlands in the WBP typically overlie deep and heterogeneous post–glacial deposits that have varying thicknesses and hydrophysical properties (Devito et al., 2005; Ireson et al., 2015). Surficial deposits range from fine– to coarse–textured, and are often layered (veneer–type), producing landscapes with varying transmissive properties and hydrologic interconnection with local, intermediate, and regional flow systems (Devito et al., 2012). As a result of this heterogeneity, the WBP typically has complex groundwater–surface water interactions (Devito et al., 2005). Furthermore, water availability in the WBP is constrained by precipitation (P) rates that are generally less than potential evapotranspiration (PET) demands (Marshall et al., 1999; Bothe and Abraham, 1993), where watersheds rely on water storage, as well as infrequent wet years over 10 to 15–year cycles (Petrone et al., 2007). The assemblage of a sub–humid climate and variable landscape configuration results in a large variation in the degree of peatland–landscape connectivity (Devito et al., 2005), resulting in various peatland types (Vitt et al., 1994), which are capable of retaining water during periods of low moisture availability (Petrone et al., 2007; Waddington et al., 2014).

As a result of the variability outlined above, numerous studies have aimed to conceptualize the hydrologic function of peatlands throughout the WBP. Considerable effort has been spent on bog and poor–fen systems in the Utikuma Region Study Area (URSA) (Ferone and Devito, 2004), and the Athabasca Oil Sands Region (AOSR) (Scarlett and Price, 2013; Wells et al., 2017) of the WBP. Conversely, the hydrologic function of base–rich fens has been explored throughout the WBP and greater Boreal Plains, including minerotrophic pond–peatland complexes in the URSA

(Smerdon et al., 2005), a moderate–rich fen in central Saskatchewan, and a saline fen in the AOSR (Wells et al. 2015a, 2015b). Moderate–rich fens have been shown to be a dominant peatland type in the AOSR (Chee and Vitt, 1989); however, to date, their hydrology remains unexplored in this region.

Understanding the hydrologic function of moderate–rich fens in the AOSR will help in conceptualizing peatland landscape connectivity in the WBP, specifically, to better predict how individual peatlands may respond to multiple environmental– and industry–related disturbances in the region. Moderate–rich fens in the AOSR are susceptible to accelerated drying and decomposition (Waddington et al., 2014), as well as wildfire (Turetsky et al., 2004), under anticipated climate change scenarios (Roulet et al., 1992). Carbon stocks within these peatlands are also particularly vulnerable to oil sands mining activities, as open–pit mining involves the large–scale removal of the surficial landscape, including the mosaic of boreal mixedwood uplands and peatlands (Daly et al., 2012; Rooney et al., 2012). Subsequently, peatland reclamation is a key feature of closure plans, as regulatory requirements require leased lands to be returned to a state of 'equivalent capability' (OSWWG, 2000). Thus, understanding the hydrologic function of moderate–rich fens is necessary for meeting these regulatory requirements.

1.1 Objectives

To help address the knowledge gaps outlined above, and further our understanding of the variability in peatland function in the WBP, a moderate–rich fen watershed (Poplar Fen) was instrumented in the AOSR, ~25 km north of the town of Fort McMurray. The primary intention was to conduct an extensive study of the hydrogeologic connectivity and hydrologic regime of the watershed. Due to the burning of the watershed in the spring of 2016, the objectives were expanded to include two additional studies that were focused primarily on wildfire. Thus, the primary objectives of this research are to:

1) Identify the hydrogeologic connectivity of Poplar Fen to the local watershed and link this connection to the hydrologic function of the watershed to better predict how moderate–rich fens in the region will respond to disturbance;

2) Characterize the ecological, physical, hydrological, and geochemical properties of margins at Poplar Fen and identify whether they act as distinct ecohydrological units, and determine how margins influence the hydrologic functioning of Poplar Fen watershed;
3) Use hydrological data to explain the observed patterns in burn severity across the watershed, and identify whether hydrological data and hydrogeological setting parameters of the watershed can serve as indicators of deep smouldering and combustion risk;
4) Characterize the hydrophysical changes to upland soils at Poplar Fen following wildfire and explore the potential implications of these changes for post–fire peatland recovery; and
5) Transfer the knowledge gained from this thesis into practical recommendations for peatland reclamation.

1.2 Organization of thesis

This thesis has been divided into six chapters. The first chapter is intended to introduce the reader to the main themes and concepts, while outlining the specific research objectives. The following four chapters are all based primarily on empirical data obtained from Poplar Fen and have been constructed to address the specific objectives outlined above.

Chapter two addresses the first primary objective of this thesis. Chapter three addresses the third primary objective, while also characterizing the hydrometeorological conditions preceding the burning of Poplar Fen watershed to determine whether these conditions were outside the range of natural WBP climate cycles. Chapter four addresses the second primary objective, while also exploring the fate of margins at Poplar Fen following wildfire. Chapter five addresses the fourth primary objective.

The four primary chapters are then followed by a conclusions chapter, which will aim to summarize all of the significant findings and contributions, and make recommendations for peatland reclamation (fifth primary objective).

2 Hydrologic function of a moderate–rich fen watershed in the Athabasca Oil Sands Region of the Western Boreal Plain, northern Alberta

2.1 Introduction

Within the Western Boreal Plain (WBP), northern Alberta, Canada, peatlands are a ubiquitous feature on the landscape, representing a large proportion of the total land area (Vitt et al., 1996). These peatlands comprise a relatively large pool of terrestrial carbon (Gorham, 1991), with stocks susceptible to enhanced drying and decomposition under anticipated climate change scenarios (Roulet et al., 1992; Waddington et al., 2014), as well as other disturbances, including oil sands mining (Rooney et al., 2012) and wildfire (Turetsky et al., 2004). This susceptibility is compounded by the sub–humid climate of the WBP, where annual precipitation is typically less than potential evapotranspiration (PET), with storage deficits replenished by infrequent wet periods occurring over 10 to 15–year cycles (Marshall et al., 1999). The combination of these stressors can induce changes to the water balance from subsequent alterations to the hydrophysical properties of peat (Waddington et al., 2014) as well as the hydrological connectivity of the peatland to the surrounding surficial geology (Devito et al., 2012).

Peatlands in the WBP range from ombrotrophic bogs to minerotrophic swamps and poor, moderate–rich, extreme–rich (Chee and Vitt, 1989), and saline fens (Wells et al., 2015a), with peatland type ultimately controlled by the local and regional hydrogeologic setting (Winter et al., 2001; Devito et al., 2005; Wells et al., 2015b). Bogs and poor–fens generally form over groundwater recharge areas, where fine–grained substrates minimize landscape connectivity and restrict recharge of peat subsurface water to underlying mineral aquifers (Ferone and Devito, 2004; Wells et al., 2017; Riddell, 2008). Conversely, base–rich fens receive solute–laden runoff and/or groundwater, and generally form over groundwater discharge areas (Siegel and Glaser, 1987; Winter et al., 2003), where coarse–grained substrates can enhance groundwater connectivity (Reeve et al., 2000) and help sustain near–surface water tables. Groundwater discharge has been linked to several important ecological and biogeochemical functions within peatlands. For example, groundwater can influence peatland surface water chemistry (Siegel, 1983) and drive the geochemical and ecological gradients associated with specific peatland types (Sjörs, 1950; Siegel, 1983; Siegel and Glaser, 1987; Chee and Vitt, 1989). Gorham (1953) suggested that modest amounts of base–rich groundwater were sufficient enough to maintain fen surface water pH above

4.5. By buffering the organic (humic and fulvic) acids that are produced in–situ through peat decomposition, base–rich groundwater can therefore inhibit the dominance of *Sphagnum* mosses that succeed in peatlands with low–pH surface waters (Dasgupta et al., 2015).

Peat accumulation (carbon uptake) is highly influenced by hydrology, with lower water tables resulting in enhanced oxygen availability and subsequent peat decomposition (Ise et al., 2008; Waddington et al., 2014). Consequently, carbon accumulation and storage in peatlands is in part controlled by water table position (Clymo, 1984; Adkinson et al., 2011). Fens are adaptive to water stress as groundwater discharge can partially offset water losses during years of low annual precipitation (Siegel and Glaser, 1987). The strength and scale of groundwater connection influences the hydraulic head distribution, and thus the patterns in discharge and flow direction (Tóth, 1999; Winter et al., 2001, 2003). Peatlands connected to intermediate/regional flow systems will receive discharge from groundwater associated with longer travel times and therefore are less susceptible to seasonal and annual hydrometeorological variability (Smerdon et al., 2005), whereas peatlands connected to shallower local flow systems receive groundwater that is more susceptible to short–term (e.g., seasonal and annual) trends in precipitation–driven recharge in adjacent topographic highs (Tóth, 1999). Thus, peatlands influenced primarily by local, rather than regional flow systems are likely to be more susceptible to vertical flow reversals in the absence of precipitation (Devito et al., 1997; Fraser et al., 2001), potentially becoming groundwater recharge areas during periods of low water availability.

Within the WBP, the hydrologic function of pond–peatland complexes have been explored in the Utikuma Region Study Area (URSA), located ~300 km north of Edmonton, AB. There, peatlands overlying clay plains and till moraines act as diffuse recharge features, with little or no supplemented discharge from adjacent uplands and underlying mineral substrates (Ferone and Devito, 2004). The hydrogeology of bogs (Scarlett and Price, 2013) and poor fens (Wells et al., 2017) in the Athabasca Oil Sands Region (AOSR) have also been shown to behave similarly to those studied in the URSA. Conversely, pond–peatland complexes in the URSA situated within coarser–grained substrates have been shown to exhibit a greater connection to regional groundwater, receiving supplemented discharge during drier periods (Smerdon et al., 2005). Similar results were illustrated at a moderate–rich fen overlying a glaciofluvial outwash plain in Central Saskatchewan, highlighting a dynamic lateral groundwater connection with adjacent

upland areas, which was enhanced during wetter conditions (Barr et al., 2012). Saline fens in the AOSR receive diffuse discharge from a saline groundwater plume sourced by the Grand Rapids formation, a regional saline aquifer (Wells et al., 2015a; 2015b).

Despite considerable efforts in characterizing their vegetation and water chemistry (Chee and Vitt, 1989; Vitt and Chee, 1990; Thormann and Bayley, 1997; Locky and Bayley, 2010), the hydrology of moderate–rich fen systems in northern Alberta remains largely unexplored (Elmes et al., 2018). A better understanding of the hydrologic function of these systems will be necessary for predicting the fate of their carbon stocks in response to multiple disturbances. The purpose of study was to examine the hydrologic setting of a moderate–rich fen watershed in the AOSR to better understand the natural variability in wetland function in the WBP. Specific objectives include: (1) identify the hydrogeologic connectivity of a moderate–rich fen to the local watershed; and (2) link this connection to the hydrologic function of the watershed to better predict how moderate–rich fen systems in the region will respond to disturbance. Here field data are presented from a moderate–rich fen watershed over a five–year period, between 2011 and 2015.

2.2 Site Description and regional hydrogeologic setting

The AOSR is located on the northeastern edge of the Alberta Basin, a sub–basin of the Western Canadian Sedimentary Basin (Grasby and Chen, 2005). The regional groundwater regime follows a south to north direction, primarily through Cambrian sandstones and Devonian through Mississippian carbonates. Cretaceous shales and silts associated with the Clearwater formation act as regional aquitards; however, interbedded sandstones often act as local and regional aquifers (Bachu, 1995). Drift thickness is variable in the region, ranging from <1 m to >200 m. The thickest drift deposits are located in topographic highs, including Muskeg Mountain (~600 m ASL) and the Birch Mountains (~800 m ASL), thinning to <20 m towards the Dover and Kearl Lake plain regions adjacent to the Athabasca River (at ~240 m ASL) (Andriashek and Atkinson, 2007). The topographic highs are underlain by cretaceous shales and sandstones, and act as regional recharge areas, creating confined regional aquifers that eventually discharge into the Athabasca River (Andriashek, 2003).

This study was conducted at ‘Poplar Fen’ (56°56′N; 111°32′W; ~320 m ASL), a 2.5 km^2 treed moderate–rich channel fen watershed (total relief: ~11 m) located 25 km north of Fort

McMurray, within the Dover Plain region of the AOSR, northern Alberta (Fig. 1). The watershed is located within the Central Mixedwood Subregion of the Boreal Plains Ecozone (Natural Regions Committee, 2006). The climate in the region is defined as sub–humid (Bothe and Abraham, 1993; Marshall et al., 1999), with annual potential evapotranspiration (PET) typically exceeding annual precipitation (P) (Devito et al., 2012). The average annual air temperature (1981–2010) is 1°C and average annual precipitation is 419 mm, with ~75% falling as rain (Environment Canada, 2017). Drift is reported to be relatively thin (<20 m) in the Poplar Fen area and is dominated by fine to coarse sand with heterogeneous deposits of boulders, gravel, silt, and clay (Andriashek and Atkinson, 2007). The site is situated within a long ~10 km belt of meltwater channels extending northward to the southern portion of the Syncrude basemine (Fig. 2–1). Prior to glaciation, relict channels in this area were incised into the Cretaceous strata (McPherson and Kathol, 1977) during a period of erosion extending from the late Cretaceous into the late Pleistocene (Andriashek, 2003). It was hypothesized that these lows were later infilled with lacustrine sediment prior to, and till and outwash during, glaciation. Following the deposition of the outwash, meltwater eroded into the channels forming them into the existing post–glacial features. Since de–glaciation, the original depositional surface has been modified by the accumulation of peat soil in topographic 'lows' and aeolian sand deposits in 'highs' (McPherson and Kathol, 1977).

Poplar Fen is composed primarily of brown moss–dominated (Goetz et al., 2014) moderate–rich channel fens (~0.7 km^2), with two additional *Sphagnum* and feather moss–dominated elongated depressional wetlands, located within upland areas and sitting at a higher elevation than the larger channel fen areas (Fig. 1). This includes a relatively small, (~0.005 km^2) wetland ("West wetland"; 56°56′4″N; 111°32′30″W) along the western portion of the watershed, and a larger (~0.03 km^2) wetland ("East wetland"; 56°56′4″N; 111°31′36″W) along the eastern portion of the watershed. The Poplar Fen watershed was delineated using an airborne LiDAR (Light Detection And Ranging) digital elevation model (Airborne Imaging Inc. licensed to the Government of Alberta). The area has been altered by linear disturbances associated with resource exploration and extraction, including the construction of several cut lines with areas cleared for drill logs, and a pipeline and corridor extending west to east along the north end of the watershed (Fig. 2–1).

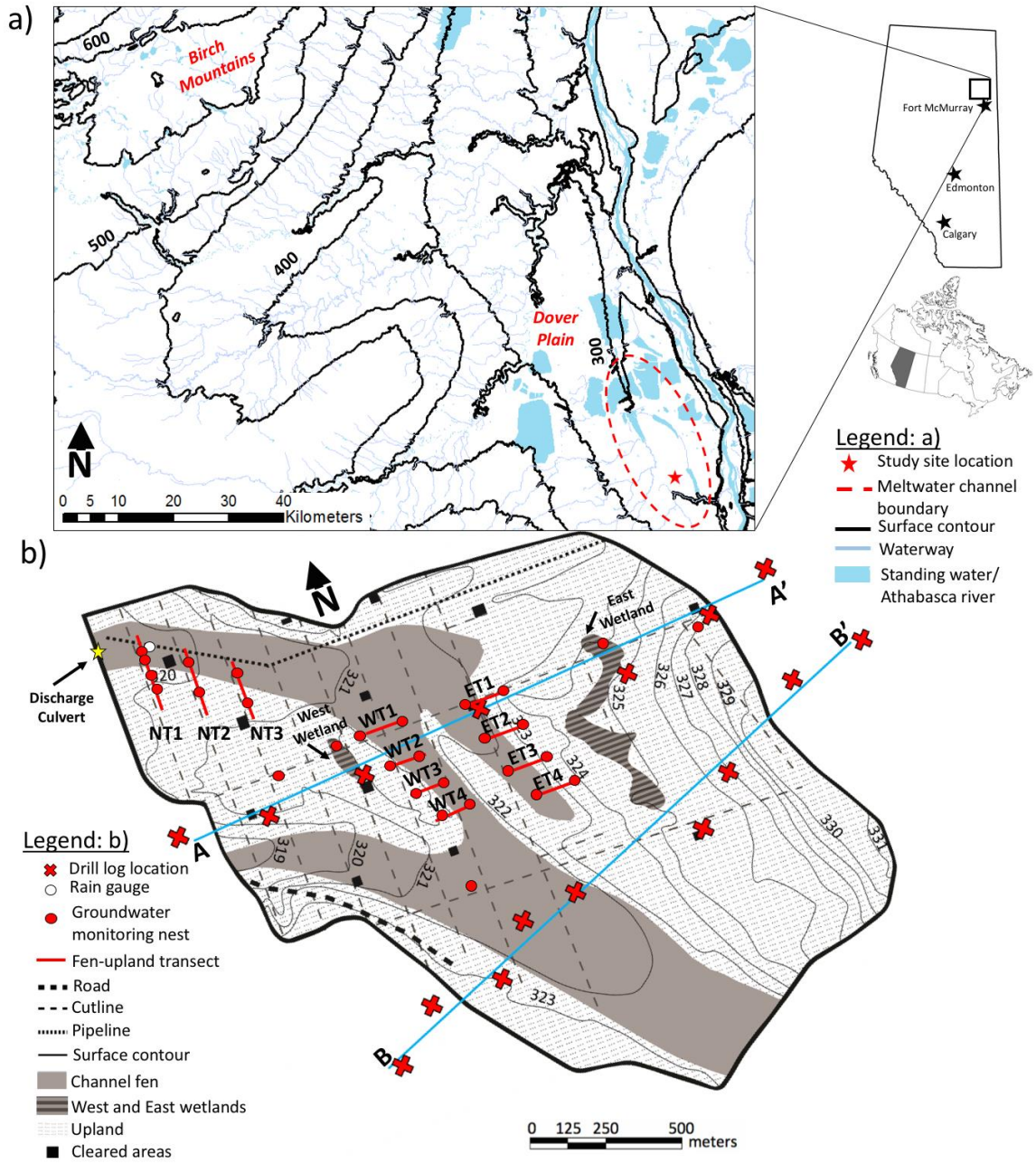

Figure 2–1. (**a**) Map showing the regional setting of the study area, and (**b**) map of Poplar Fen study site, including transect locations and instrumentation. The channel fen extends south of the watershed boundary, but has a hydraulic gradient towards the south.

Tamarack (*Larix laricina*) and black spruce (*Picea mariana*) are the dominant tree species within Poplar Fen, with saplings (<1 m height) dominant in the West wetland, saplings and mid–sized trees (<3 m height) dominant in channel fen areas, and taller trees (>3 m height) dominant in the East wetland. Surface cover in moderate–rich channel fen areas is characterized primarily by mosses *Tomenthypnum nitens*, *Aulacomnium palustre*, *Pleurozium schreberi*, and from the

genus *Sphagnum* (*S. fuscum* and *S. capillifolium*). Surface cover in the East and West wetland areas is dominated primarily by *S. fuscum*, and feathermosses *Hylocomium splendens,* and *P. schreberi*. Upland areas are dominated by *P. mariana* and feather mosses in riparian zones, with jack pine (*Pinus banksiana*) and aspen (*Populus tremuloides*) mixedwood overstorey and lichen ground cover in topographically higher areas.

2.3. Methodology

Field lithology drill logs were obtained from Suncor Energy Inc. (personal communication), and used to construct geologic cross–sections of Poplar Fen. Logs included interpretations of specific geological sequences extending down to the Precambrian Shield, which were ultimately used to construct cross–sections. Two primary west–east transects (A–A' and B–B' in Fig. 2–1) were drawn for the watershed, extending through several land types. To aid with the interpolation of shallow substrate attributes between drill logs (e.g., surface elevation, peat thickness, and mineral grain size directly underlying the basal peat), information obtained during groundwater monitoring nest installation was also used in producing the cross–sections.

Hydrological investigations at Poplar Fen began in June of 2011, and instrumentation initially comprised three transects at the northwestern portion of the channel fen (NT1–NT3; Fig. 2–1), extending southward with nests installed along the fen–upland ecotone. In 2014 and early 2015, additional nests were installed elsewhere throughout the watershed to capture a greater representative area. Nests were installed at several fen and adjacent upland locations, comprising four transects along a narrow and gentle–sloping upland on the west side of the watershed (WT1–WT4; Fig. 2–1) to the adjacent fen, and four transects along a more expansive and steeper upland on the east side of the watershed (ET1–ET4; Fig. 2–1) to the adjacent fen. A nest was also installed in both the West and East wetlands (Fig. 2–1). Nests were also installed into margins at all transects, although water levels and hydraulic gradients are not reported in this study. Screened wells and piezometers (20 cm screened intake) were constructed from PVC (2.5 cm inner diameter) pipe and installed into the different substrates in grouped nests. Nests typically comprised a fully–slotted well, with piezometers installed in mid–peat (0.6–0.75 m depth) and underlying mineral (1.25–1.5 m depth). The depth to water table and piezometer head at nests were measured manually on a weekly basis during the spring and summer from 2011–2015 and once in October for all years

with the exception of 2014. A continuous record of channel fen water table was obtained at a nest in NT1 using a logging pressure transducer (from 2011–12; Schlumberger Mini–Diver) or a capacitance water level recorder (from 2013–15; Odyssey Dataflow Systems Ltd.). Average manual water was then extrapolated into a continuous record, based on highly correlated values between average manual water table and logged water table. Saturated hydraulic conductivity (K_{sat}) of peat and underlying mineral was determined by bail tests on all piezometers installed at Poplar Fen between 2011–15 in the fen and margin zones using the hydrostatic time–lag method (Hvorslev, 1951). Triplicate K_{sat} measurements were performed on all piezometers in which the arithmetic average was taken. For the upper 60 cm of peat, K_{sat} was determined in the lab using peat cores extracted from channel fen (n= 2), Margin (n= 2), and West wetland (n= 1) areas. Cores were extracted using a Wardenaar coring device and samples were frozen and shipped for processing at the lab. Cores were subdivided into 10–cm stratigraphic intervals, and horizontal and vertical K_{sat} were determined using a constant head method (e.g. Freeze and Cherry, 1979). Lab and field K_{sat} values were grouped and arranged by depth to estimate average K_{sat} versus depth, which were later used in groundwater flux calculations.

Darcy's Law (Freeze and Cherry, 1979) was used to estimate groundwater fluxes in and out of the channel fen (NT1–NT3) and West wetland areas:

$$q = -K \frac{dh}{dl} \quad (2\text{–}1)$$

where q is the specific discharge (m s^{-1}), K is the saturated hydraulic conductivity (m s^{-1}), and dh/dl is the hydraulic gradient (dimensionless).

Vertical fluxes were calculated using vertical hydraulic gradients between the mid–peat and underlying mineral layer for each channel fen nest and for the West and East wetlands. Vertical area–weighted groundwater flux rates (mm d^{-1}) were estimated at each nest (with the exception of the East wetland) by multiplying the vertical hydraulic gradient by a weighted harmonic mean saturated hydraulic conductivity between the piezometers measured, incorporating all available K_{sat} data at Poplar Fen. This mean is typically used for calculating vertical flux rates through horizontally layered strata (Freeze and Cherry, 1979). Given negligible differences between laboratory–measured vertical and horizontal K_{sat} (not shown), an anisotropy of 1 was used for

field–measured K_{sat} values.

Horizontal groundwater fluxes, laterally into the channel fen, were calculated using the head differences in channel fen and upland water table elevations. First, a depth–weighted arithmetic mean K_{sat} of the peat was calculated, the mean typically used for calculating flux rates for horizontal flow through horizontally layered strata (Freeze and Cherry, 1979). To prevent overestimation of K_{sat}, weighted arithmetic means were calculated individually for fen and margin areas, given their unique peat physical properties and water table depths. Weighted arithmetic means were calculated for fen and margin at each transect depending on their average water table position. Once a mean K_{sat} value was calculated for fen and margin, a harmonic mean was taken between fen, margin, and upland K_{sat}. Final K_{sat} values were then multiplied by the horizontal hydraulic gradient to calculate the specific discharge fluxes (mm d^{-1}) at each transect. Average fluxes were applied across a flow face (thickness and length of NT1–NT3 peat flow face) to obtain a volumetric flux (m^3). Then, the volumetric flux was divided by the estimated fen surface area of NT1–NT3 (~47,000 m^2) to which this flow face was assumed to contribute to.

Precipitation was measured in an open area of the site with a logging Onset RG3–M tipping bucket rain gauge. Missing daily totals were supplemented with rainfall data for the Poplar Fen area (township: T092R10W4), which were estimated using an inverse-distance weighting interpolation procedure (IDW) (Alberta Agriculture and Forestry, 2017).

In August 2014, June 2015, and July 2015, porewater samples were taken from specific nests within the channel fen, West and East wetland, and upland water table wells, as well as specific underlying mineral piezometers at channel fen nests and the West wetland. All water samples were sent for laboratory analysis of major cations and anions, as well as oxygen ($\delta^{18}O$) and hydrogen (δD) isotopes. All water samples were filtered within 24 hours using 0.45 μm nitrocellulose membrane filters. Samples for ion analyses were stored in 60 mL high–density polyethylene bottles and kept frozen prior to analyses. Isotope samples were stored in tightly sealed 20 mL scintillation vials with no head space, at 4°C, for isotope analyses. Major ions were measured with a Dionex ICS–1600 Method EPA 300.0 with AS–DV auto–sampler, with analytical precision to ±1.0 mg L^{-1} or less. Isotopes were measured with a Picarro L2120–i Cavity Ring–

Down Spectroscopy analyzer. This technique yields an analytical precision of ±0.4‰ for δD and ±0.2‰ for $\delta^{18}O$.

2.4. Results

2.4.1 Lithology

Within the watershed boundaries – along cross–sections A–A' and B–B' – there was a combined average drift and recent sediment thickness of 12.3 m overlying the Cretaceous Clearwater formation (Fig. 2–2). Although not reported in the lithology drill logs, a thin (~0.1 m) silty sand layer is dominant at most channel fen nest locations, detected during well and piezometer installations. A similar underlying silty sand layer is located at the West wetland at ~1 m depth below ground surface (b.g.s.); however, between this and the peat layer is a ~0.5 m thick sand layer. Underlying the peat at the East wetland is a ~1 m sand layer, which is underlain by a clay layer (≥0.5 m). The uppermost mineral sediment is composed of coarse outwash sand and gravel, which averages 6.2 m in thickness, ranging from 0.5–13.4 m (Fig. 2–2). Outwash depth is thicker, more elevated, and more consistent along the more elevated eastern side of the watershed. Underlying the outwash is a fine–grained silt–dominated till unit, which averages 5.3 m in thickness, ranging from 0–9.5 m. Underlying the silty–till is the Clearwater formation, a known regional aquitard, which varies in thickness and grain size, ranging from sandy silt to pure clay, and has an average combined thickness of 10.9 m. Underlying the Clearwater formation is the bitumen–bearing McMurray formation, which has an average depth below ground surface of 22.7 m.

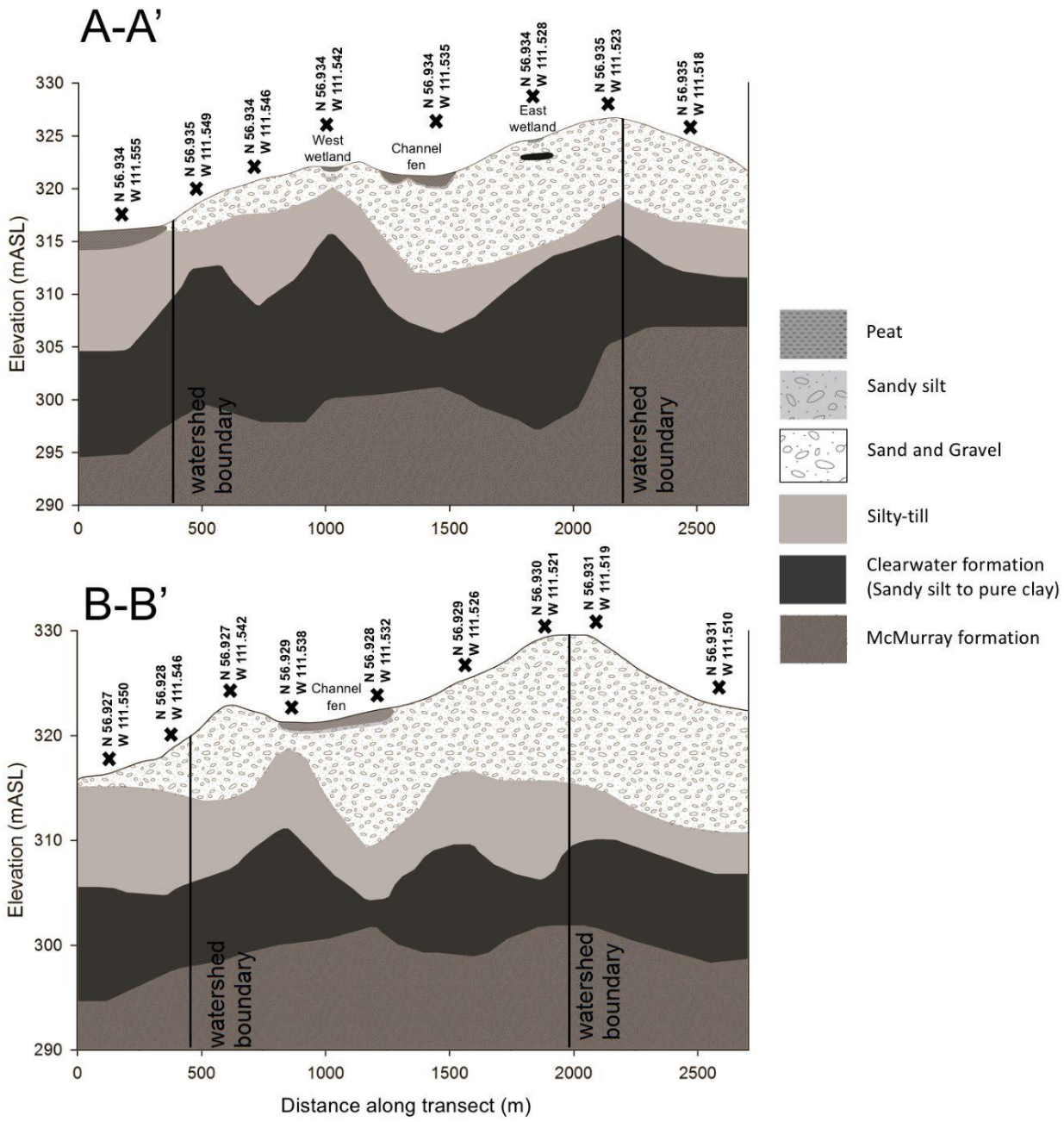

Figure 2–2. Field lithology drill logs of transects A–A' and B–B' (vertical exaggeration = 4.6) at Poplar Fen watershed (see Figure 1 for locations).

2.4.2 Hydraulic Conductivity

Peat thickness measured in this study ranged from 1.3–1.5 m in channel fen areas, commonly thinning to 0.3–0.7 m in margins between fen and upland; however, drill logs obtained for the area report peat thickness can reach up to 3 m. Peat depth averaged ~0.5 m in the West

wetland and ~0.3 m in the East wetland. K_{sat} of the channel fen peat declined with depth by orders of magnitude, ranging from 4.7 x 10^{-3} m s^{-1} in the upper 10 cm to as low as 1.2 x 10^{-8} m s^{-1} at the basal layer (Fig. 2–3). The peat at the base of the channel fen (1.0–1.1 m depth) had a geometric mean K_{sat} of 4.5 x 10^{-7} m s^{-1}, ranging from 3.1 x 10^{-5} m s^{-1} to 1.2 x 10^{-8} m s^{-1} (n=11), spanning three orders of magnitude (Fig. 2–3). Directly underlying the channel fen peat (below 1.2–1.5 m) is a ~0.3 m thick, heterogeneous mineral layer above the outwash layer, ranging from fine–medium sand to silty sand. K_{sat} in this layer and the outwash layer ranged by four orders of magnitude, and had a geometric mean of 5.6 × 10^{-6} m s^{-1} (n=33). K_{sat} measured at the West wetland ranged by two orders of magnitude, from 3.5 × 10^{-3} m s^{-1} at the surface, to 2.7 × 10^{-5} m s^{-1} at the basal layer (0.5–0.6 m depth). Directly underlying the West wetland is a ~0.4 m thick sand layer (K_{sat} not measured at this depth). Below the sand layer (at 1 m depth b.g.s.) is a silt–dominated layer with a K_{sat} of 3.4 × 10^{-8} m s^{-1}. K_{sat} was not measured for the peat layer at the East wetland; however, the sand–dominated mineral layer directly underlying the peat (0.3–1.4 m) had a measured K_{sat} of 1.0 × 10^{-5} m s^{-1}. Underlying the sand layer is a clay–dominated layer which had a K_{sat} of 3.9 × 10^{-10} m s^{-1} (not shown).

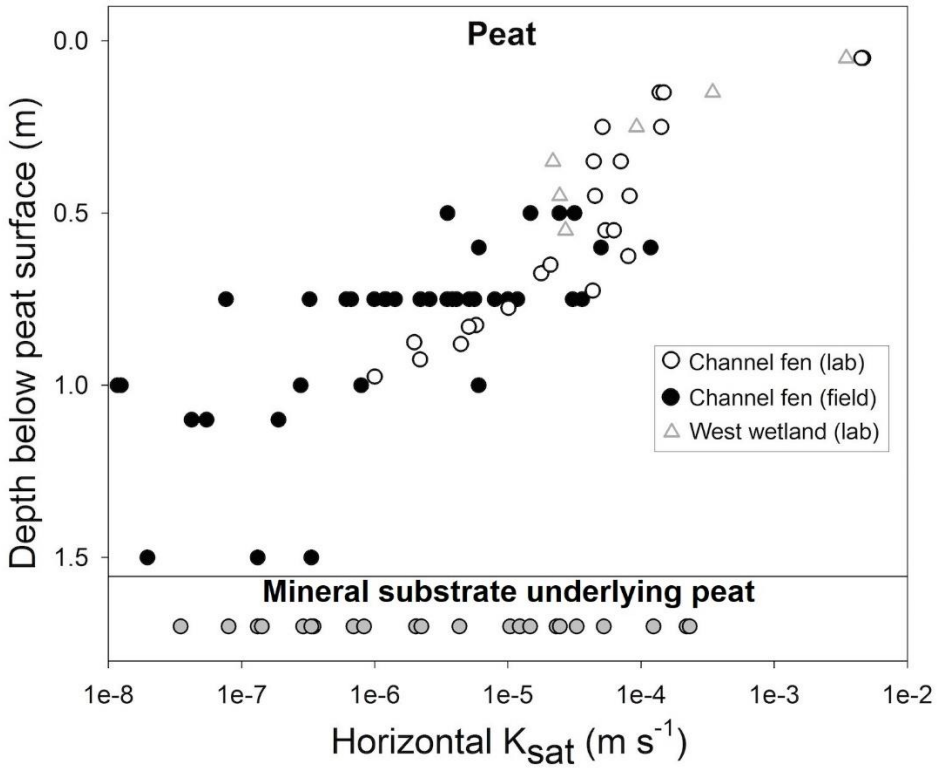

Figure 2–3. Laboratory (0–0.6 m) and field estimates (0.6–1.5 m) of saturated horizontal hydraulic conductivities for channel fen and West wetland peat and underlying mineral sediments.

2.4.3 Hydrology

2.4.3.1 Water table

The average channel fen water table range at NT1–NT3 was ~0.77 m (+0.1 m to –0.66 m) between Jun. 08, 2011 and Oct. 04, 2015 (Fig. 2–4a). The general five–year water table trend was relatively low water tables (dry conditions) at the beginning (2011 to mid–2012), increased water table in the middle years (late 2012 to mid–2014), and lower water tables in a drying period towards the end (mid–2014 to late 2015) of the 5–year record (Fig. 2–4a). Over this time, horizontal hydraulic gradients were relatively stable down the channel fen towards the culvert (location shown in Fig. 2–1), averaging 0.0026 ± 0.0005 (SE) (data not shown on Fig. 2–4). Horizontal groundwater flow was typically low during the drier periods (2011 to Summer 2012, 2015), ranging from 0.004–0.254 mm d^{-1} (average = 0.05 ± 0.01 (SE) mm d^{-1}). During wet periods (Fall 2012–2014), horizontal flow was higher, ranging from 0.07–0.30 mm d^{-1} (average = 0.26 ± 0.01 (SE) mm d^{-1}).

2.4.3.2 Vertical groundwater connection between channel fen and underlying outwash

Between 2011 and 2015, hydraulic head in the underlying outwash aquifer (Fig. 2–4b) and vertical hydraulic gradients between the peat and underlying mineral substrate at the channel fen (Fig. 2–4c) varied in correspondence with diurnal and seasonal precipitation trends. Vertical flow direction at NT1–NT3 fen nests (location shown in Fig. 2–1) was downward (indicating groundwater recharge) throughout 2011, corresponding to a period of low water tables and below average rainfall (Fig. 2–4a). Over this period vertical discharge averaged –0.13 mm d^{-1} (Table. 2–1). In 2012, several relatively large rain events had occurred (Fig. 2–4a), with several vertical flow reversals occurring during these events (Fig. 2–4c). For the majority of this field season, vertical flow was directed primarily upwards (indicating groundwater discharge), with average vertical discharge equaling +0.04 mm d^{-1}. Discharge conditions persisted throughout 2013 until Aug. 2014, during an extended period of abundant rainfall and high fen water tables, reaching upward gradients as high as +0.016 (Fig. 2–4c). Throughout this period, average vertical discharge equaled +0.13 mm d^{-1} (Fig. 2–4c). In July 2014, fen water tables began declining steadily into the fall (Fig. 2–4a), and another vertical flow reversal was initiated, back to groundwater recharge, with weighted average vertical discharge equaling –0.04 mm d^{-1} (Fig. 2–4c). Spring 2015 exhibited

high (near–surface) fen water tables (Fig. 2–4a), and at this time, Poplar Fen was a groundwater discharge area. However, throughout the growing season, several more flow reversals were initiated, including recharge during a period of low rainfall in June, discharge in mid–July during a period of increased rainfall, and recharge from early August until the late fall (Fig. 2–4c). Over this period vertical discharge averaged –0.09 mm d^{-1} (Table. 2–1). The annual net groundwater fluxes measured over each respective field season were –13.9 mm in 2011 (111 days), +8.1 mm in 2012 (170 days), +17.8 mm in 2013 (147 days), +5.2 mm in 2014 (84 days), and –11.0 mm in 2015 (125 days).

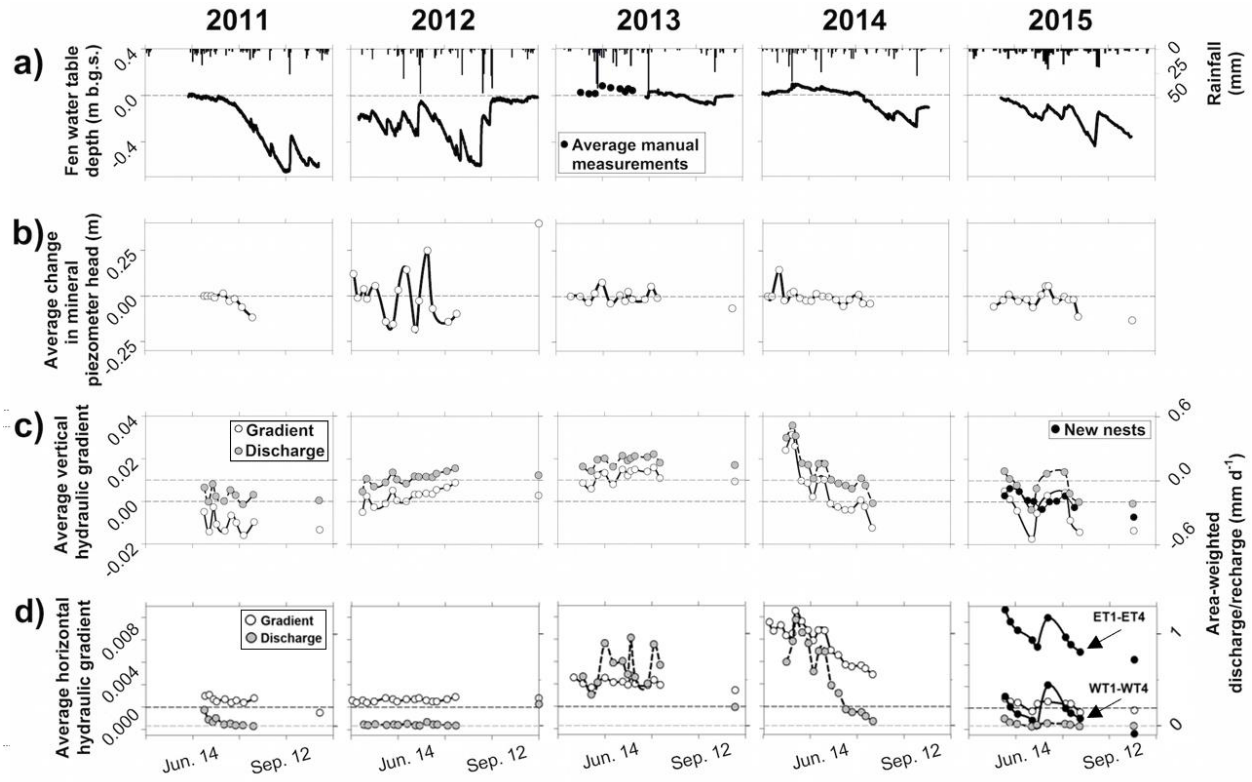

Figure 2–4. Average hydrological results for NT1–NT3 (see Fig. 1) from 2011–2015, including (**a**) channel fen water table with daily regional precipitation illustrated, (**b**) change in hydraulic head since last measurement in outwash piezometers underlying channel fen areas, (**c**) average vertical hydraulic gradients between channel fen peat and underlying mineral substrate (open and black circles) and corresponding average vertical groundwater fluxes (grey circles), and (**d**) average horizontal hydraulic gradients between upland and channel fen (open and black circles) and corresponding average horizontal groundwater fluxes (grey circles). Also included are vertical (**c**) and horizontal (**d**) hydraulic gradients for newly installed 2015 nests (black circles). Positive gradients and fluxes represent flow towards the fen. Note that calculated discharge in (**c**) and (**d**) in 2015 correspond only to gradients measured at NT1–NT3 and not the newly installed nests.

Average vertical hydraulic gradients measured at NT1–NT3 (–0.008) were lower in 2015 than those calculated from new nests (WT1–WT4; ET1–ET4; Fig. 2–1) that were installed in 2014

and 2015 (–0.001) (Fig. 2–4c). The newer nests exhibited flow reversals throughout 2015 in response to precipitation; however, vertical hydraulic gradients did not reach values as low as those measured at NT1–NT3 and therefore did not experience the same variation (Fig. 2–4c). This resulted in lower loss (–0.02 mm d^{-1}) of water to the underlying outwash aquifer compared to NT1–NT3 (–0.11 mm d^{-1}).

2.4.3.2 Lateral upland–channel fen groundwater connection

The fen to upland slope along NT1–NT3 (Fig. 2–1) averaged 0.5% and had a relief of ~1.1 m. Horizontal hydraulic gradients between fen and upland at these transects were positive throughout most of the five–year record (Fig. 2–4d), indicating that the lateral flow was directed primarily towards the fen (average: +0.001). On average, horizontal gradients were weaker by an order of magnitude than vertical gradients (see Fig. 2–4c). Flow reversals occurred only in late June, mid–August, and early October 2015, corresponding to periods of low rainfall. Average horizontal discharge ranged from –0.01 to +1.15 mm d^{-1} (Fig. 2–4d). During drier periods characterized by lower rainfall and water tables (Aug. 2011–Aug. 2012, 2015; Fig. 2–4a), horizontal discharge averaged +0.01 mm d^{-1}. During wetter periods characterized by higher rainfall and water tables (Fall 2012–July. 2014; Fig. 2–4a), horizontal discharge averaged +0.50 mm d^{-1}. The annual net groundwater fluxes measured over each respective field season were +2.8 mm in 2011 (111 days), +10.7 mm in 2012 (170 days), +79.2 mm in 2013 (147 days), +44.5 in 2014 (84 days), and +1.2 mm in 2015 (125 days).

Table 2–1. Summary of estimated vertical and horizontal groundwater fluxes averaged (weighted) annually for 2011–2015 field seasons, along with average daily precipitation over the same time period. Note: a negative gradient and flux represents a loss of water from the fen.

Year	2011	2012	2013	2014	2015
Vertical discharge to fen					
Average vertical hydraulic gradient between fen and underlying outwash	–0.011	+0.004	+0.011	+0.006	–0.008
Average groundwater exchange (mm d^{-1})	–0.13	+0.04	+0.12	+0.06	–0.09
Horizontal discharge to fen					
Average horizontal hydraulic gradient between fen and upland	+0.0004	+0.0007	+0.0019	+0.0017	+0.0001
Average groundwater exchange (mm d^{-1})	+0.03	+0.06	+0.54	+0.53	+0.01

In the more expansive East upland (transects ET1–ET4; average upland to channel fen

slope = 1.5%; total relief = ~7.0 m), horizontal hydraulic gradients in 2015 were stronger by an order of magnitude along this flow face than those measured at NT1–NT3 (Fig. 2–4d). Although weakening in the absence of precipitation, horizontal hydraulic gradients at ET1–ET4 remained positive in 2015 and no flow reversals were detected over this relatively dry summer. This resulted in horizontal discharge ranging from +0.09 to 1.08 mm d^{-1} (not shown on Fig. 2–4d). Conversely, average horizontal gradients at the narrower and more gently–sloping West upland (transects WT1–WT4; average upland to channel fen slope = 0.5%; total relief = ~1.0 m) were generally lower and more variable than at NT1–NT3 (Fig. 2–4d). This resulted in horizontal discharge ranging from –0.08 to +0.19 mm d^{-1} (not shown on Fig. 2–4d).

2.4.3.4 Hydrology of West and East wetlands

Water tables in the East and West wetlands were below ground surface for the entire instrumental period (Fig. 2–5a). Water table position was nearly identical between the East and West wetlands in 2014. Conversely, water tables differed more in 2015, as the West wetland was consistently lower (Fig. 2–5a); it had fallen below the base of the peat layer and into the underlying sand layer (not shown) by October, 2015.

Vertical hydraulic gradients differed notably between wetlands (Fig. 2–5b). Vertical gradients were negative in the East wetland throughout all of 2014–15, indicating that the peat was recharging the underlying mineral layers throughout the whole instrumental record. In contrast, vertical flow reversals were detected in the West wetland during both years. Unlike in channel fen areas, where gradients became positive in response to rainfall, vertical flow direction showed opposite patterns in the West wetland, as it became a recharge zone during wetter periods and a discharge zone following extended periods of water table drawdown (Fig. 2–5b). Due to the relatively high saturated hydraulic conductivity of the basal peat layer (Fig. 2–3), vertical flux rates in the West wetland were typically higher compared to the channel fen, ranging from –0.91 mm d^{-1} during wet periods to +0.70 mm d^{-1} during dry periods. Due to insufficient information on the hydraulic properties of the 30 cm deep peat in the East wetland, fluxes were not calculated.

Horizontal gradients also differed greatly between wetlands in 2015 (Fig. 2–5c). Horizontal gradients between the West wetland and adjacent uplands were negative throughout the entire sampling period, indicating that the wetland received no supplemented lateral discharge, and

instead, recharged the adjacent uplands. Contrary to the West wetland, a strong and consistent positive gradient was measured between the East wetland and the upland to the east throughout 2015 (Fig. 2–5c).

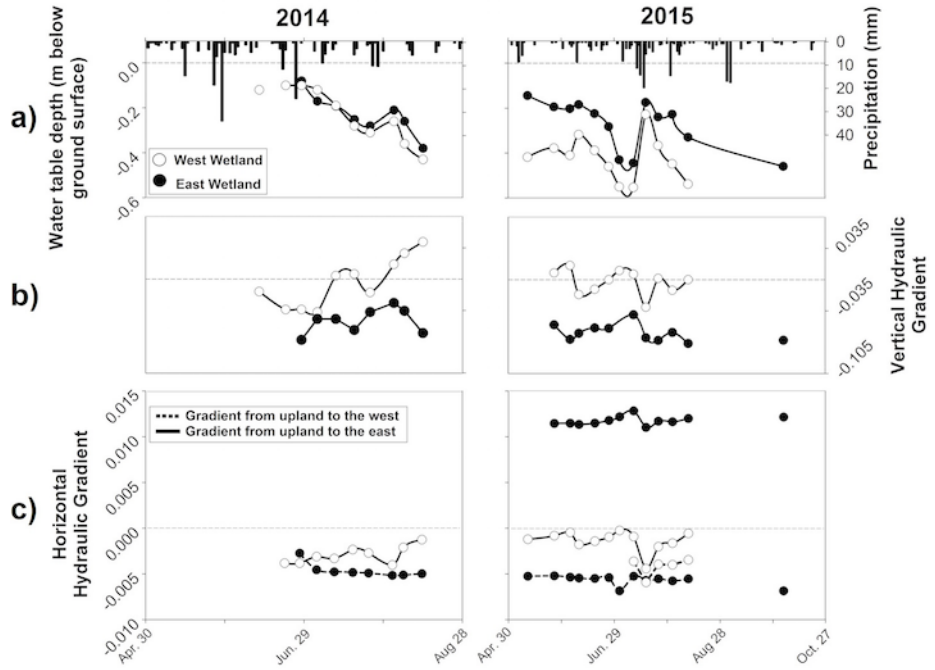

Figure 2–5. (**a**) Comparison of water table position, (**b**) vertical hydraulic gradients between wetland water table and underlying mineral, and (**c**) horizontal gradients between wetland water table and upland to the west (hashed lines) and east (solid lines) of the West and East wetland areas (see Fig. 1).

2.4.4 Water chemistry

Porewater samples obtained from channel fen, underlying outwash, and upland pipes all had similar pH (6.8–7.0), electrical conductivity (EC; 411–532 µS cm^{-1}), and concentrations of calcium (Ca^{2+}; 59–79 mg l^{-1}) and magnesium (Mg^{2+}; 13.9–17.1 mg l^{-1}) (Fig. 2–6). Comparatively, the West and East wetland wells, as well as the sandy silt layer underlying the West wetland, had lower pH (4.5–5.6), EC (109–165 µS cm^{-1}), Ca^{2+} (8.2–14.2 mg l^{-1}), and Mg^{2+} (1.2–2.6 mg l^{-1}). All locations had similar chloride (Cl^{-}) concentrations, ranging from 1.3–3.5 mg l^{-1} (Fig. 2–6).

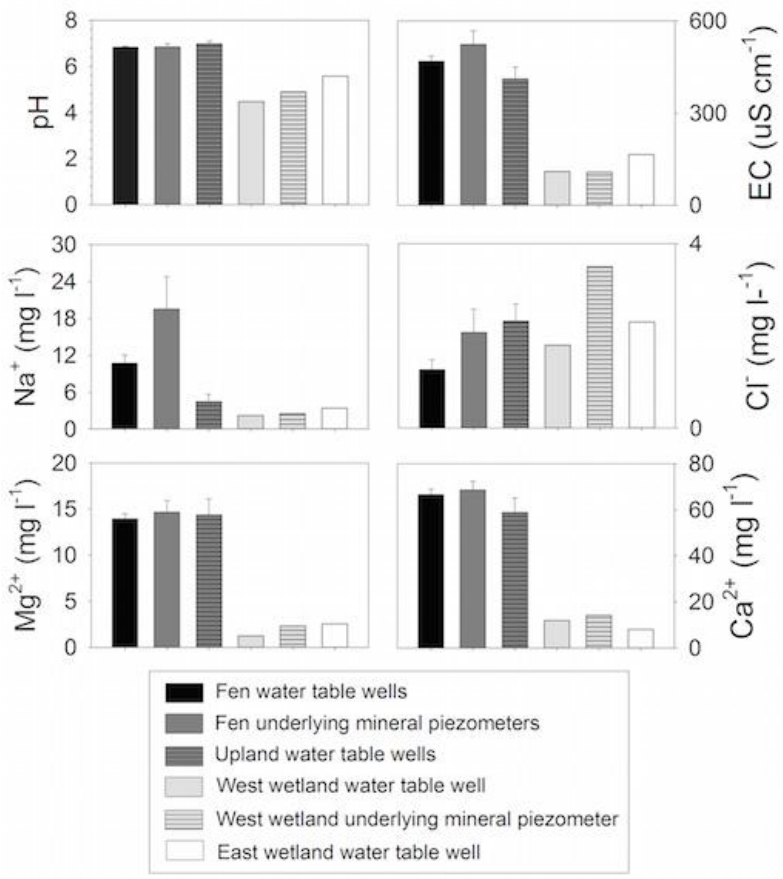

Figure 2–6. Average pH, electrical conductivity (EC), and concentrations of major cations (Na^+, Ca^{2+}, and Mg^{2+}) and Cl^- for samples obtained from channel fen, upland, and West and East wetland wells, as well as underlying mineral piezometers from channel fen and West wetland nests obtained throughout 2015.

All water samples obtained from these three locations appeared to be of similar recent meteorological origin, plotting close to the LMWL, and showing little or no evidence of isotopic enrichment or depletion. The West wetland water table well sample plotted close to the corresponding underlying mineral piezometer, both in the middle of the LMWL. The East wetland water table in June 2015 was virtually similar in isotopic composition to upland water table samples obtained during that period. However, by July, 2015, the East wetland water table and corresponding underlying sand piezometer sample had isotopic composition characteristic of late summer precipitation (Fig. 2–7).

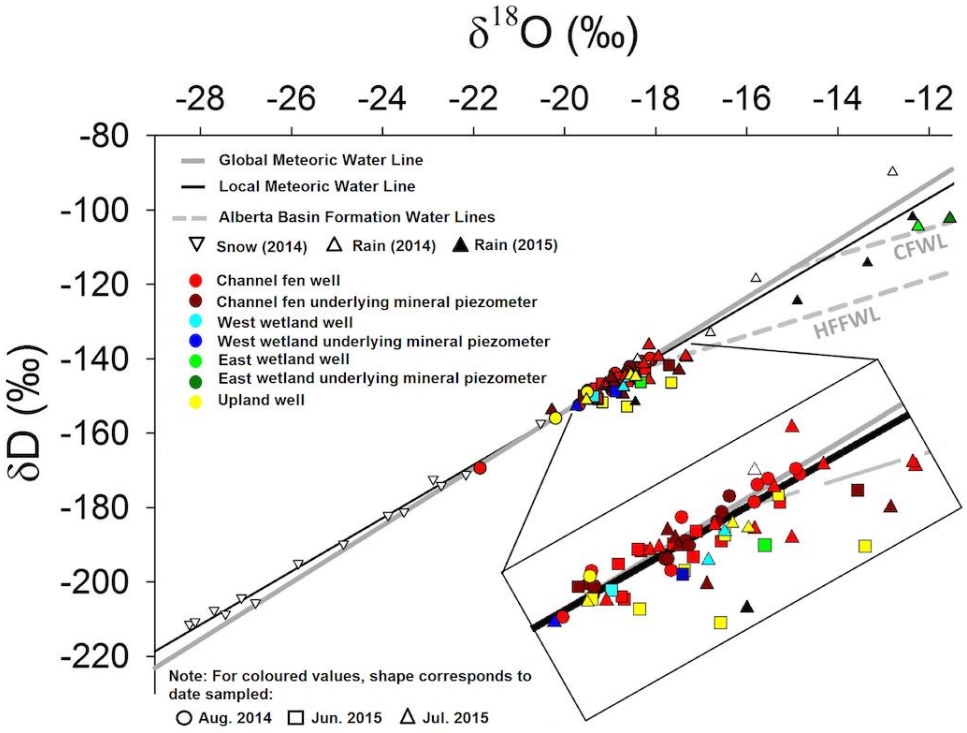

Figure 2–7. Isotopic signatures $\delta^{18}O$ and δD for precipitation obtained ~5 km from Poplar Fen (used to produce LMWL), and for water samples obtained at channel fen, West and East wetlands, and upland water table wells and underlying outwash piezometers (see legend for colour scheme), at Poplar Fen in August, 2014 (circles), June, 2015 (squares), and July, 2015 (triangles). Additional water lines were plotted, including the GMWL, as well as water lines of regional Alberta Basin formation water samples reported in Connolly et al., 1990 (CFWL) and Hitchon and Friedman, 1969 (HFFWL), adapted from Lemay, 2002.

2.5 Discussion

2.5.1 Hydrogeologic Setting of Poplar Fen Watershed

Based on what was observed at Poplar Fen, the following conceptual model is proposed (Fig. 2–8), which highlights the hydrogeologic setting and hydrologic function of fens and uplands that are thought to be typical of moderate–rich fen watersheds in the AOSR. Given that this study included two seasons with less than typical rainfall, the conceptual model may be a useful guide for understanding the likely response of moderate–rich fens in the AOSR under a warmer climate. Below, the field results and key processes are discussed while referring to this conceptual model.

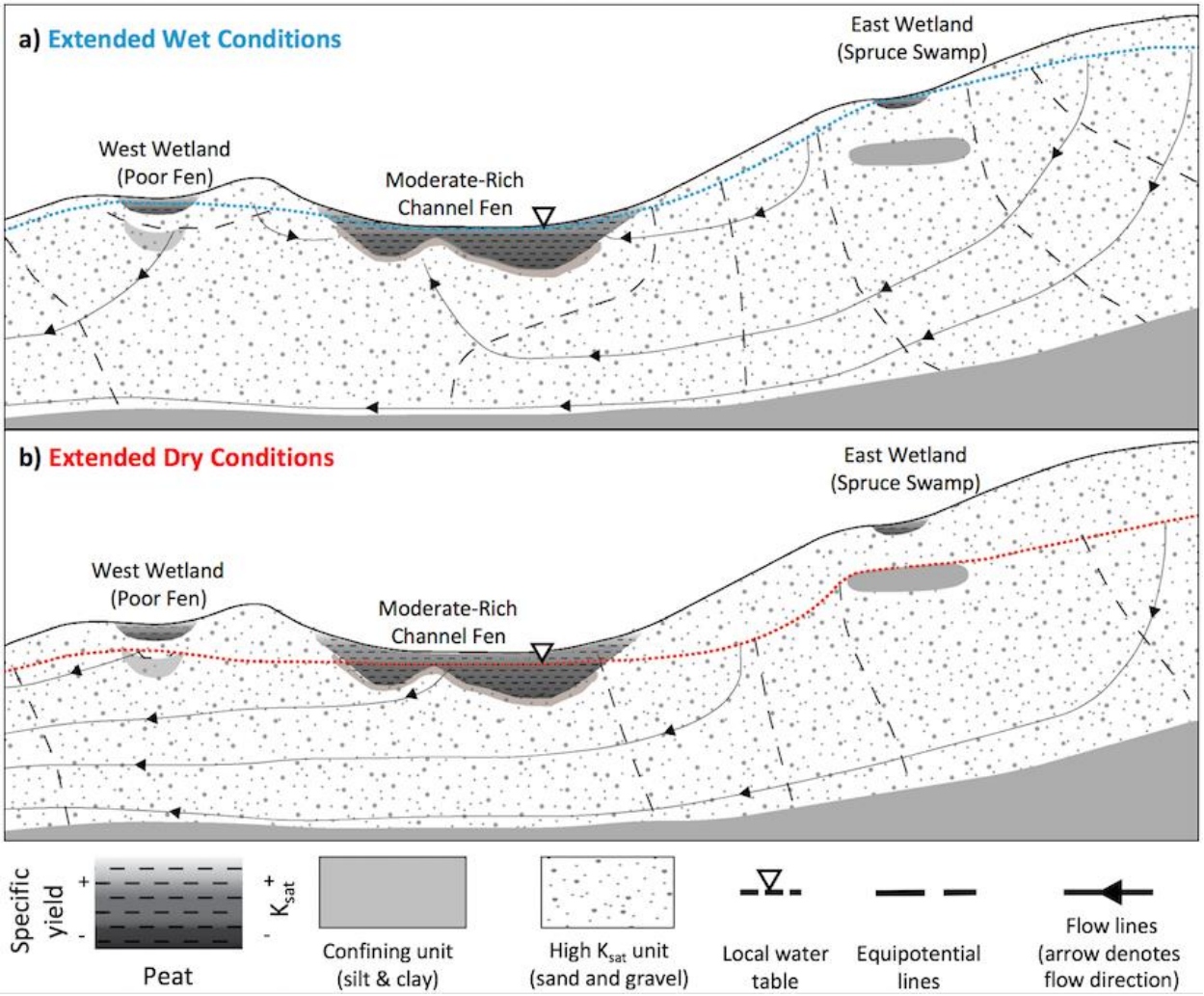

Figure 2–8. Conceptual model of fen landscape connectivity at Poplar Fen for moderate–rich channel fen, poor–fen, and spruce swamp systems, comprising lithological information from cross–section A–A' (Fig. 2) during typical wet and dry conditions observed between 2011–15. Due to insufficient hydrological information below 2.0 m, equipotential and flow lines are idealized.

Field lithology drill logs identified a veneer–type layering of coarse– over fine–grained glacial deposits over the Cretaceous Clearwater formation at Poplar Fen. This establishes a relatively thick (~16 m) and shallow aquitard throughout the watershed (Fig. 2–2). The combined low K_{sat} units constrict the connectivity between the watershed and underlying regional flow systems. Overlying the aquitard, outwash sand and gravel are the dominant sediment textures in adjacent uplands and outwash underlying the channel fen. These higher K_{sat} units allow for a local unconfined flow–system to develop, which focusses discharge to low–lying channel fen areas. The silty sand layer underlying the channel fen, although thin and heterogeneous, limits the strength of this connection, lowering specific discharge during wet periods, while also reducing water loss

(via downward flow through the basal peat) during drier periods. In addition, the West and East wetlands have a relatively shallow, low K_{sat} unit underlying the organic soil, which helps confine the downward flow of subsurface water and promotes more saturated peat–forming conditions.

Vertical recharge–discharge patterns between the peat and underlying outwash aquifer were variable both spatially and temporally over the five–year instrumental period at channel fen nests (Fig. 2–4c). Vertical flow reversals occurred several times (Fig. 2–4c), with discharge conditions (upward flow from underlying outwash to peat) initiating and persisting over relatively wet periods, and recharge conditions (downward flow from peat to underlying outwash) over extended dry periods (summarized in Fig. 2–8). These flow patterns are different from those reported on pond–peatland complexes overlying outwash sediments at the URSA (Smerdon et al., 2005), a spring fen (Siegel and Glaser, 1987) and raised–bog (Glaser et al., 1997) in northwestern Minnesota, and fens overlying esker aquifers in northern Finland (Kløve et al., 2012). These locations comprise relatively thick coarse-grained sediments that extend deeper than those underlying Poplar Fen, and subsequently, water table drawdown is moderated by more consistent sources of groundwater discharge, which the authors all attribute to deep regional flow. The variability in hydraulic head in the relatively thin coarse–grained outwash sediment underlying Poplar Fen, in correspondence with short-term precipitation trends, indicates a local groundwater flow–system characterized by short travel times (Tóth, 1999; Kløve et al., 2012). Although localized, this hydrogeologic setting is different from bog and poor fen watersheds connected to local flow systems at URSA (Ferone and Devito, 2004), where low K_{sat} clay or till underlying the peat was found to confine the hydrological connectivity between peatlands and underlying groundwater. Thus, flow direction and magnitude at Poplar Fen are more responsive to precipitation–driven recharge from adjacent uplands leading to subsequent discharge from underneath the channel fen (Fig. 2–8a). However, without a regional groundwater connection to supplement discharge during extended dry periods, recharge conditions will likely become more dominant in moderate–rich fens with a climatic and hydrogeologic setting similar to Poplar Fen (Fig. 2–8b), rendering them susceptible to enhanced water table decline during dry periods.

Horizontal recharge–discharge patterns between upland and channel fen were also highly variable between 2011–2015 (Fig. 2–4d); however, the flow direction was typically from upland to fen with flow reversals only occurring during in the fall of 2011 and throughout 2015, two

relatively dry years (Environment and Climate Change Canada, 2018). During these dry periods (2011 and 2015), discharge from upland to fen averaged +0.05 and +0.02 mm d^{-1}, roughly equaling lateral discharge (0.04 and 0.02 mm d^{-1}) measured down the fen towards the culvert during those years, respectively. Conversely, during wetter periods (2013–2014), specific discharge fluxes along the NT1–NT3 flow face became higher by up to several orders of magnitude (Fig. 2–4d). This resulted in average area–weighted fluxes of +0.54 and +0.53 mm d^{-1}, roughly two times higher than the lateral discharge measured down the fen during those years, respectively. The results presented in this study differed from poor–fen and bog systems studied at the URSA, where fine–grained sediment dominant in the uplands limited connectivity, resulting in negligible groundwater fluxes (Ferone and Devito, 2004). Results were more similar to those reported on a minerotrophic fen overlying a coarse-grained glaciofluvial outwash plain in central Saskatchewan (Barr et al., 2012), where bidirectional flow was measured between fen and adjacent black spruce– and jack pine–dominated upland areas, with higher groundwater fluxes directed towards the fen during wet periods.

The difference in lateral flux rates to channel fen areas between dry and wet years at Poplar Fen is explained largely by the hydraulic conductivity of the upper peat, which increases by several orders of magnitude from base to surface (Fig. 2–3), and is regarded as a common physical characteristic of peat (Price and Maloney, 1994; Hoag and Price, 1995; Ferone and Devito, 2004; Whittington and Price, 2006; Wells et al., 2017). The presence of the water table within shallower and relatively high K_{sat} layers had greatly increased the transmissivity of the fen peat layer. In addition, the hydraulic gradient between upland and fen becomes much higher during wet periods as the fen water table reaches the surface and specific yield approaches 1, causing it to rise at a slower rate than the upland water table. These two primary attributes, when combined, produce a transmissivity feedback mechanism (Bishop, 1991; Waddington et al., 2014), which conveys relatively higher groundwater fluxes from upland to fen (summarized in Fig. 2–8). Despite these high fluxes, margin water table position exhibited a relatively important control on the overall transmissivity of the fen–upland flow path, due to its lower water tables and therefore lower arithmetic K_{sat}. This suggests that margins operate as distinct hydrological units and should be understood better in future studies. Conversely, lower horizontal gradients during dry periods (Fig. 2–4d), along with the water table (Fig. 2–4a) positioned in deeper, lower K_{sat} peat (Fig. 2–3), result in fluxes that are much lower (Table 2–1). This weak connection during flow reversals, however,

results in negligible flux rates from fen to upland. This negative feedback is regarded as an important feature for water conservation in peatlands (Waddington et al., 2014); however, it does not account for potential water losses via transpiration by aspen trees (deep clonal roots) via hydraulic lift from deeper substrates and adjacent wetlands (Depante et al., 2016). Therefore, uplands may still act as water sinks despite this limited hydrological connection between fen and upland.

Transects NT1–NT3 provided replicates of a similar upland–fen setting that is common in the watershed, but not ubiquitous. Additional insight is gained from installations and 2015 data from WT1–WT4 and ET1–ET4, which illustrate contrasting patterns of landscape connection. The West upland–fen transect is short, and thus the contributing area (estimated across the slope from first to last transect) to the fen is small (~0.05 km^2). Consequently, its hydraulic gradients were more variable than NT1–NT3, and susceptible to flow reversals. In contrast, the East upland contributing area was larger (~0.68 km^2) and steeper (relief ~7 m) than the West upland (see Fig. 2–8). This yielded stronger and consistently positive flow towards the fen in 2015 (cf. Hokanson et al., 2016). It also explains why the local vertical hydraulic gradients in the channel fen remained stronger than those at NT1–NT3. This upland apparently plays a pivotal role in providing water to the channel fen areas in Poplar Fen watershed.

The West wetland had a net loss of groundwater to adjacent uplands throughout 2014 and 2015, as evidenced by consistent negative horizontal hydraulic gradients. However, vertical hydraulic gradients were susceptible to flow reversals during both years (Fig. 2–5b), and in contrast to channel fen areas, the West wetland became a groundwater recharge area during periods of high precipitation. The elevation and position relative to the adjacent upland can explain why the West wetland became a recharge zone during wet periods (Fig. 2–8), as uplands and topographic highs typically recharge topographic lows (Tóth, 1999; Winter, 1999). Conversely, flow reversals in the West wetland occurred in between rainfall events in the summer. It is postulated that although the wetland is a predominant recharge feature, the relatively low specific yield (~0.08) of humified peat causes water table drawdown at a faster higher rate than the decrease in hydraulic head in the underlying outwash aquifer. Large fluctuations in the vertical hydraulic gradient resulted, and when multiplied by the relatively high harmonic mean hydraulic conductivity of the West wetland peat, resulted in vertical groundwater fluxes that were up to

twenty times higher than those measured in channel fen areas. This dynamic groundwater connection can help explain why the water table declined below the base of the peat in the West wetland twice in 2015, highlighting its heavy reliance on rainfall for a stable source of water storage.

The East wetland was characterized by negative vertical hydraulic gradients throughout 2014 and 2015 (Fig. 2–5b), suggesting that it is a prominent recharge feature for the watershed. This is likely due to the relative position of the wetland, located within an expansive upland system and at an elevation ~2.5 m higher than the channel fen area directly to the west. The East wetland, with an organic layer thickness of only ~30 cm, does not classify as a peatland, and has characteristics more like a basin swamp (NWWG, 1997). It hosts peat–forming mosses (*S. fuscum* and *P. schreberi*), as the underlying low K_{sat} clay layer (4.0×10^{-10} m s^{-1}) helps to sustain high, yet strongly variable, water tables. In addition, the strong positive horizontal hydraulic gradients measured from the upland to the wetland (Fig. 2–5c) highlight the importance of throughflow as a means of maintaining high water tables in the East wetland.

Geochemical results supported the lithological and hydrological evidence of a localized flow system influencing recharge–discharge patterns at Poplar Fen. Virtually indistinguishable pH and similar EC and Ca^{2+} and Mg^{2+} concentrations between channel fen, underlying outwash aquifer, and upland suggests that waters in these locations are of similar origin. Furthermore, Cl^- concentrations 4.7 times lower than SO_4^{2-} concentrations (not shown in Fig. 2–6) in the underlying outwash aquifer points to local groundwater, as Cl^- is typically the dominant anion in deep regional groundwater due to a longer time and distance of travel (Domenico, 1972). Lower pH, EC, Ca^{2+}, and Mg^{2+} in the West and East wetlands points to a reliance on precipitation–driven recharge rather than groundwater, suggesting that these wetlands act predominantly as recharge rather than discharge features within the watershed. The δ^2H and $\delta^{18}O$ signatures also confirmed the dominance of a local–flow system at the Poplar Fen watershed (Fig. 2–7). Channel fen and West and East wetland water table well samples and corresponding underlying mineral substrates and adjacent upland samples were nearly indistinguishable in isotopic composition between 2014 and 2015. Samples from the majority of these locations plotted in the middle of the LMWL, suggesting that they receive recently precipitated meteoric water in the form of both snowfall and rainfall. Groundwater sourced by a regional (older) groundwater would plot elsewhere on the $\delta^{18}O/\delta D$ plot,

along a water line (e.g., CFWL & HFFWL; Figure 2–8) with a different slope and δD–excess (y–intercept) more reflective of the hydrometeorological conditions (e.g., relative humidity and temperature) during the time of recharge (Kendall and Caldwell, 2006). The heavy reliance on precipitation, combined with relatively low pH and base cation concentrations, suggests that the West wetland functions as a poor or intermediate fen (Chee and Vitt, 1989; Vitt et al., 1995).

The results from this study suggest that peatlands in the region that are fed by localized flow systems are particularly susceptible to drainage and drying under a climate characterized by warmer and drier conditions (Flannigan et al., 2016), especially during extended drought periods that are becoming more frequent (IPCC, 2013). Unlike fen systems connected to regional groundwater sources (Winter et al., 2003; Smerdon et al., 2005; Kløve et al., 2012), those with only a local hydrogeological connectivity similar to Poplar Fen may receive substantially less groundwater discharge from coarse–grained uplands and underlying mineral aquifers during periods of water table drawdown. Consequently, these fen systems may be subjected to enhanced peat decomposition and carbon release (Roulet et al., 2007), as well as seral succession to more ombrogenous peatlands characterized by shifts in vegetation community composition to more drought–tolerant species (e.g., *Hylocomium splendens*; Vitt, 1990).

Caution is required in generalizing the results of this study of one moderate–rich fen system to all such systems in the AOSR, although it does include a variety of transects and wetland configurations. The plain regions of the AOSR are typically dominated by outwash sand and gravel; however, are not all situated within meltwater channel features (McPherson and Kathol, 1977). Slight modifications in grain size, watershed area, and topographic relief may result in large differences in the connection to, and scale of, groundwater flow systems (Reeve et al., 2000; Tóth, 1999; Winter, 2001). The results presented in this study are consistent with conceptual models developed for the Utikuma Region Study Area (Devito et al., 2005; 2012), which stress the need for careful consideration of the local physiography when predicting the hydrologic function of peatlands on this heterogeneous and low–relief post–glacial landscape. It is recommended that additional hydrological studies be conducted on base–rich fen systems overlying coarse–grained glacial deposits in the AOSR outside of the Poplar Fen vicinity. This will help refine our understanding of the potential variability in hydrogeological connectivity of peatlands in the WBP and how they will respond to future climate– and potential human–related disturbances.

2.6 Conclusions

Groundwater flow direction between moderate–rich fen areas and the surrounding mineral landscape was transient during the 2011–2015 sampling period at Poplar Fen, changing between recharge and discharge during dry and wet periods, respectively. The variability in vertical and horizontal hydraulic gradients in response to precipitation patterns, along with supporting lithological and geochemical evidence, points to the dominance of a local flow–system generated by precipitation–driven recharge in the upland areas of Poplar Fen. During years of above average precipitation, connection is strong, with discharge higher than dry years by orders of magnitude. These results are contrary to results from previous studies of peatlands connected to deep regional flow systems (Siegel and Glaser, 1987; Glaser et al., 1997; Winter et al., 2013; Smerdon et al., 2005; Kløve et al., 2012), where peatland water levels are moderated by more consistent sources of groundwater discharge characterized by longer travel times (Tóth, 1999). This local groundwater connection, however, may render Poplar Fen, and peatlands of a watersheds with a similar hydrogeologic connectivity more susceptible to dramatic changes in the face of climate change, including drainage, enhanced peat decomposition, seral succession and wildfire.

2.7 Acknowledgements

The authors wish to thank C. Wells, D. Price, M. Fraser, J. Sherwood, R. Menzies, and J. Asten for their assistance in the field, and to E. Kessel for comments and suggestions on an earlier version of the manuscript. We gratefully acknowledge funding from a grant to Jonathan S. Price from the National Science and Engineering Research Council (NSERC) of the Canada Collaborative Research and Development Program, co–funded by Suncor Energy Inc., Imperial Oil Resources Limited, and Shell Canada Energy.

3 Hydrometeorological conditions preceding wildfire, and the subsequent burning of a fen watershed in Fort McMurray, Alberta, Canada

3.1 Introduction

The sub–humid Athabasca oil sands region (AOSR) of the Western Boreal Plain (WBP) comprises a mosaic of small lakes, forested uplands, and wetlands primarily as peatlands (Devito et al., 2012). Bogs are defined as ombrogenous peatlands, receiving water exclusively from atmospheric sources (Ingram, 1983). Conversely, fens receive water from both atmospheric and surface water and/or groundwater sources. In the WBP, fens are distinguished into three primary types (poor, moderate–rich, and extreme–rich) based on differences in water chemistry, indicator plant species, and species richness (Vitt et al., 1995). In the AOSR, moderate–rich fens are the primary peat–forming wetland (Chee and Vitt, 1989). The hydrology of bog (Scarlett and Price, 2013), poor fen (Ferone and Devito, 2004; Wells et al., 2017), and saline fen (Wells et al., 2015a, b) systems have been studied in the WBP; however, the hydrology of moderate–rich fen systems in the AOSR remains largely unexplored.

Water availability in the WBP is constrained by annual precipitation rates that are typically less than potential evapotranspiration demands (Marshall et al., 1999; Bothe and Abraham, 1993). Consequently, the timing, frequency, and magnitude of wildfires are dictated by variability in the hydrometeorological conditions over the growing season (Abatzoglou and Kolden, 2011; Flannigan and Harrington, 1988), where moisture deficits accumulate in upland duff (Keith et al., 2010) and near–surface peat horizons (Lukenbach et al., 2015) over extended dry periods. Consumption of surface and ground fuels in flaming and smouldering combustion during wildfires in the WBP can total 3 kg m^{-2} (Forestry Canada Fire Danger Group, 1992) to upwards of 4 kg m^{-2} in forested peatlands dominated by conifers (Benscoter and Wieder, 2003). Wildfire affects a variable, yet considerable area (~208 000 ha; 2006–2015), of Alberta on an annual basis (Government of Alberta, 2017). During these fires large quantities of terrestrial carbon stock held within WBP peatlands are liberated to the atmosphere, estimated at 4700 Gg C released per year, from continental western Canada alone (Turetsky et al., 2002); the peat is vulnerable to combustion and deep smouldering (Benscoter et al., 2011; Turetsky et al., 2011). Over the past decade, there has been increasing concern over longer fire seasons in Alberta (Wotton and Flannigan, 1993; Flannigan et al., 2013; Kirchmeier–Young et al., 2017) and an increase in large high–intensity

wildfires (Tymstra et al., 2007) and total burned area each year (Podur and Wotton, 2010).

The majority of summer wildfires are ignited by lightning (Tymstra et al., 2005), when wildfire behaviour can be predicted by drying signals in shallow forest duff horizons with relatively simple drying mechanisms (Wotton et al., 2005). Unlike summer fires, spring wildfires usually have human–caused ignition sources (e.g. recreational vehicle exhausts or unextinguished cigarettes) and are harder to predict given that widespread fires occur regardless of the presence of moisture deficits (Amiro et al., 2009). These spring fires therefore possess less obvious antecedent moisture signals, given that they occur post–snowmelt, an important rewetting period for wetlands and forested uplands in the region (Smerdon et al., 2008; Redding and Devito, 2011).

In Canada, early spring fire susceptibility is typically predicted with the Canadian Forest Fire Weather Index (FWI) System, a component of the Canadian Forest Fire Danger Rating System (CFFDRS) (Lawson and Armitage, 2008). The Drought Code (DC) is a component of the FWI which applies to slow–drying deep forest organic layers often found throughout the WBP, which are layers that can enhance wildfire intensity (Van Wagner, 1987). The DC is a semi–physical model which uses precipitation inputs and predicts water loss (as a function of daily noon temperature and day length) to estimate the moisture content of deep organic layers that typically dry logarithmically based on an estimated 53–day period required to lose two–thirds of held moisture (Lawson and Armitage, 2008). Values of the DC range from 0 (saturated soils at surface) to over 800 (residual soil moisture only), representing the origins of the index as representing the slow drying of stored water in Pacific coastal slash fuels (Turner, 1972). DC values have been related to the peatland water table (Waddington et al., 2012) as well as the extent of the peatland burned area (Turetsky et al., 2004). These DC calculations, although based on typical wetting and drying rates of relatively deep upland fuels (Lawson and Armitage, 2008) and regarded as general estimates, can be important predictors for fire managers immediately following snowmelt, especially when additional soil moisture information is lacking. Given the large moisture deficits that can develop in deeper upland organic layers, the DC is overwintered to incorporate the effect of fall DC and winter precipitation into the next year's starting value. Overwintering calculations generally include estimates of total winter precipitation from nearby climate stations, along with two estimated coefficients, which include a carry–over effect to adjust for antecedent (fall) moisture conditions, and the wetting–efficiency fraction of the snowpack to the specific soil layer

(Lawson and Armitage, 2008). These coefficients, however, can be ignored if direct measurements of recharge into forest soils are available.

During the spring of 2016, the ~590 000 ha Horse River wildfire spread into the city of Fort McMurray and subsequently advanced across the boreal mosaic of mixedwood uplands and peatlands. The destructive nature of the Horse River wildfire, specifically the imminent threat to nearby inhabitants causing widespread evacuation (MNP, 2017) and the subsequent 3.58 billion (CAD) of direct insurance and infrastructure losses that resulted (IBC, 2016), motivated the investigation of the hydrological and meteorological conditions that led up to the fire. Currently, it is unknown if the exceptionally warm and dry conditions were also manifested by significant moisture deficits in the peatland watersheds surrounding the community. This study provides a useful means of explaining why watersheds in the region are especially vulnerable to wildfire in the early spring and how management agencies can better detect these early moisture signals that are a potential indicator of future high–intensity spring wildfires.

We capitalize on an opportunity to explore pre–fire hydrometeorological data obtained from "Poplar Fen" from 2011 to 2016, which is an instrumented moderate–rich fen watershed that burned on 17 May 2016. Some of the data presented in this paper were expanded from data and ideas presented in chapters 2 (fen chapter) and 4 (margin chapter). The specific objectives of this research are: (1) to use a combination of historical climate and field hydrological data to characterize the hydrometeorological conditions preceding the burning of a moderate–rich fen watershed to determine whether these conditions were outside the range of natural WBP climate cycles; (2) to use these hydrological data to explain the observed patterns in burn severity across the watershed; and (3) to identify whether hydrological data and hydrogeological setting parameters of the watershed can serve as indicators of deep smouldering and combustion risk.

3.2 Study Site

Situated within the Athabasca region of the Boreal Plains Ecozone (Ecoregions Working Group, 1989), Poplar Fen (56°56′ N, 111°32′ W; Fig. 3–1) is a ~2.5 km^2 treed moderate–rich fen watershed located 25 km north of Fort McMurray, Alberta (Fig. 3–1). This watershed is characterized by low relief topography (~10m), with undulating sand and gravel uplands and interconnected moderate–rich fens. Average annual air temperature (1981–2010) is 1°C; average

annual precipitation is 419 mm, with ~75% falling as rain (Environment Canada, 2017).

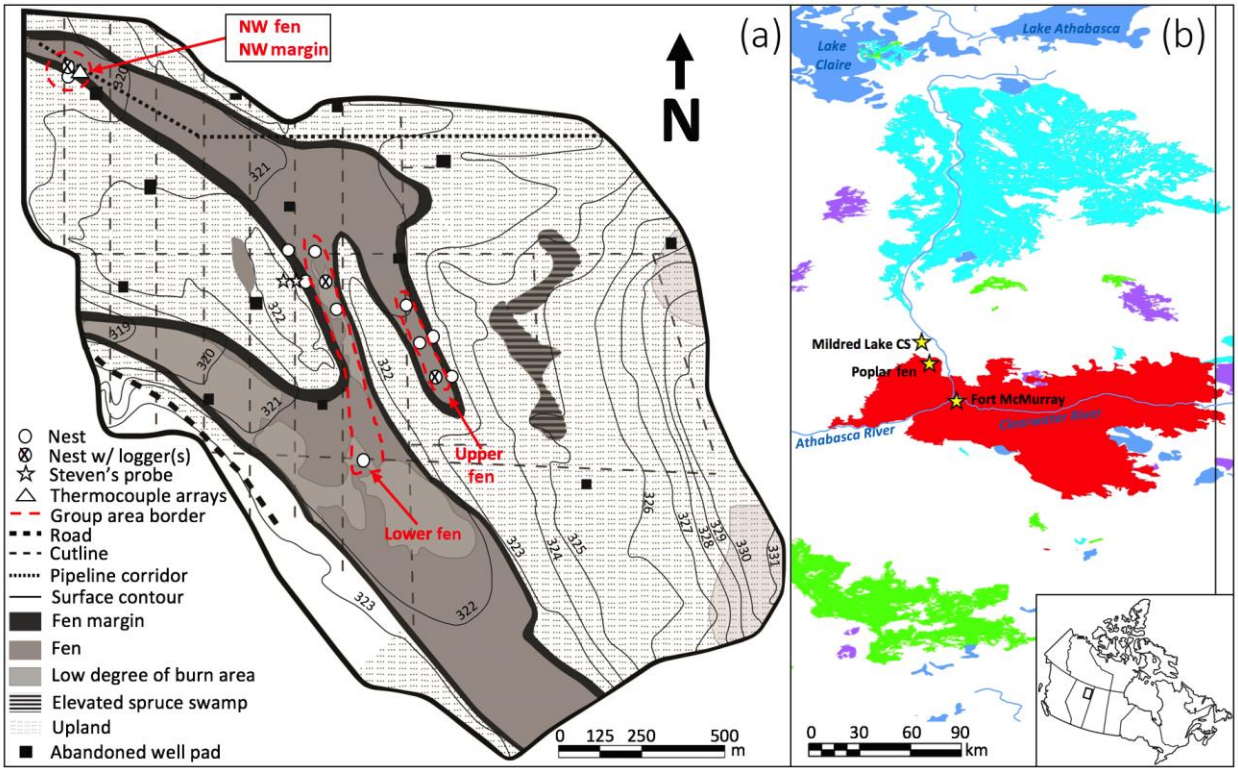

Figure 3–1. Map of the Poplar Fen watershed (**a**; 56°56′ N, 111°32′ W). The entire area was burned with the exception of areas highlighted in light grey. Included is an inset of northeastern boreal Alberta (**b**) showing the burned area during years of high spring fire frequency, including 1998 (purple), 2002 (green), 2011 (cyan), and 2016 (red).

The fen areas at Poplar Fen are underlain by thin (~10 cm) heterogeneous deposits of fine–grained silty sand of relatively low hydraulic conductivity that constrict recharge to an underlying outwash sand and gravel layer and favour saturated peat–forming conditions. Maximum peat depth ranges from 1.2–3.0 m, decreasing to <0.5 m along the margin tracts between fen and upland. Ground surface and water table elevations generally decrease from upland to margin to fen, as well as from southeast to northwest. Uplands are underlain by Brunisols in topographic highs and by Luvisols in riparian areas.

Tamarack (*Larix laricina*) and black spruce (*Picea mariana*) are the dominant tree species within moderate–rich fen areas, with a surface cover of the mosses *Tomenthypnum nitens*, *Aulacomnium palustre*, *Pleurozium schreberi*, and from the genus *Sphagnum* (*S. fuscum* and *S. capillifolium*). Margins are characterized by a sparse *P. mariana* overstorey, with *S. fuscum* and the feather mosses *Hylocomium splendens* and *P. schreberi*. Upland areas are dominated by *P.*

mariana and feather mosses in riparian zones, with jack pine (*Pinus banksiana*) and aspen (*Populus tremuloides*) mixedwood overstorey and lichen ground cover, in topographically higher areas.

3.3 Methodology

3.3.1 Historical data collection

A 20–year record of meteorological data was obtained from Alberta Agriculture and Forestry through the Alberta Climate and Information Service (Alberta Agriculture and Forestry, 2017). This included daily values of precipitation (rainfall and snowfall) and air temperature, which were estimated for the Poplar Fen area (township: T092R10W4) using an inverse-distance weighting interpolation procedure (IDW). Data from 2 to 7 stations were used for the IDW over the 20–year period with the nearest station (Mildred Lake; Fig. 3–1) located ~12 km from Poplar Fen. Rainfall and snowfall were totaled for every hydrological year (1 October–30 September). Additional average daily wind speed and relative humidity values were obtained from the Mildred Lake climate station for the 2015–2016 winter and early spring (Alberta Agriculture and Forestry, 2017). A 7–year record of snow–water equivalent (SWE), the depth of water contained within the snowpack, was also obtained from a snow pillow located at Gordon Lake, ~70 km from Poplar Fen (Alberta Environment and Parks, personal communication). This record provided information on SWE accumulation/ablation as well as peak SWE prior to snowmelt from October 2009 to April 2016. Snow–free conditions were estimated for each year by identifying the day when <20 % of the snow mass was remaining.

3.3.2 Field data collection

Hydrological data were collected between 2011 and 2016. Initial instrumentation included a water table monitoring well in a fen area (NW fen), located in the northwest section of the watershed, and a well in the adjacent margin area (NW margin), located ~140 m south of the fen well (Fig. 3–1) and ~0.65 m higher in elevation. The NW fen water table was monitored from June 2011 to May 2016 using either a logging pressure transducer (from 2011 to 2012; Schlumberger Mini–Diver) or a capacitance water level recorder (from 2013 to 2016; Odyssey Dataflow Systems Ltd.). In spring 2015, additional groundwater monitoring focused on two fen areas located at contrasting low (lower) and high (upper) topographic elevations, which varied by ~0.7 m (Fig. 3–

1). Groundwater monitoring nests were installed in the lower (n = 4) and upper (n = 3) fen areas and adjacent margins (n = 4) (Fig. 3–1). Screened wells and piezometers (20 cm screened intake) were constructed from PVC (2.5 cm I.D.) pipe and installed into the different substrates in grouped nests. Nests typically comprised a fully slotted well, with piezometers installed in mid–peat (0.6–0.75m depth) and underlying mineral substrate (1.25–1.85 m depth). Logging pressure transducers were installed in a well and in a piezometer situated in the underlying mineral layer, for one nest each in the lower and upper areas (Fig. 3–1). Nests were measured manually on a weekly basis between May and August 2015 and again in early October. Vertical hydraulic gradients were calculated between the water table and hydraulic head in the underlying mineral layer for each nest in the lower and upper fen areas using standard methods (Freeze and Cherry, 1978). Fen ground temperatures were monitored within close proximity to the NW fen well between fall 2012 and summer 2016 using two thermocouple arrays, buried at 0.1 and 0.2 m depth below surface. Temperatures were logged half–hourly and daily averages were calculated for each depth.

Precipitation was measured in an open area of the site with a logging Onset RG3–M tipping bucket rain gauge; missing daily totals (October–May) were supplemented with interpolated rainfall data for the Poplar Fen area (Alberta Agriculture and Forestry, 2017). Between 21 March and 19 April 2016, snow surveys were conducted using a Meteorological Service of Canada (MSC) snow tube. Measurements of snow depth were taken at 178 locations, ~10 m apart along a zigzag transect that extended through all major land classes for Poplar Fen (Fig. 3–1). SWE was recorded every ~20 m. Peak SWE was represented by the first snow survey on 21 March 2016 and an area–weighted SWE contribution for each land class was estimated from the proportional area for each respective class.

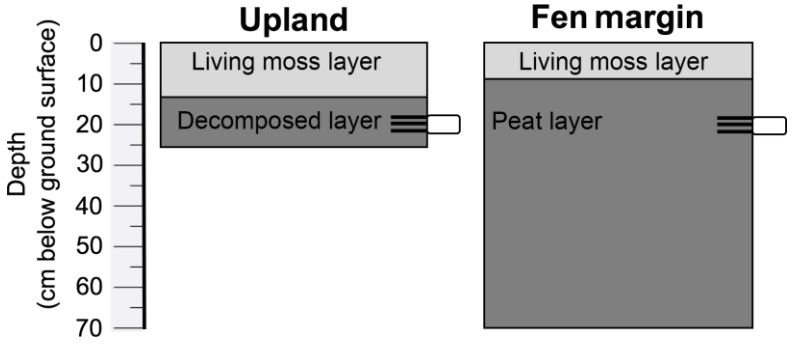

Figure 3–2. Moisture probe profiles in upland duff and fen margin peat.

Volumetric water content (VWC) was recorded half–hourly from June 2015 to May 2016 in upland duff and margin peat soils with arrays of Stevens Hydra Probe II (Figs. 3–1, 3–2). Two weeks of data (2–17 May 2016) could not be salvaged due to fire damage to the logger. The probes were calibrated in the laboratory to the respective soil types.

3.3.3 Drought Code

The Drought Code (DC) was calculated using the "cffdrs" package in the R statistical program (R Core Team, 2016) for the 2015 growing season using data obtained from the Mildred Lake climate station (Alberta Agriculture and Forestry, 2017). This included noon measurements of air temperature and cumulative precipitation from the previous 24 h. The DC was started on 12 April 2015, following 3 days of noon temperatures of 10°C or higher, using default presets, including a starting DC of 15. The starting DC becomes less imperative over a fire season as it will be corrected after sufficient rainfall (Alexander, 1982). Thus, an overwintering procedure is essential for improving accuracy predominantly in the early months of a fire season. The DC was run until 31 October 2015 (a standardized end date) and the code then overwintered for spring 2016 using a range of different approaches following methods outlined by Van Wagner (1987). The startup moisture equivalent (Q_S) of the DC was determined by Eq. (3–1):

$$Q_S = aQ_f + b(3.94r_w), \quad (3–1)$$

where Q_f is the moisture equivalent of the DC on October 31, 2015; r_w is total winter precipitation (mm); and a and b are coefficients chosen to estimate the carry–over fraction of last fall's moisture and estimate the fraction of snowmelt retained in the duff layer, respectively. Q_f is calculated by Eq. (3–2):

$$Q_f = 800 \exp(-DC_f/400), \quad (3–2)$$

where DC_f is the final DC value on 31 October 2015. The startup DC value can then be calculated from Eq. (3–3):

$$DC_S = 400 \ln(800/Q_S), \quad (3–3)$$

The values for a and b in Eq. (3–1) are typically determined by provincial fire management

agencies (Lawson and Armitage, 2008). Though organic soil moisture data are available in this instance, in this study we examine both the observed soil moisture data and the variations on DC start and overwinter values using less detailed information to compare predictions of organic soil moisture at the time of the fire made without the benefit of in situ observations.

Startup and overwinter upland duff DC were calculated four different ways (Table 3–1), each reflecting specific information of the hydrometeorological environment. For scenario 1, startup DC was estimated for the upland duff from a linear regression between DC and measured duff VWC from 27 June to 31 October 2015 and calculated based on the starting VWC for 19 April. Scenarios 2–4 were then calculated with the overwintering procedure (Eqs. 3–1, 3–2, and 3–3). For scenario 2, the startup DC was calculated using total winter precipitation values obtained from the Fort McMurray airport climate station and default carry–over and wetting–efficiency values (0.75) from the cffdrs package (Lawson and Armitage, 2008). For scenario 3, the startup DC was calculated from peak SWE data from snow survey data of Poplar Fen and carry–over (0.5) and wetting–efficiency (1.0) values used by Alberta Agriculture and Forestry. Scenario 4 applied the directly measured duff recharge (a mm value input, inferred from the upland duff site moisture probe) to the overwintering procedure, which eliminated the need for a precipitation value as well as estimates of carry–over and wetting efficiency. Following these methods, four differing startup DC values were generated for the upland duff. The DC was then calculated four times, corresponding to each startup DC value, starting on 19 April and were ran until 17 May 2016.

Table 3–1: Summary of scenarios used for calculating a starting DC for April 19, 2016.

Scenario #	**Carry–over *a***	**Wetting–efficiency *b***
1) Expected DC values based on observed relationship between 2015 VWC and DC.	N/A	N/A
2) Overwintering procedure with default CFFDRS values (Lawson and Armitage, 2008) using precipitation from Fort McMurray airport.	0.75	0.75
3) Overwintering procedure with Alberta Agriculture and Forestry values with Poplar Fen manual SWE data.	0.5	1
4) Overwintering procedure with upland duff: Using measured 32 mm snowmelt recharge (Oct. 31 – Apr. 19).	1	1

3.3.4 Burn depth and fuel consumption

Measurements of burn consumption of organic soils were made in fen, margin, and upland areas that burned using differential GPS (Leica GS14 GNSS) survey data obtained pre– (October 2015) and post–fire (October 2016) from well–inferred surface (elevation of PVC top minus distance to ground surface) elevations; the difference between soil surface elevations at piezometer nests were compared between pre– and post–fire. This included nests from Poplar Fen in addition (5 fen, 5 margin, and 10 upland nests) to those identified in Fig. 3–1 (not shown). Average vertical elevation (surface) change was calculated for each nest location. Depth changes were averaged for burned fen, margin, and upland organic soils, and these depths were multiplied by previously measured average bulk density values for each soil type to estimate terrestrial fuel loss.

3.4 Results

3.4.1 Hydrometeorology

Precipitation observations from 1996 to 2016 interpolated for Poplar Fen averaged 380 ± 17(SE) mm total precipitation with 284 ± 15 mm falling as rain and 96 ± 6 mm as snow (Table 3–2). For the 4 hydrologic years of high burned area in the spring, total winter snowfall was below average for all years except for 1997–1998. The lowest total snowfall was measured in hydrologic years 1998–1999, 1999–2000, and 2008–2009 – all years with low burned area in the spring. Peak SWE from the Gordon Lake snow pillow from 2009 to 2016 (Fig. 3–3) averaged 120 ± 10 mm. Peak SWE prior to snowmelt in hydrological years 2010–2011 and 2015–2016 was not especially low, and, despite the modest SWE available for melt, the snow–free day of the year (80 % of peak SWE melted) during these years was not significantly earlier than the other 5 years on record. Total rainfall was below average in only 2 (1997–1998 and 2010–2011) of the 4 hydrological years with large spring burned areas; the bulk of precipitation occurred in the summer for all 4 years (Table 3–2). Cumulative post–melt rainfall until 15 May averaged 25.5 ± 3.3(SE) mm between 1997 and 2016 (Fig. 3–3). A total of 3 of 4 hydrological years with high burned area in the spring were below the 20–year average rainfall, with 2001–2002 being the lowest and 1997–1998 just above average. In 2015–2016, only 8.5 mm of rain fell following snowmelt prior to ignition of the Horse River wildfire, and only 0.3 mm fell over the next 2 weeks leading up to the burning of the Poplar Fen watershed (Fig. 3–3). The hydrological year with the lowest early spring cumulative

rainfall in the 20–year record was 2007–2008 (1 mm), which was a year of low burned area in the spring (Natural Resources Canada, 2018). However, during this year a total of 151 mm of snow fell in the area, which is 55 mm more than the 20–year average (Table 3–2), and snow–free conditions were not reached until 30 April.

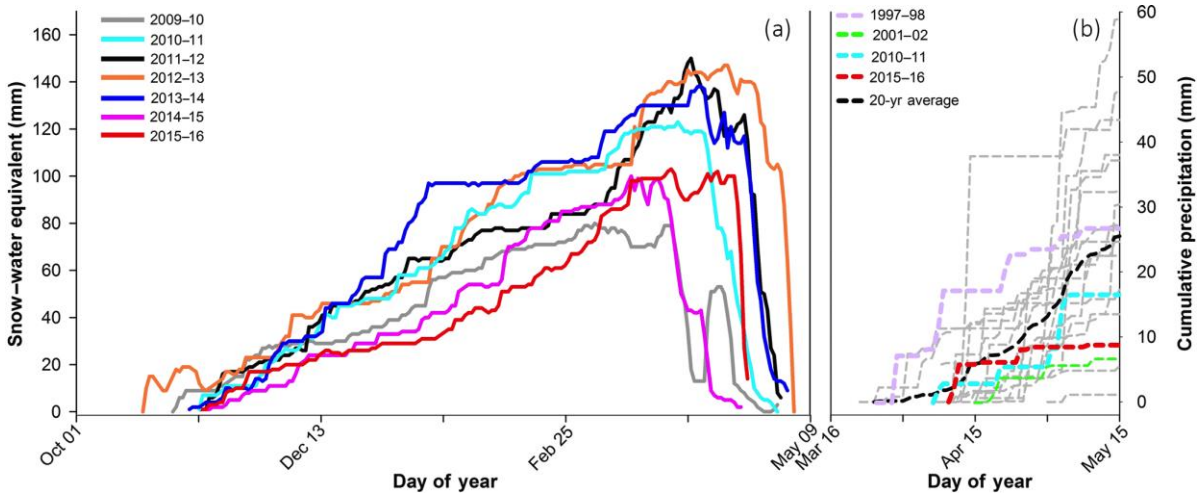

Figure 3–3. Measured accumulation and ablation of SWE at Gordon Lake snow pillow (**a**), and interpolated cumulative early spring rainfall from 1996 and 2016 at Poplar Fen (**b**). Coloured lines in graph (**b**) correspond to years of high burned area in the spring, including 1997–1998 (726 968 ha), 2001–2002 (496 515 ha), 2010–2011 (806 055 ha), and 2015–2016 (663 529 ha) (Natural Resources Canada, 2018).

Table 3–2: Total hydrological year rainfall and snowfall from 1996–2016, interpolated for the Poplar Fen area. Asterisks correspond to years of high burned area in the spring.

Year	Total	Rain	Snow
1996–97	467	354	114
1997–98*	265	156	109
1998–99	280	227	53
1999–20	395	331	64
2000–01	356	277	79
2001–02*	396	322	75
2002–03	424	306	118
2003–04	396	286	110
2004–05	523	385	138
2005–06	409	303	106
2006–07	352	215	137
2007–08	387	235	151
2008–09	269	210	58
2009–10	421	330	90
2010–11*	235	156	78
2011–12	430	343	88
2012–13	481	373	109
2013–14	375	298	77
2014–15	326	235	91
2015–16*	412	329	82

Over the 2015–2016 winter (mid–October–mid–April), average air temperatures were −6.5°C, which is 2.9°C warmer than for the previous 19–hydrological–year (1996–2015) average (−9.4°C). Periodic warm spells were observed in late January and February, when air temperatures rose above freezing for several consecutive days (Fig. 3–4a). Manual snow measurements yielded

an area–weighted average peak SWE of 105 mm (Fig. 3–4d) on 21 March 2016, which is 2 mm higher than the peak measured at the Gordon Lake snow pillow. In spring 2016, the primary snowmelt period occurred between 21 March and 19 April. Air temperatures did not deviate far from the 20–year normal during this time, with the exception of 27–30 March, when daily maximum air temperatures in the area rose to over 9°C. The strongest deviation prior to the fire was measured following snowmelt when maximum daily air temperatures reached 27 and 33°C in April and May, respectively. At this time, average daily relative humidity decreased (Fig. 3–4b) and average daily wind speeds exceeded 20 km hr^{-1} prior to the fire's ignition (Fig. 3–4c).

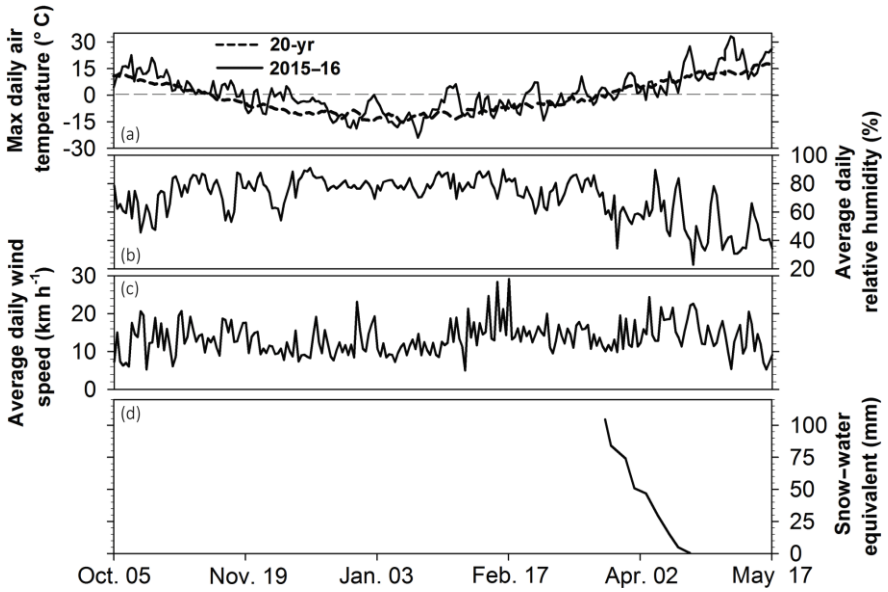

Figure 3–4. Daily records of (**a**) maximum air temperature (with 20–year average), (**b**) average daily relative humidity, and (**c**) average daily wind speed at Mildred Lake climate station from 5 October 2015 to 17 May 2016, and (**d**) measured area–weighted SWE for Poplar Fen in 2016.

3.4.2 Hydrology

The NW fen (Fig. 3–1) water table range was ~0.79 m (+0.12 m to −0.66 m) between 8 June 2011 and 17 May 2016 (Fig. 3–5). Average NW margin water table was 0.32 m lower than NW fen between 2011 and 2015. Both NW fen and margin exhibited relatively low water tables (dry conditions) at the beginning, increased water table in the middle years (wetter conditions), and lower water tables in a drying period towards the end of the 5–year record. The late fall and early spring NW fen water table was near or above ground surface in hydrological years 2012–2013 and 2013–2014 (Fig. 3–5), which corresponded to delayed ground thawing at 0.1 and 0.2 m peat depths until mid–May. Conversely, the year 2014–2015 water table was ~0.2 m b.g.s. (below

ground surface) in the fall and at the surface in the early spring, which began to decline rapidly in June (Fig. 3–5). This hydrological year corresponded with delayed ground thawing until mid–May at only 0.2 m peat depth. Furthermore, between 2011 and 2015, NW fen water table underwent periods of decline over the summer in all years except 2013. By early fall, the NW fen water table in all 5 years reached an annual low and, in 2012–2014, rose in the late fall prior to freeze–up. Conversely, rainfall was not sufficient in 2011 and 2015 to raise the fall NW fen water table above the low levels observed in the summer (Fig. 3–5).

The 2015–2016 hydrological year began with water levels that were among the lowest in the 6–year record (Fig. 3–5). By the end of winter, all manually surveyed fen monitoring wells were empty of water (water tables >0.8 m b.g.s.). The comparison of fall 2015 logged water levels to manual winter 2016 observations (before snowmelt recharge and before pressure transducers were installed for the 2016 field season) evidenced an additional 0.12–0.26 m water table decrease, demonstrating mid–winter water table decline and drying of overlying peat substrate. Ground thawing at 0.1–0.2 m depth occurred in mid–April (earlier than 2013–2015) toward the end of snowmelt, and at this time (16 April 2016) the NW fen water table had increased to 0.67m b.g.s. The remaining snowmelt period initiated a water table rise of 0.46 to 0.21 m b.g.s. on 3 May which then decreased in the total absence of rainfall to 31 cm b.g.s on 17 May, the day that the Poplar Fen area burned over (Fig. 3–5).

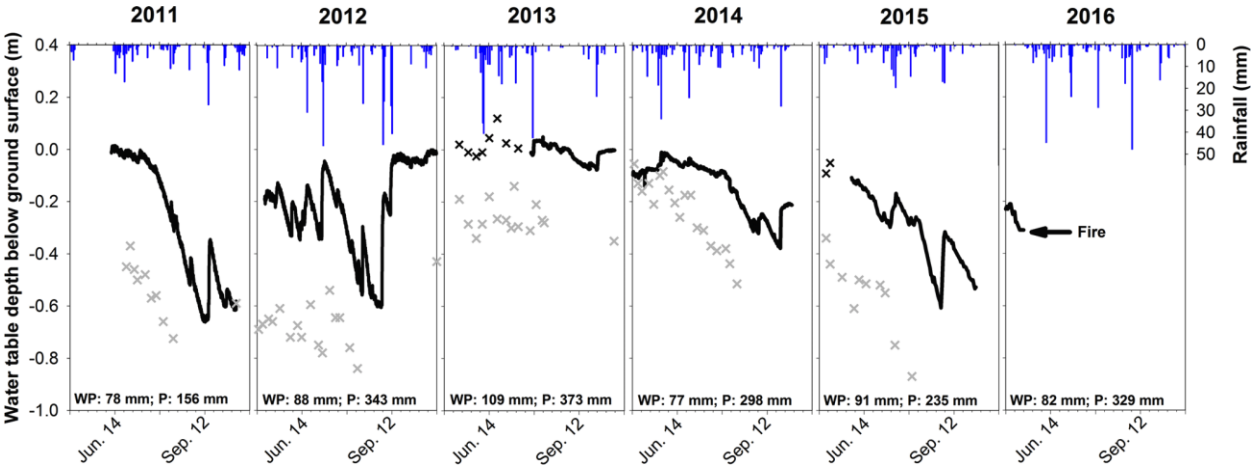

Figure 3–5. Logged (lines) and manually ("x" symbols) recorded water table position at NW fen (black) and NW margin (grey) (see Fig. 1), from 2011 to 2016, with field–measured rainfall (P), and total winter precipitation (WP) interpolated for the Poplar Fen area.

To examine how fen areas of varying topographic position were wetting and drying over the 2015 growing season, water table and hydraulic gradients were compared between the

contrasting upper and lower fen areas (Fig. 3–6). Average water table depth below surface differed by 0.05 m between upper (0.22 ± 0.05 (SD) m) and lower (0.17 ± 0.04 (SD) m) fen nests. In both areas, the hydraulic head in underlying mineral layers mirrored the water table profile (Fig. 3–6). Vertical hydraulic gradients (a metric of groundwater recharge–discharge) in both upper and lower fen areas were strongest when water tables were highest and weakened (less groundwater recharge to the fen) during periods when rainfall was less abundant. Throughout the entire monitored period, the lower fen nests had the strongest average hydraulic gradients (0.021 ± 0.008(SE)), showing groundwater discharge that remained positive throughout the measurement period. Conversely, upper fen nests had weaker hydraulic gradients (−0.007 ± 0.004(SE)), which experienced flow reversals (downward), and were negative throughout most of the year. Margin areas exhibited the lowest water tables, as well as hydraulic gradients (−0.03 ± 0.03(SE)) (recharge), over the 2015 growing season (Fig. 3–6).

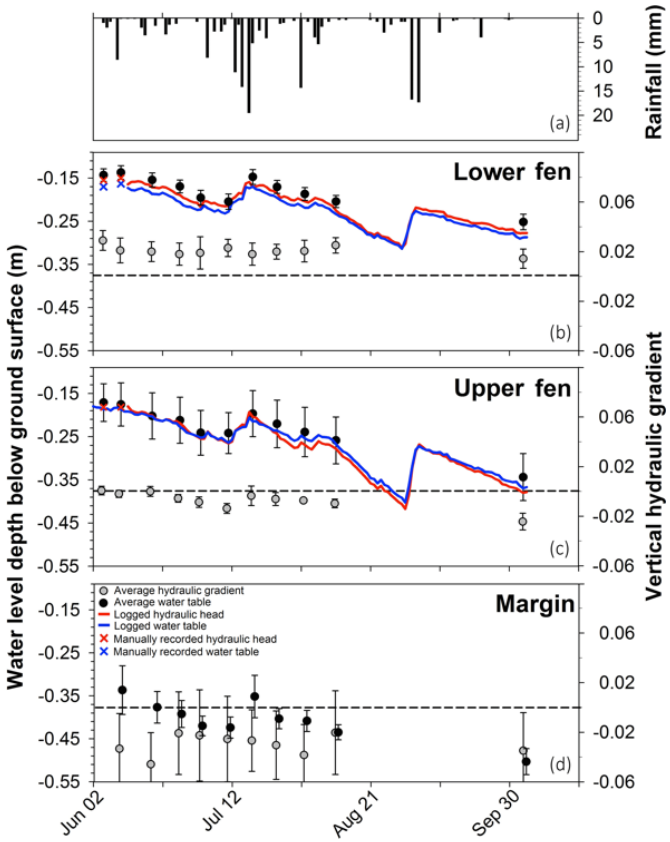

Figure 3–6. Average (SE) water table (black circles) and vertical hydraulic gradient (grey circle) between the water table and underlying mineral substrate for lower and upper fen, and margin areas, along with logged (line) and manually recorded ("x" symbol) water table (blue) and hydraulic head (red) for lower and upper fen areas in 2015. A negative hydraulic represents a loss of water from the fen to the underlying mineral substrates. Rainfall is also illustrated.

Between June and October 2015, duff and margin peat VWC (both at ~0.2m b.g.s.) averaged 0.33 and 0.41 m^3 m^{-3}, respectively, with a higher coefficient of variation for duff (0.21) compared to margin (0.06) peat (Fig. 3–7). The duff experienced extended drying periods in the summer–fall and, by freeze–up, reached the minimum VWC for 2015 (0.24 m^3 m^{-3}). Margin peat VWC had also reached a minimum by fall (0.39 m^3 m^{-3}); however, values were similar to late spring 2015 VWC (~0.42 m^3 m^{-3}). During winter 2015–2016 (31 October–21 March), VWC in the duff and margin peat decreased an additional 0.06 and 0.03 m^3 m^{-3}, respectively, and, following snowmelt, increased from 0.19 to 0.32 m^3 m^{-3} and 0.36 to 0.38 m^3 m^{-3}, respectively. Two weeks prior to the Horse river wildfire, upland duff and margin peat VWC were 0.31 and 0.37 m^3 m^{-3}, respectively (Fig. 3–7), and likely continued to decrease prior to the fire in the absence of rainfall.

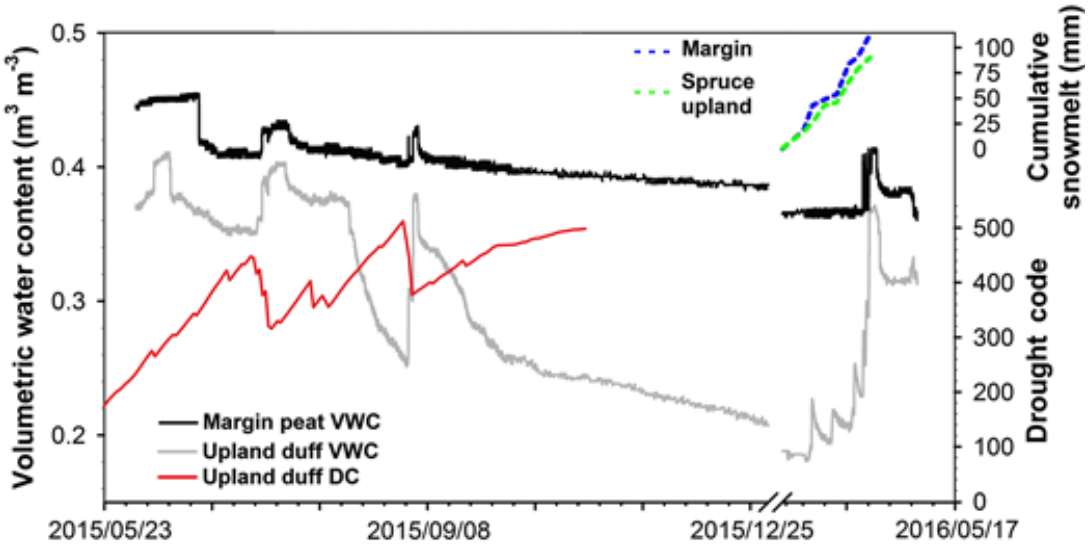

Figure 3–7. Volumetric water content (m^3 m^{-3}) for upland duff and margin peat from 2 June 2015 to 2 May 2016, including with average 2016 snowmelt recharge (mm) for upland and margin, and Drought Code from May to October 2015.

3.4.3 Drought Code

Following the first month of startup in 2015, the DC illustrated an inverse relationship with upland duff VWC ($r = -0.94$; $p<0.001$) (Fig. 3–7); the dry conditions caused DC to increase from 18 to 496, between 12 April and 31 October. VWC on 31 October and the corresponding DC were chosen to represent the final fall moisture and DC equivalent values for the various overwintering DC calculations. The overwintering period ran from 31 October 2015 to 19 April 2016, the day following 3 consecutive days with noon air temperatures ≥12°C. For scenario 1, the 2016 spring startup DC was predicted based on the relationship between upland duff DC and VWC in 2015,

and a 2016 spring startup DC of 357 was estimated given a starting soil moisture of 0.37 m^3 m^{-3} (Fig. 3–7). Scenarios 2 and 3 produced startup values using the overwintering procedure with standard carry–over and wetting–efficiency coefficients, resulting in startup DCs of 242 and 212, respectively. Scenario 4 used the overwintering procedure with no precipitation values or default coefficients, but rather with directly measured duff recharge from 31 October to 19 April. Snowmelt increased duff VWC by 0.13 m^3 m^{-3} in the ~0.25m thick soil horizon, resulting in 32 mm of recharge (35% of estimated upland snowfall), yielding a startup DC of 321. DC was then calculated from 19 April to 17 May 2016, and all starting DCs increased 131 units over that time period (Table 3–3).

Table 3–3. The 19 April 2016 startup and final 17 May DCs for Poplar Fen using four different scenarios.

Scenario #	***Carry–over a***	***Wetting–efficiency b***	**Starting DC on April 19, 2016**	**Final DC on May 17, 2016**
1) Expected DC values based on observed relationship between 2015 VWC and DC	N/A	N/A	357	488
2) Overwintering procedure with default CFFDRS values (Lawson and Armitage, 2008) using precipitation from Fort McMurray airport	0.75	0.75	242	373
3) Overwintering procedure with Alberta Agriculture and Forestry values with Poplar Fen manual SWE data	0.5	1	212	344
4) Overwintering procedure with upland duff: Using measured 32 mm snowmelt recharge (Oct. 31 – Apr. 19)	1	1	321	452

3.4.4 Burn depth and fuel consumption

The greatest depth of burn was measured in the margins (0.13 ± 0.01 m) with lower (0.10 ± 0.02 m) burn depths measured at upland locations (Table 3–4). Burn depth values in burned fen areas were 78–83% lower than margin and upland areas. Estimated fuel consumption rates (depth of burn × average bulk density) generally echoed the trends in surface change with slight differences due to higher bulk density measured in margin peat. No surface changes or fuel consumption were observed in the lower fen area.

Table 3–4: Average (± SE) surface change and fuel consumption in upland, margin, and fen at Poplar Fen.

Type	Measured Ground Surface Change (m)	Pre–Burn Bulk Density (kg m^{-3})	Estimated Fuel Consumption (kg m^{-2})
Duff	0.10±0.02	70	7.0±1.2
Margin	0.13±0.01	98	13.0±1.2
Fen (burned)	0.02±0.002	70	1.6±0.06
Fen (unburned)	0	70	0

3.5 Discussion

3.5.1 Pre–fire meteorology

Within the Boreal Plain region of northeastern Alberta, average precipitation is less than potential evapotranspiration in most years (Bothe and Abraham, 1993). Consequently, water deficits are common in the WBP, relying on infrequent wet periods every 10–15 years to replenish storage deficits (Marshall et al., 1999; Devito et al., 2005). Historical precipitation data illustrate that rain and snow patterns are variable in the WPB (Table 3–2; Fig. 3–3). Total snowfall was near or below average in years during which spring wildfires burned large areas. Although modest snowfalls are a recurring influence, they do not necessarily dictate fire magnitude; a total of 5 years with spring wildfires of low burn area were identified, possessing similar (or lower) total snowfall values than large spring burn area years (Table 3–2). Earlier snowmelt can extend the dry WBP spring and drying of organic soils, which could therefore extend the period over which spring fires can be generated (Westerling et al., 2006). However, the timing of snowmelt in the WBP does not appear expedited in years of large burned area in the spring, with no significant patterns in the timing of snow–free conditions observed in the 7–year Gordon Lake snow pillow record (Fig. 3–3). However, years of high total annual snowfall all align with years with low burned area in the spring (Table 3–2). This suggests that large SWE can contribute to decreasing the total annual area burned in the spring. Low and infrequent early precipitation events occurred in 3 of 4 years with high burned area in the spring. However, due a large proportion of rainfall in continental western Canada generally occurring in summer (Smerdon et al., 2005), dry early spring is not exceptional and not restricted to years of high burned area in the spring. The year with the lowest early spring

cumulative rainfall in the 20–year record was 2008; however, above–average snowfall and late snow–free conditions decreased wildfire susceptibility in the spring, further demonstrating the importance of a large snowmelt for reducing wildfire vulnerability (CFRC, 2001).

The 2015–2016 hydrological year experienced the second warmest winter temperatures over the past 20 years. Periodic rises in air temperature above freezing conditions throughout the winter (Fig. 3–4a) supplied energy for mid–winter snowmelt and sublimation (Pomeroy et al., 1998), potentially decreasing available peak SWE for the spring snowmelt period. The modest snowpack melted over a 31–day period. Immediately following snowmelt, high air temperatures, low relative humidity, and high wind speeds (Fig. 3–4b and c) created weather conditions optimal for the spread of wildfire (Van Wagner, 1977). Similar mild winter temperatures and warm, dry spring conditions were present in previous years of high spring time burned area in 1968, 1998, 2002, and 2011. These years produced fires of a similar magnitude and total area burned to the Horse River wildfire of 2016 (Hirsch and de Groot, 1999; Tymstra et al., 2005; FTCWRC, 2012).

3.5.2 Pre–fire hydrology

A 5–year (2011–2016) water table record illustrated the susceptibility of Poplar Fen to extended drying periods, with years of high spring (2011 and 2016) and summer (2015) burned area corresponding with low water table position (Fig. 3–5). At Poplar Fen, water tables also decreased over winter periods in the absence of precipitation–driven recharge. These prolonged periods of water table decline were evidenced by logged water table and mineral piezometer observations from the lower and upper fen areas (Fig. 3–6). In these areas, the hydraulic head in the underlying mineral substratum (~1.5 m b.g.s.) closely mimicked the pattern of the water table, suggesting that the underlying groundwater at Poplar Fen is derived mostly from local recharge, rather than from regional groundwater, which would have a more stable hydraulic head (Siegel and Glaser, 1987). Therefore, peatlands that are supplied mainly by local groundwater (such as Poplar Fen) become particularly vulnerable to wildfire during high–risk fire weather conditions (Lukenbach et al., 2017).

Spring NW fen water table position was also related to the persistence of a frozen upper saturated zone. For example, near–surface water tables in fall of 2012 and 2013 (Fig. 3–5) allowed for relatively homogenous overwinter freezing of the upper saturated zone (Price, 1983), which

reduced the permeability of the peat (Roulet and Woo, 1986; Quinton et al., 2009) and helped store subsurface water over the winter periods (Price and FitzGibbon, 1987). Ground ice persisted into mid–late May in 2013 and 2014, thus limiting snowmelt water infiltration (Roulet and Woo, 1986) and subsurface water loss to the underlying silty sand and outwash layers (Price and FitzGibbon, 1987). Conversely, the shallow (0–0.2 m) peat had reached above freezing temperatures by the end of snowmelt (mid–April) in 2016, suggesting that low (~0.55 m b.g.s.) fall 2015 water tables had prevented the near–surface ground ice. Consequently, the entire saturated zone was free to recharge the underlying mineral layers over the 2015–2016 winter, and meltwater infiltrated readily (during the 2016 snowmelt period) to recharge the relatively deep water table. Thus, high antecedent fen water levels provide an important mechanism for overwinter storage and maintaining higher spring water levels.

Post–snowmelt 2016, the NW fen water table (0.3 m b.g.s.) was ~0.3m lower than the water table observed mid–June 2011 (Fig. 3–5), a period without rainfall and with high burned area in the spring when the 2011 Richardson Fire reached a size similar to the Horse River wildfire (Pinno et al., 2013). Surprisingly, spring 2016 water tables were more comparable to levels measured in the spring of 2012 (Fig. 3–5), a year of low burned area in the spring. The lower burned area was likely attributed to larger and more frequent rainfall events (an additional 14 mm) recorded in the region during the 2012 spring season. Peatland water table position, therefore, likely cannot serve as a stand–alone metric for estimating fen wildfire susceptibility in the region without considering the moisture deficits that can accumulate above the water table in the absence of precipitation.

Soil moisture in upland duff and margin peat followed a drying trend throughout 2015. Following snowmelt in 2016, water contents in the upland duff and margin peat were not sufficiently higher than values observed in fall of 2015 (Fig. 3–7). These data suggest that there was no net wetting to the organic near–surface soils in the upland or margins at Poplar Fen from snowmelt infiltration. This soil moisture deficit was further enhanced by the lack of spring precipitation and increased evaporative demand (Hayward and Clymo, 1983) driven by the low humidity, high temperatures, and winds at the time of the Horse River wildfire (Fig. 3–4). This deficit would have increased the available fuels for the wildfire allowing for significant combustion of these organic layers (Table 3–4).

3.5.3 Assessing the hydrometeorological conditions preceding the Horse River wildfire and burning of Poplar Fen

The historical meteorological and field hydrological data illustrate the susceptibility of regionally abundant WBP peatland watersheds to wildfire during extended dry periods. Results suggest that the wildfire at Poplar Fen, and the greater Horse River wildfire, was not simply a consequence of anomalous drought climate conditions, but rather interconnected hydrometeorological factors not uncommon to the Western Boreal Plain, occurring at least twice in the 5–year instrument record. These factors included low autumn soil moisture and water tables, modest snowfall, overwinter drainage, insufficient spring rainfall, and high spring air temperatures and winds. The synchronicity of these factors, occurring in the same hydrological year, combined with mature tree stands with high accumulated fuels ubiquitous to the region, likely contributed to the large magnitude Horse River wildfire. The similarities of the hydrometeorological events preceding the Horse River wildfire with previous years (1968, 1998, 2002, and 2011) of similar burned area in the spring (Hirsch and de Groot, 1999; Tymstra et al., 2005; FTCWRC, 2012) suggest that the mild and/or dry fall, winter, and spring conditions conducive for spring fire occur frequently in the region with a recent recurrence interval of 5 years. Moreover, conditions favouring spring wildfire may be enhanced by climate change, given the responsiveness of forest fuel moisture to changes in temperature and precipitation (Weber and Flannigan, 1997; Flannigan et al., 2016).

3.5.4 Differences in burn severity within Poplar Fen

During summer 2015, vertical hydraulic gradients decreased in all fen and margin wells over periods of low precipitation. In lower fen these remained positive throughout the 2015 sampling period (Fig. 3–6), indicating upward groundwater discharge into the basal peat (water gain to peatland) from the underlying silty sand and outwash layers. In upper fen regions, these values were always lower and eventually became negative over time in the absence of rainfall, suggesting a flow reversal (downward) and loss of water from the basal peat to the underlying silt layer. Margin areas, located at a higher topographic position between fen and upland, exhibited the strongest negative hydraulic gradients, suggesting that these areas were recharging the underlying mineral layers throughout the entire year. These subtle differences in topographic

position therefore played a large role in the observed differences in burn severity between these areas (Table 3–4). Hence, treed headwater moderate–rich fens and fen margin tracts in the WBP may be particularly vulnerable to wildfire.

3.5.5 Soil moisture: an early indicator of spring wildfire danger

The 2015 moisture conditions observed in the upland duff of Poplar Fen were represented reasonably well with the DC. The DC was overwintered for 2016 using a range of startup values from different methods (Table 3–3). Scenarios 2 and 3 produced DCs that were lower than the expected DC (scenario 1), since carry–over and wetting–efficiency coefficients overestimated the recharge to the duff layer by 15–21%. These default coefficients may not have accounted for the high sublimation rates caused by low relative humidity and high solar radiation, common to the western boreal forests of Canada (Burles and Boon, 2011). The lower recharge values measured at Poplar Fen (35% of melt water) may also be due to moisture deficits that accumulated since the summer of 2015, as a high proportion of the available meltwater went towards recharging the unsaturated mineral soil underlying the duff. The startup DC that was calculated using the directly measured duff recharge (scenario 4) was much closer to the expected DC, suggesting that the overwintering calculation is suitable for the duff layer at Poplar Fen when VWC is directly measured.

Due to differences in soil bulk density and depth of burn, average duff fuel consumption was ~50% less than the consumption observed in margins (Table 3–4). The observed duff fuel consumption at Poplar Fen (~7.0 kg m^{-2}), along with the VWC–inferred expected (488) and overwintered (452) final duff DC values, were both in line with fuel consumption and DC estimates from interior Alaska (Kane et al., 2007) and are on the higher end of DCs measured from other burned boreal forest fires throughout continental western Canada (de Groot et al., 2009). Thus, the overwintering procedures that were calculated using default wetting–efficiency coefficients produced lower final DC values that did not reflect the fuel consumption rates measured at Poplar Fen. The observed range in overwintering DC calculations in Table 3 highlights the difficulties in determining a proper startup DC for watersheds that experience periods of prolonged drying prior to snowmelt. These overwintering calculations have a substantial impact on DC values calculated for the following growing season, predominantly in the early spring. Estimations based on VWC

measurements may therefore produce more accurate and conservative spring DC values, given that the selected coefficients may not properly represent the hydrological and meteorological processes occurring in the Western Boreal Plain during the snowmelt period.

3.4 Conclusions

This study applies a combination of pre–fire and historical hydrometeorological data from a moderate–rich fen watershed to contextualize the conditions preceding the 2016 Horse River wildfire. The fire was manifested by dry hydrometeorological conditions extending back to summer 2015. This included low fall soil moisture, modest snowfall, and no spring rainfall, with above–average spring air temperatures and high winds also prevalent – conditions not uncommon in the sub–humid WBP. It was ultimately the less frequent synchronization of these factors that led to a wildfire of this size and observed depth of burn in boreal forests and wetlands as well as the associated fuel losses. These coinciding hydrometeorological conditions share stark similarities with previous years with large burned areas from spring fires, namely 1968, 1998, 2002, and 2011, which may support the notion that fires of this magnitude are a function of WBP climate cycles. However, as natural as these factors may be, spring conditions conducive to wildfire could be enhanced by climate change, given the responsiveness of these boreal watersheds to changes in temperature and precipitation.

Field data from Poplar Fen confirmed that moisture deficits accumulated between summer 2015 and the Horse River wildfire the following spring. Following a relatively mild winter, the modest 2016 snowmelt did not raise upland duff and margin peat moisture above fall 2015 values. This was in part due to the hydrogeological setting of Poplar Fen, as water tables and hydraulic head decreased in the absence of localized precipitation–driven recharge from adjacent uplands, with no evidence of a regional groundwater connection to supplement discharge during extended dry periods. We propose that headwater peatlands in this region fed by localized flow systems will be particularly susceptible to water table fluctuations under a drying climate, rendering them more vulnerable to burning from wildfire.

The dry conditions and subsequent duff fuel consumption observed at Poplar Fen in the spring of 2016 were difficult to illustrate with the Drought Code when carry–over and wetting–efficiency coefficients were applied to the overwintering procedure. Closer agreement was found

when directly measured duff soil moisture recharge was applied to the overwintering procedure in place of the coefficients. In order to better gauge the susceptibility of WBP headwater systems to wildfire in the spring, management strategies could therefore benefit from monitoring soil moisture at different land classes and watersheds. These data would allow for more accurate overwintering DC calculations and would provide managers more time to prepare for a fire season by considering additional indicators that can be detected earlier.

3.5 Acknowledgements

The authors wish to thank C. Wells, G. Sutherland, D. Price, E. Kessel, and J. Asten for their assistance in the field. We gratefully acknowledge funding from a grant to Jonathan S. Price from the National Science and Engineering Research Council (NSERC) of the Canada Collaborative Research and Development Program, co–funded by Suncor Energy Inc., Imperial Oil Resources Limited, and Shell Canada Energy. The authors would additionally like to thank Ralph Wright at Alberta Agriculture and Forestry for help with obtaining historical data as well as Tom Schiks for comments on an earlier version of the manuscript.

4 The hydrologic role of fen margins in the low–relief Western Boreal Plain, northern Alberta, Canada, prior to, and following, wildfire

4.1 Introduction

In the sub–humid Western Boreal Plain (WBP), northern Alberta, wetlands are a dominant feature on the landscape, occurring primarily as peatlands (Vitt et al., 1996). These peatlands overlie a generally deep and heterogeneous surficial geology (Andriashek, 2003; Devito et al., 2012), resulting in complex groundwater interactions with surrounding mixedwood uplands and underlying aquifers (Bachu et al., 1993; Devito et al., 2005; Devito et al., 2012). This results in a wide range of peatland types, which range from ombrogenous bogs to geogenous and/or saline fens (Vitt et al., 1995; Wells et al., 2015a). The variability in form and hydrologic function is ultimately influenced by the hydrogeologic setting, which determines the degree of interaction between a peatland and surrounding landscape (Winter et al., 1999; 2001; Devito et al., 2005; 2012). There has been considerable research conducted on the hydrology of peatlands in the WBP (Ferone and Devito, 2004; Scarlett and Price, 2013; Lukenbach et al., 2015; Wells et al., 2015a; 2015b; Hokanson et al., 2016; Wells et al., 2017; chapter 1), which all outline the overall importance of hydrogeological setting on peatland hydrologic function. Recent studies have also outlined potential gradients that may exist from peatland to margin to upland based on differences in vegetative characteristics (Bauer et al., 2009), peat depth (Bhatti et al., 2006), water table trends (Dimitrov et al., 2014), hydrophysical peat properties, and groundwater connectivity (Lukenbach et al., 2015; Hokanson et al., 2016).

The term ‘lagg’ is applied to the margin of domed bogs and adjacent upland; laggs are regarded as distinct landscapes and hydrological units (Howie et al., 2011; Langlois et al., 2015). These are low–lying areas that are developed on a break in slope that initiates a convergence of runoff and groundwater from both bog and upland (Langlois et al., 2015; Fig. 3b). This creates a variably saturated and relatively minerotrophic zone that supports a mix of swamp and/or fen plant species (Howie et al. 2011). Although laggs typically do not contribute a groundwater flux to adjacent and topographically higher domed bogs (Ingram, 1983; Langlois et al., 2015), they have been shown to exhibit an important hydrological function and control over the growth of bogs, primarily in helping retain higher water tables in the upper, more elevated sections of the peatland (Belyea and Baird, 2006; Langlois et al., 2015). Contrary to bogs, fens do not have elevated domes

and the topographic gradient is downward from upland to margin to fen, and hydraulic gradients therefore typically follow the topography. For example, marginal fen areas located at relatively high topographic positions have been shown to provide a direct source of lateral groundwater flow to lower–lying peatland areas. However, reversals in the hydraulic gradient, from fen to upland, have also been detected in the WBP (Ferone and Devito, 2004; chapter 2).

Within the WBP, the majority of research on fen margins has been conducted in the Utikuma Region Study Area (URSA) (Devito et al., 2012). For example, bog and poor–fen margins were described by Ferone and Devito (2004), who illustrated that water table mounds can develop at margins during periods of high water availability. The authors illustrated how these mounds were important for generating horizontal hydraulic gradients between peatlands and adjacent ponds, which helped maintain pond water levels. Lukenbach et al. (2015) measured a greater degree of soil moisture variability at margins compared to lower–lying peatlands. This left margins at a greater susceptibility to drying due to their relatively high bulk density, and more vulnerable to combustion and deep smouldering from wildfire. Hokanson et al. (2016) later discovered that variability in burn severity between margins was primarily attributed to differences in hydrogeologic setting, as margin areas underlying coarse– rather than fine–textured glaciofluvial sediments had a stronger groundwater connection, which minimized water table and soil moisture variability, thus reducing the susceptibility to combustion and deep smouldering.

In the Athabasca oil sands region (AOSR) of the WBP, moderate–rich fens are a prominent peatland type (Chee and Vitt, 1989). Prior hydrological studies in this region have generally not focused on moderate–rich fens and associated margins, despite the susceptibility of these systems to changes from climate warming and industry, predominantly oil sands mining. Large tracts of peatlands are stripped for mining, with overburden materials, including the terrestrial vegetation, stockpiled or used as construction materials (Alberta Environment, 2014). Subsequently, wetland reclamation is a mandatory element of closure plans, and regulatory requirements require lands to be returned to a state of ‘equivalent capability’. Given the importance of landscape connectivity on ecosystem health in the AOSR (Devito et al., 2012; Wells et al., 2015a; 2015b; Wells et al., 2017; Elmes et al., 2018 (chapter 2)), understanding the hydrologic function of moderate–rich fens is essential for meeting these regulatory requirements.

In chapter 2, the hydrogeological connectivity of a moderate–rich fen watershed (Poplar Fen) in the AOSR was explored, situated within a sand and gravel–dominated meltwater channel belt, ~30 km north of Fort McMurray. Lithological, geochemical, and hydrological evidence pointed to the dominance of a locally–driven flow system providing groundwater to low–lying fen areas, where thick (~16 m) low hydraulic conductivity till and shale units acted as aquitards constraining connectivity between the fen and deep regional groundwater. During periods of high moisture availability, sufficient precipitation–driven recharge to adjacent uplands resulted in relatively strong and consistent hydrological connection from an underlying outwash aquifer (via vertical flow) and from adjacent uplands (via lateral flow) to fen areas. In chapter 2, the hydrology of channel fen areas was specifically addressed, while acknowledging the importance of understanding margins as separate hydrological units. Furthermore, Poplar Fen burned over in May 2016, as part of the greater Horse River Wildfire (MNP, 2017) and in chapter 3 (Elmes et al., 2018) the hydrometeorological conditions leading up to the wildfire were explored. Field results obtained in 2015 from Poplar Fen highlighted the susceptibility of the watershed to water table and soil moisture decline due to groundwater recharge conditions over rain–free periods. Margins exhibited lower average water tables than fen areas over the 2015 summer, and consequently burned much more severely than the adjacent fen.

This study expands on concepts raised in chapter 2, focusing specifically on margin areas. The objectives are to: 1) characterize the ecological, physical, hydrological, and geochemical properties of margins at Poplar Fen and identify whether they act as distinct ecohydrological units; 2) determine how margins influence the hydrologic functioning of Poplar Fen watershed; and 3) identify how their hydrology is affected by wildfire. Here, seven years of hydrological data are evaluated from Poplar Fen, five years leading up to wildfire, and two years following wildfire.

4.2 Study Site

This study is conducted in the AOSR of the WBP. Here, the average annual air temperature (1981–2010) is 1°C and average annual precipitation is 419 mm, with ~75 % falling as rain (Environment Canada, 2017). The climate in the AOSR is defined as sub–humid, where potential evapotranspiration (PET) often exceeds annual precipitation (Marshall et al., 1999).

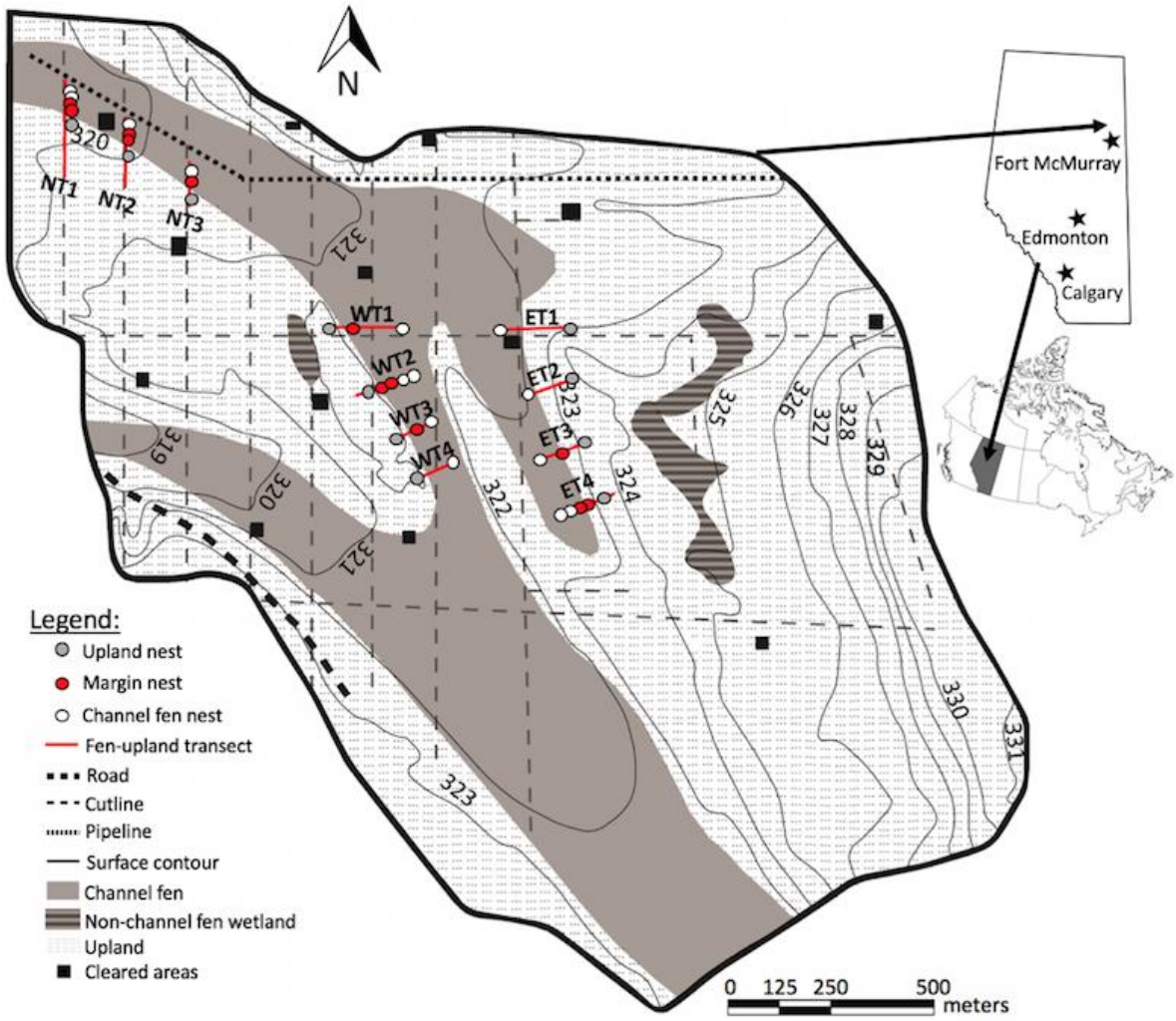

Figure 4–1. Map of Poplar watershed with location of fen upland transects.

Poplar Fen (56°56′ N, 111°32′ W; Fig. 4–1) is a ~2.5 km^2 treed moderate–rich fen watershed located 25 km north of Fort McMurray, Alberta (Fig. 4–1), within the Athabasca oil sands region of the Boreal Plains Ecozone (Ecoregions Working Group, 1989). The watershed is situated within a ~10 km long meltwater channel belt characterized by outwash sand and gravel (McPherson and Kathol, 1977). Lithological logs reported in chapter 2 show that the watershed is

underlain by two relatively thick aquitards which constrain groundwater connectivity between Poplar Fen Watershed and regional aquifers. These include a ~6.0 m thick silty till unit, and the Clearwater formation, a known regional aquitard with an average measured thickness at Poplar Fen of ~10 m. The watershed is characterized by low relief (~10 m) with channel fen–upland slopes that range from 0.5–1.5%. Due to the gentle slopes between fen and uplands, peatlands are fairly expansive at Poplar Fen, where peat depth reduces to <0.7 m in the peat–forming riparian transition zones (hereafter referred to as margins) between upland and fen (Fig. 4–1). These margin areas have been observed to have different vegetation communities than those observed in lower–lying fen areas.

4.3 Methodology

4.3.1 Ecology

During the summer of 2015, vegetation surveys were conducted on 10 m^2 plots placed along the upland–fen ecotone at WT2 (n= 5) and ET4 (n= 4) (see Fig. 4–1). Locations of plots were chosen strategically based on observed differences in elevation and community composition. Within each plot, three 1 m^2 quadrats were chosen randomly for vegetation surveys. Percent cover of each species (mosses/lichens, forbs, graminoids, and shrubs/trees) was determined visually within each quadrant and was then averaged for the entire plot. Due to the three–dimensional vegetation cover, percent cover often exceeded 100%. As a result, percent cover of each species was converted to a relative proportion.

4.3.2 Hydrology and physical characteristics

A network of three transects (NT1–NT3; Fig. 4–1) were originally installed in the northwest portion of Poplar Fen in 2011, extending southward with well and piezometer nests installed into channel fen (n = 5; hereafter referred to as fen), margin (n = 4), and upland (n = 3) areas. Fen nests were typically installed near the center of the fen, and nests in the margins were installed at the lower slope of the margin toward the fen (n = 2), or at the upper slope of the margin closer to the upland (n = 3). In 2015, eight additional transects (WT1–WT4, ET1–ET4) were installed elsewhere throughout the watershed. Within these newly–installed transects, five (WT1–WT3, ET3–ET4) had nests installed into margin areas (Fig. 4–1). One nest was installed into an

upper slope, and the remaining four were installed at the toe slope of the margin where peat depth was 0.6–0.7 m. These nests located at different positions were installed to explore potential differences in groundwater connectivity for margin areas of varying topographic positions. Screened wells and piezometers (20 cm screened intake) were constructed from PVC (2.5 cm I.D.) pipe and installed into the different substrates in grouped nests. Nests typically comprised a fully–slotted well, with piezometers installed in mid–peat (only in fen areas) and underlying mineral substrate. Upon installation, peat depth was recorded along with an estimate of the texture of the underlying mineral substrate. Nests were measured manually on a weekly basis during the spring and summer from 2011–2015 and once in October for all years except for 2014. Following the burning of Poplar Fen in May, 2016, select nests in NT1, NT3, and the newly installed transects were repaired over the 2016 field season. Nests were measured on a roughly weekly basis between June and August and again in October of 2016, and four times between May and August of 2017. A continuous record of fen water table was obtained at a nest in NT1 using either a logging pressure transducer (from 2011–12, 2016–17; Schlumberger Mini–Diver) or a capacitance water level recorder (from 2013–15; Odyssey Dataflow Systems Ltd.). Average manual water was then extrapolated into a continuous record, based on highly correlated values between average manual water table and logged water table. During periods when logger data were unavailable, manual averages were supplemented. Pipe top and corresponding ground elevations were measured using a dual–frequency survey–grade differential global positioning system (DGPS; Leica Viva GS14, 2014). Survey precision was set at 0.003 m (z) and 0.005 m (x, y) and points were only recorded when these conditions were met. Additional ground elevation measurements were made randomly along WT2 and ET4 where ecological analyses were conducted.

Field measurements of saturated hydraulic conductivity (K_{sat}) were made using bail tests on all fen and margin piezometers installed at Poplar Fen between 2011–15 using the hydrostatic time–lag method (Hvorslev, 1951). Triplicate measurements were performed on all piezometers and K_{sat} at each piezometer was computed by calculating the arithmetic mean. For the upper 0.4–0.6 m of peat, K_{sat} was determined in the lab using peat cores extracted from fen (n= 2) and margin (n= 2) areas. Cores were extracted using a Wardenaar coring device and samples were frozen and shipped for processing at the lab. Cores were subdivided into 10–cm stratigraphic intervals, and horizontal (K_H) and vertical (K_V) K_{sat} were determined using standard methods (e.g. Freeze and

Cherry, 1979). Specific yield (drainable porosity under gravity), porosity, and bulk density were also measured for each interval.

Vertical hydraulic gradients between the water table and underlying mineral layer were calculated weekly for all margin nests. A total of three t–tests were then employed to test for significant differences in vertical hydraulic gradients in 2015 between margin areas of varying topographic positions (toe, lower, upper). Vertical fluxes were calculated individually from hydraulic gradients between the water table and underlying mineral layer for margin nests. Between 2011–15, only nests from NT1–NT3 were included in the weekly average vertical gradient calculations (reported in the results section), and between 2016–17, all recovered nests were included. Vertical area–weighted groundwater flux rates (mm d^{-1}) were estimated each sample day for each nest by multiplying the vertical hydraulic gradient by a weighted harmonic mean saturated hydraulic conductivity between the peat and mineral piezometers. This mean is typically used for calculating vertical discharge through horizontally layered strata (Freeze and Cherry, 1979).

Horizontal groundwater connectivity over the upland–fen ecotone was explored by calculating horizontal hydraulic gradients from head differences between upland and margin and between margin and fen. Horizontal groundwater fluxes, the rate at which groundwater flows horizontally through the unconfined peat aquifer, were calculated by multiplying the horizontal hydraulic gradient by a depth–weighted arithmetic mean K_{sat}, of the peat, which changes depending on water table position. This method is typically used for calculating horizontal discharge through horizontally layered strata (Freeze and Cherry, 1979). Weighted arithmetic means were calculated individually for fen and margin areas at each of the three NT transects. The same methods were applied to all salvaged transects post–fire between 2016–17. Due to insufficient information regarding changes to peat K_{sat} following the fire, original pre–fire K_{sat} data were used in the post–fire calculations. The implications of this limitation will be addressed in the discussion.

To explore the relative importance of vertical versus horizontal groundwater fluxes, horizontal specific discharge rates between upland and margin and margin and fen were transformed into area–weighted (mm d^{-1}) fluxes. First, average specific discharge fluxes were

multiplied by a 1x350 m flow face (thickness and length of NT1–NT3 flow face) to obtain a volumetric flux (m^3). Then, the volumetric upland to margin flux was divided by the estimated margin surface area of NT1–NT3 (~21,000 m^2), and the volumetric margin to fen flux was divided by the estimated fen surface area of NT1–NT3 (~26,000 m^2), to which these flow faces were assumed to contribute to.

Precipitation was measured in an open area of the site with a logging Onset RG3–M tipping bucket rain gauge. Missing daily totals were supplemented with interpolated rainfall data for the Poplar Fen area (Alberta Agriculture and Forestry, 2017).

4.3.3 Geochemistry

In August, 2014, water samples were obtained from selected wells and piezometers at NT1–NT3. In June, 2015, another round of water sampling was conducted on a select number of the newly installed nests, which were primarily wells at that point. Following extensive instrumentation over the growing season, another round of water sampling was conducted on select wells and piezometers from the newly installed nests, with high resolution sampling in the west and east margin zones. All water samples taken from Poplar Fen were filtered within 24 hours using 0.45 μm nitrocellulose membrane filters. Samples were stored in 60 mL high–density polyethylene bottles and kept frozen prior to analyses. Geochemical analyses were completed at the Biotron Experimental Climate Change Research Centre at Western University. Major ions were measured with ion chromatography.

4.4 Results

4.4.1 Vegetation Composition

The upland plots at each margin transect were at the highest topographic position along both ecotones and had the lowest organic layer thickness (~0.2 m; appendix A.1). At these upland locations, richness was limited to ten and sixteen distinct species at the west and east margin transects, respectively. Upland quadrats were composed primarily of feathermosses (*Pleurozium schreberi, Hylocomium splendens,* and *Dicranum polysetum*), along with small proportions of forbs (*Viola canadensis*, *Rosa acicularis, Vaccinium myrtilloides,* and *V. vitis–idaea*), horsetail (*Equisetum scirpoides, E. arvense*), and shrubs/saplings (*Rhododendron groenlandicum* and *Picea*

mariana) (appendix A.1). Across both ecotones, surface elevation decreased (Fig. 4–2) and community composition gradually transitioned with species richness increasing. In margin areas (West margin transect: 30 and 55 m across ecotone; East margin transect: 50 m across ecotone), feathermosses were still dominant; however, *R. groenlandicum* and *P. mariana* became more dominant, along with several species of mosses (*Sphagnum fuscum, Polytrichum strictum, Aulacomnium palustre,* and *Tomenthypnum nitens*), forbs (*Smilacina trifolia*, *Oxycoccus microcarpus*), graminoids (*Carex aquatilis*) and shrubs/saplings (*Larix laricina, Salix planifolia,* and *S. pedicellaris*) (appendix A.1). Farther across the ecotone, within lower lying fen plots (Fig. 4–2), species composition changed, and richness increased. Species found in uplands and margins, including feathermosses, became virtually absent, and fen quadrats were dominated by *T. nitens* and *L. laricina*, and comprised a mixture of populations of several different mosses (*S. warnstorfii, S. angustifolium, Drepanocladus aduncus, Campyllium stellatum, Mnium stellare, Calliergon giganteum,* etc.), forbs (*Potentilla palustre*, *Pyrola asarifolia*, *Stellaria longifolia*, *Caltha palustris*, and *Galium triforum*), graminoids (*E. fluvial, Carex leptalea, C. gynocrates, C. disperma, C. diandra, C. prairea, C. tenuiflora, C. paupercula, C. pauciflora*), and shrubs (*Salix candida, Betula pumila,* and *S. pedicellaris*) (appendix A.1).

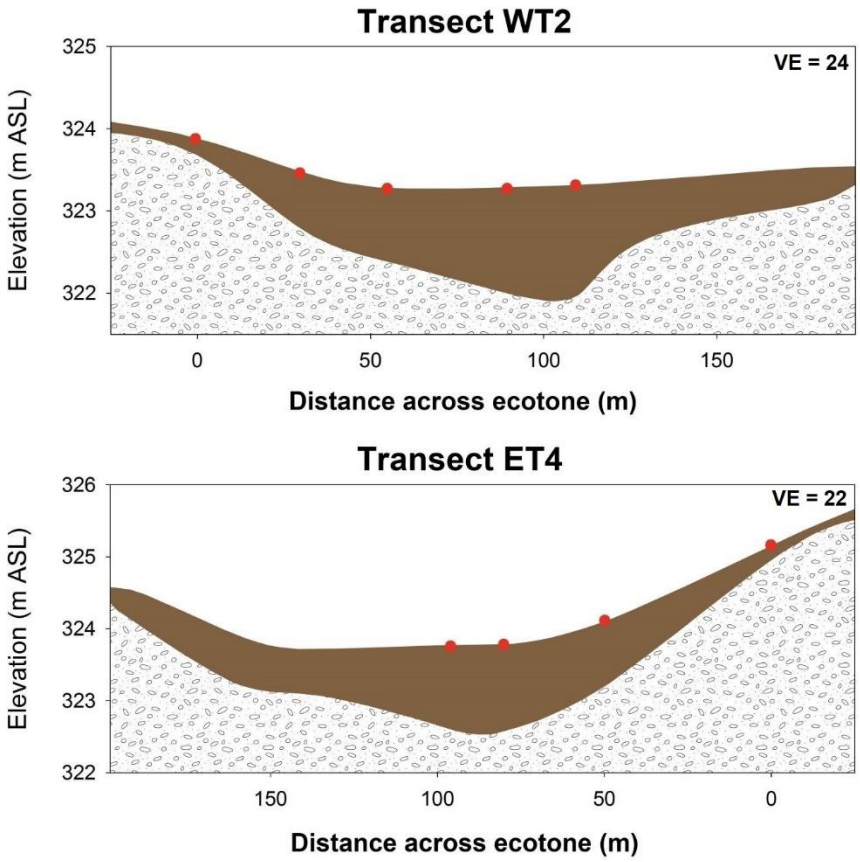

Figure 4–2. Cross–sections of transects WT2 and ET4 with locations of vegetation survey plots (red dots).

4.4.2 Topography and peat physical properties

Along WT2, total relief is 0.58 m, slope is 0.5% (Fig. 4–2), and margin (n = 16) and fen (n = 9) ground elevation measurements differ by an average of 0.18 m. This transect has a lower relief and slope compared to ET4 (1.26 m and 1.4%, respectively) (Fig. 4–2), where margin (n = 14) and fen (n = 12) ground elevations differ by an average of 0.24 m. Little difference in bulk density was observed between fen and margin cores in the upper 0.3 m (Fig. 4–3). However, below 0.3 m below ground surface (b.g.s.), bulk density was consistently higher in margin cores at both locations. Little difference was found in specific yield between fen and margin cores. For both fen cores and the WT2 margin core, anisotropy was close to 1 at most depths. Greater differences were measured for the ET4 margin core, as K_H was higher than K_V for all intervals below 0–10 cm (Fig. 4–3), and anisotropy increased from 0.7 to 50 towards the bottom of the core.

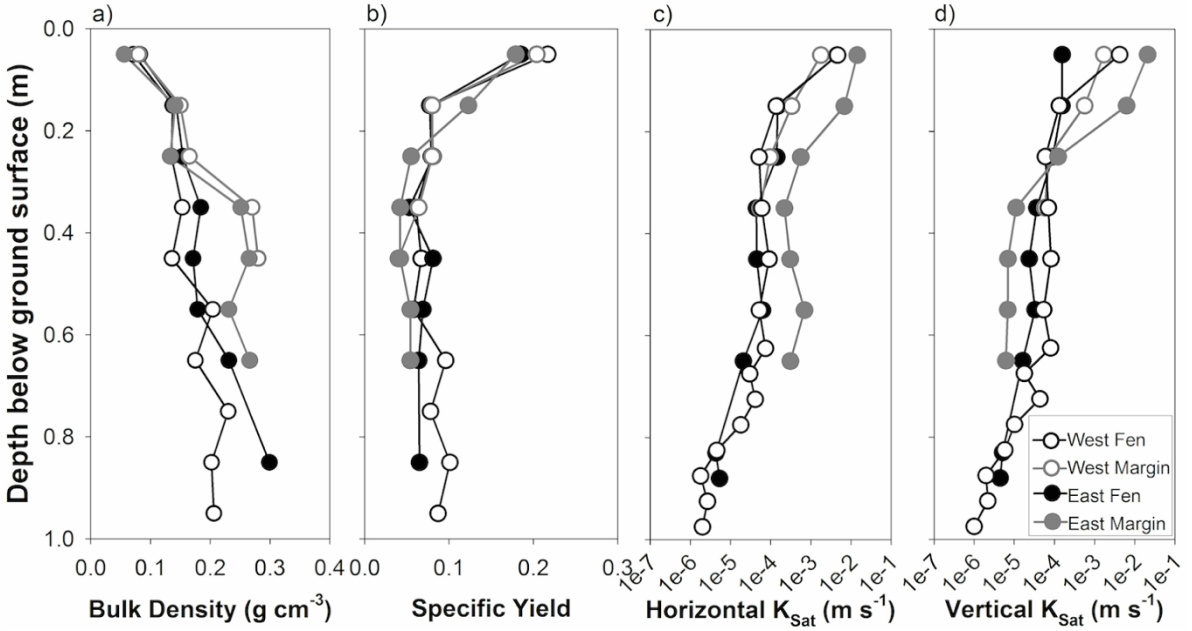

Figure 4–3. Physical properties of peat cores obtained WT2 and ET4 (see Fig. 1 and 2), including (**a**) bulk density, (**b**) specific yield, (**c**) horizontal K_{sat}, and (**d**) vertical K_{sat}.

Laboratory–measured K_H was plotted alongside field–measured K_H values (Fig. 4–4). In the top 40 cm, margin K_{sat} was typically higher than in the fen; however, margin peat had comparable values at 0.5 m b.g.s. Basal margin peat (0.6–0.7 m b.g.s.) had a geometric mean K_H of 7.0×10^{-7} m s^{-1}, an order of magnitude higher than basal fen peat (1.1–1.5 m b.g.s.), which had a geometric mean K_H of 7.6×10^{-8} m s^{-1}. The weighted arithmetic mean K_H of both fen and margin peat decreased logarithmically with decreasing water table (Fig. 4–4), as higher K_H near surface layers become unsaturated, and therefore do not contribute flow. Weighted arithmetic mean K_H was higher in margin peat at a given water table depth compared to fen peat, until the water table went below 0.5 m b.g.s. Field measured K_H of underlying mineral sediment were different by an order of magnitude between fen (n= 22) and margin (n= 9) nests, with means of 3.5×10^{-5} and 1.3×10^{-4} m s^{-1}, respectively (Fig. 4–4). Both locations experienced high variance, with a coefficient of variation of 1.97 and 1.28 for fen and margin underlying mineral substrate K_H, respectively.

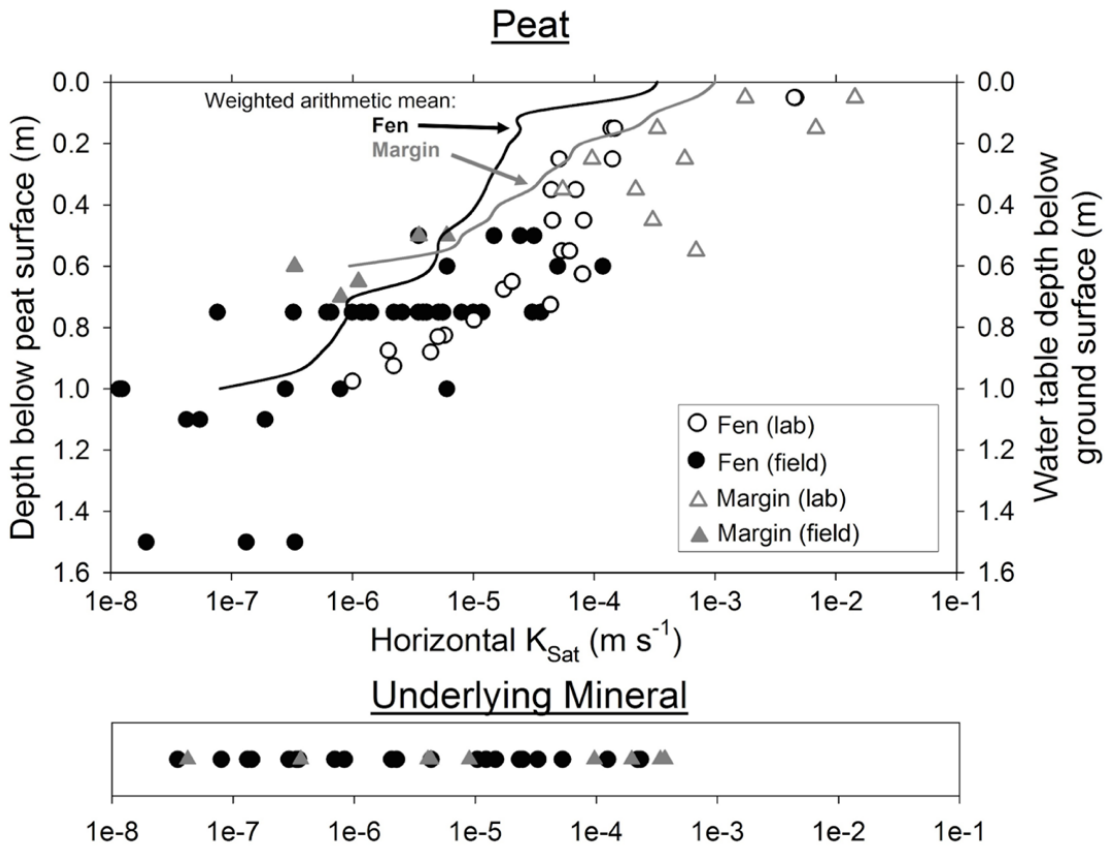

Figure 4–4. Lab (open symbols) and field (closed symbols) measured saturated horizontal hydraulic conductivity in fen (circles) and margin (triangles) of Poplar Fen, along with changes in the weighted arithmetic mean K_H of fen (black line) and margin (grey line) peat with change in water table position.

4.4.3 Hydrological comparison of fen and margin areas, pre–fire

Fen and margin water tables are illustrated in Fig. 4–5 and summarized in Table. 4–1. The five–year fen (2011–2015) water table trend was relatively low water tables (dry conditions) at the beginning (2011–Sep. 2012; mean = 0.29 m b.g.s.), increased water table in the middle years (Sep. 2012– Sep. 2014; mean = 0.01 m b.g.s.), and lower water tables in a drying period towards the end of the record (Sep. 2014–Oct. 2015; mean = 0.18 m b.g.s.) (Fig. 4–5a). Margin water tables exhibited similar temporal patterns; however, they were lower than the fen for the entire five–year, pre–fire instrumental period by an average of 0.22 m (Table 4–1). Both areas experienced variation in water table over this period (Fig. 4–5a), with standard deviations of 0.2 and 0.18 m for fen and margin areas, respectively. The 2015 season ended with fall water tables that were among the lowest observed in the five–year record. The following spring, the logged fen water table at NT1 was 0.31 m b.g.s. by May 17, 2016, the day that Poplar Fen began to burn over (Fig. 4–5a). No records of margin water table were made during this time.

Vertical flow direction between the fen and the underlying outwash aquifer was transient during 2011–2015, with flow reversals occurring in 2012, 2014, and 2015. Vertical hydraulic gradients in fen areas averaged +0.001 (Table 4–1), and were positive throughout the majority of the five–year pre–fire period (Fig. 4–5b). In contrast, vertical hydraulic gradients in margin areas were negative throughout the entire five–year pre–fire record (Fig. 4–5b), averaging –0.02 (Table 4–1). Contrary to fen areas, where gradients were highest (positive) during the wet years (2013–2014), the lowest (most negative) vertical hydraulic gradients in margin areas were measured during this time (Fig. 4–5b). As margins exhibited a higher basal peat K_{sat} than fens by roughly an order of magnitude (Fig. 4–4), absolute vertical fluxes were higher in the margin over the five–year pre–fire instrumental period. Over this period, vertical fluxes in margin areas averaged –0.63 mm d^{-1}, indicating strong recharge (downward flow) to the underlying outwash aquifer, whereas vertical fluxes in the fen averaged +0.03 mm d^{-1} (Fig. 4–6). Since vertical hydraulic gradients were strongest during wet periods (Fall 2012–Summer 2014; Fig. 4–5c), recharge was the highest during this time, averaging –0.86 mm d^{-1}, with fluxes as large as –1.15 mm d^{-1} (Fig. 4–6). Conversely, during drier periods marked by lower water tables (2011, 2015) (Fig. 4–5a), margin recharge to the underlying outwash aquifer was ~48% lower, averaging –0.45 mm d^{-1} (Fig. 4–6). Between 2011–15, average daily vertical fluxes amounted to ~18–51% of the average daily rainfall recorded over the respective field seasons (Table 4–1).

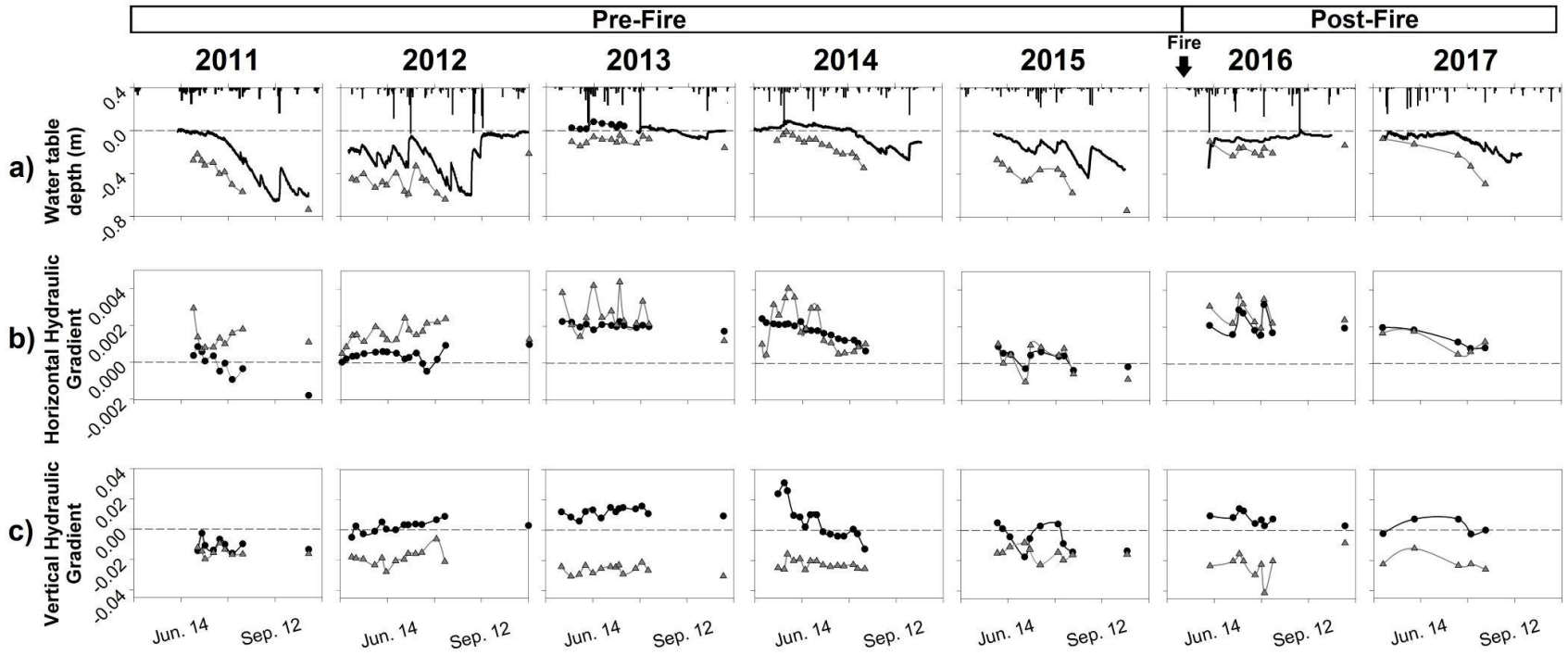

Figure 4–5. Average hydrological results for NT1–NT3 (see Fig. 1) from 2011–2015, and for salvaged nests along NT1 and WT and ET transects from 2016–2017, including (**a**) extrapolated (lines) and/or manually (circles) recorded fen (black) and margin (grey) water table position and daily regional precipitation, (**b**) average horizontal hydraulic gradient between upland and margin (grey) and margin and fen (black), and (**c**) average vertical hydraulic gradients between peat and underlying mineral substrate in fen (black) and margin (grey) areas. Note that positive gradients signify a gain in groundwater from underlying mineral substrate or upland to peat.

Large differences were found in the vertical groundwater connectivity of margin areas of varying topographic positions. For example, nests located at upper margin locations typically had the strongest gradients in 2015, which were always negative (mean = –0.04), and therefore had the greatest measured downward flux (mean = –1.24 mm d^{-1}) to the underlying outwash aquifer. Conversely, both nests located at lower margin areas still had negative vertical hydraulic gradients throughout the entire year. However, gradients in lower margin nests (mean = –0.02) were significantly ($t_{36.2}$ = –4.5, p = 0.0001) higher (less negative) than upper margin nests, resulting in a lower downward flux (mean = –0.64 mm d^{-1}) to the underlying outwash aquifer. The greatest differences were measured at margin nests located at toe slopes, where vertical hydraulic gradients were typically positive (mean = +0.001). The vertical hydraulic gradients measured at these nests were significantly higher than nests at both lower ($t_{53.2}$ = –7.8, p = 2.3^{-10}) and upper ($t_{43.9}$ = –9.2, p = 9.5^{-12}) margin areas, yielding a gain in groundwater (mean = +0.04 mm d^{-1}) from the underlying outwash aquifer. In general, nests located at lower margin areas experienced the lowest variation, and several nests at both toe and upper margin areas experienced relatively high variation.

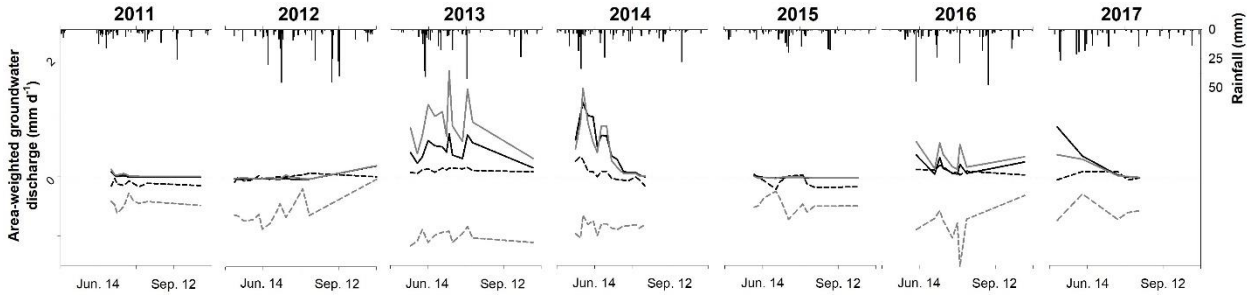

Figure 4–6. Average area–weighted groundwater fluxes over the instrumental record, for NT1–NT3 from 2011–2015, and all salvaged nests from 2016–2017, including lateral fluxes between upland and margin (solid grey), margin and fen (solid black), and vertical fluxes between margin (dashed grey) and fen (dashed black) peat and underlying mineral substrate. Note that a positive horizontal flux represents a gain to the lower surface elevation, and a negative vertical flux represents a loss from margin peat to underlying mineral substrate.

Upland–margin and margin–fen (horizontal) hydraulic gradients followed patterns similar to vertical hydraulic gradients over the five–year pre–fire period (Fig. 4–5b). Water table position exhibited a large control on the weighted arithmetic mean of fen and margin peat (Fig. 4–4) and therefore the overall flux of groundwater (Fig. 4–6). The highest hydraulic gradients were measured during periods of high rainfall fall (2012–summer, 2014) (Fig. 4–5b), with fluxes from upland to margin and margin to fen averaging +0.70 and +0.47 mm d^{-1}, respectively, during this time. During periods of low rainfall (2011 and 2015), horizontal hydraulic gradients were typically

lower (Fig. 4–5b), and with the relatively low water table positions during this time (lower mean K_{sat}), fluxes averaged +0.008 and +0.002 mm d^{-1} to margin and fen areas, respectively. Flow reversals (towards the upland) occurred in margin areas only in the summer and fall of 2015 (Fig. 5b), and due to the relatively low water tables at the time (Fig. 4–5a), represented a negligible loss of groundwater (–0.003 mm d^{-1}) away from the margin (Fig. 4–6). Flow reversals from fen to margin were more common, albeit still rare, occurring in 2011, 2012 and 2015 (Fig. 4–5b), and also represented a negligible loss of groundwater (–0.001 mm d^{-1}) away from the fen (Fig. 4–6).

Table 4–1. Summary of average daily hydrological results from 2011–2017, including rainfall, fen and margin water table position, horizontal and vertical hydraulic gradients, and corresponding average area–weighted groundwater fluxes (mm d^{-1}) for each hydraulic gradient.

	2011	**2012**	**2013**	**2014**	**2015**	**2016**	**2017**
Average rainfall May 01–Oct. 01 (mm d^{-1})	1.1	2.5	2.0	1.9	1.3	2.0	1.4
Water Table (m b.g.s.)							
Fen (±SE)	–0.26 ±0.02	–0.26 ±0.02	–0.01 ±0.00	–0.17 ±0.01	–0.33 ±0.01	–0.03 ±0	–0.12 ±0.01
Margin (±SE)	–0.36 ±0.04	–0.49 ±0.02	–0.09 ±0.01	–0.12 ±0.02	–0.4 ±0.03	–0.19 ±0.02	–0.19 ±0.06
Horizontal Flow (mm d^{-1})							
Margin–Fen	+0.01	+0.05	+0.43	+0.51	+0.005	+0.17	+0.27
Upland–Margin	+0.02	+0.07	+0.79	+0.46	+0.004	+0.30	+0.19
Net flux to margin	+0.01	+0.02	+0.36	–0.05	–0.001	+0.13	–0.08
Vertical Discharge mm d^{-1})							
Fen	–0.13	+0.04	+0.12	+0.06	–0.09	+0.10	+0.06
Margin	–0.45	–0.45	–1.02	–0.82	–0.46	–0.66	–0.52

4.4.4 Hydrological comparison of fen and margin areas, post–fire

The hydrometeorological conditions leading up to the Horse River Fire and burning of Poplar Fen were summarized in Elmes et al. (2018; (chapter 2)), which confirmed the accumulation of moisture deficits prior to the fire, between summer 2015 and early spring 2016. Following the fire, the greatest depth of burn was measured in the margins (0.13 ± 0.01 m) with lower (0.02 ± 0.002 m) burn depths measured at fen areas (Elmes et al., 2018 (chapter 2)).

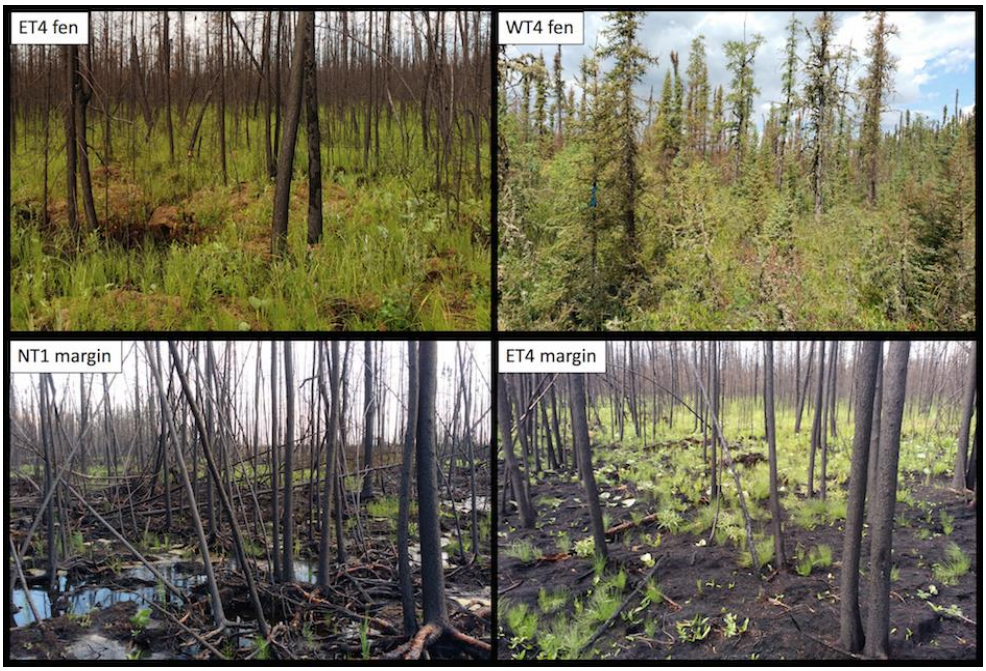

Figure 4–8. Photos of taken at several transect locations two months following the wildfire (refer to Fig. 1).

A relatively wet summer occurred in 2016, following the burning of Poplar Fen on May 17. Over the 2016 field measurement period (May 17– Oct. 16), the watershed had received ~306 mm of rainfall, 36 mm more than the May–Oct. average for 2011–15. Over the 2016 post–fire field season (Jun–Oct), average fen water tables remained close to surface (with ground surface ~0.02 m lower), averaging 0.07 m b.g.s. (Fig. 4–5a). Due to differences in surface change from the fire (Fen = 0.02 m; Margin = 0.13 m; Elmes et al., 2018 (chapter 2)), margin water tables (0.14 m b.g.s.) were deeper relative to ground surface than fen water tables by only 0.07 m (Table 4–1).

Average vertical hydraulic gradients remained positive (upward) in fen areas throughout all of 2016, and were negative (downward) in margin areas for the entire year (Fig. 4–5c), with groundwater fluxes averaging +0.10 and –0.66 mm d^{-1}, respectively (Fig. 4–6; Table 4–1). In 2017, average vertical hydraulic gradients in margins remained negative throughout the entire monitoring period (Fig. 4–5c), with fluxes averaging –0.66 mm d^{-1} (Fig. 4–6). In 2016 and 2017, average annual vertical fluxes in margins amounted to 33% and 37% of the rainfall recorded over the respective field seasons (Table 4–1).

Horizontal hydraulic gradients between 2016–17 followed patterns similar to those observed from 2013–14 (Fig. 4–5b), as upland water table elevations were higher than in adjacent margin areas, and margin water table elevations higher than in adjacent fen areas. In 2016, upland–

margin gradients were higher than margin–fen, with the strongest connection following rainfall events. Horizontal hydraulic gradients remained strong and positive throughout the entire 2016 field season (Fig. 4–5b) with groundwater fluxes to margin averaging +0.30 mm d^{-1} (Fig. 4–6). In 2017, gradients from upland to margin remained strong during the first half of the field season, decreasing in the late summer (Fig. 4–5b), with fluxes averaging +0.19 mm d^{-1} (Fig. 4–6).

4.4.5 Geochemistry

For water samples obtained in the summer of 2015 (pre–fire), fen porewater chemistry had EC and cation concentrations in between those measured in the margin peat porewater and in piezometers underlying the fen in the outwash aquifer. In contrast, margin porewater exhibited strong similarities in geochemical composition with samples obtained from upland wells, rather than samples from the outwash underlying the margin (Fig. 4–9). For example, margin porewater and upland well water samples both exhibited relatively higher chloride and sulphate, and lower sodium concentrations compared to the other locations. pH was circumneutral, and EC was relatively high for all samples obtained from fen, margin, underlying outwash and upland wells/piezometers (Fig. 4–9).

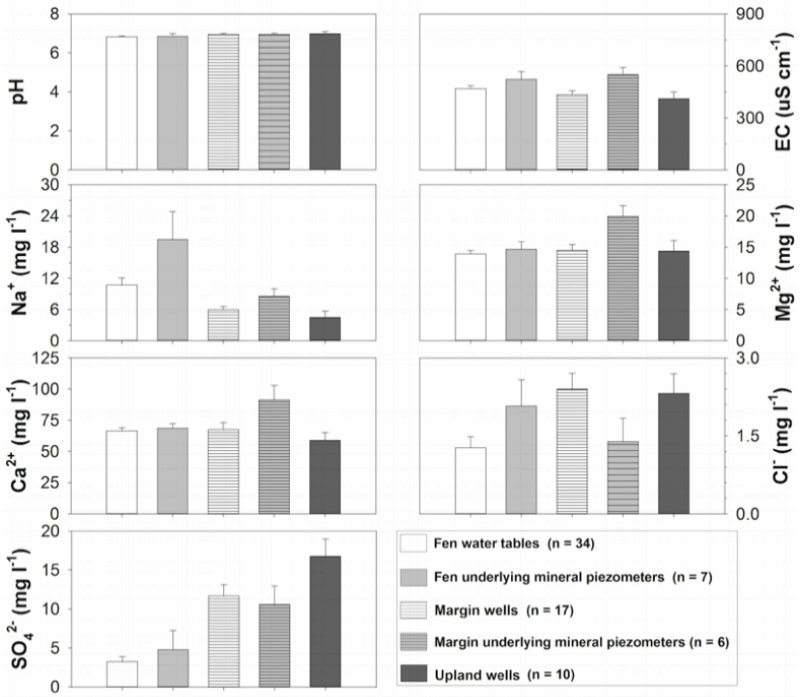

Figure 4–9. Average pH, electrical conductivity (EC), and concentrations of major cations (Na^+, Ca^{2+}, and Mg^{2+}) and anions (Cl^- and SO_4^{2-}) for samples from fen and margin wells and underlying mineral piezometers, as well as upland wells, obtained throughout 2015 at Poplar Fen.

4.5 Discussion

4.5.1 Margins as distinct ecological and hydrological units

Ecological results identified a transition in community composition along the upland–fen ecotone at transects WT2 and ET4 (appendix A.1). Uplands were composed primarily of feathermosses characteristic of boreal forests overlying mineral soils (Bauer et al., 2009). Across the ecotone, there was an increase in species richness, as well as the appearance of several peatland indicator species (cf. Vitt and Chee, 1990) in margin areas (appendix A.1). Although still dominated by feathermosses, the appearance of peatland indicator species suggests that margins are located within a transition zone characterized by more saturated conditions that support the presence of peatland vegetation (e.g. *T.* nitens, *Carex spp.*, *Equisetum spp*; Chee and Vitt, 1989; Vitt and Chee, 1990). Furthermore, the appearance of *T. nitens* (appendix A.1), a moderate–rich fen indicator species (Chee and Vitt, 1989), suggests that margin vegetation can access circumneutral, ion–rich water, pointing to an influence of groundwater.

The ET4 margin had higher bulk density and K_H, and lower specific yield at depth compared to fen peat (Fig. 4–3), but no distinct difference was observed in the peat from the WT2 margin and fen. However, given the effect of vegetation composition on peat K_{sat}, differences in peat physical properties would be expected. Margins exhibited deeper water tables (cf. Ferone and Devito, 2004; Lukenbach et al., 2015; Hokanson et al., 2016) throughout the five–year pre–fire instrumental period (Fig. 4–5a), and thus presumably have deeper oxidized conditions and more peat decomposition (Roulet et al., 2007). This causes structural changes (Waddington et al., 2014) that affect physical parameters (Ise et al., 2008; Waddington et al., 2014). Interestingly, conflicting differences in anisotropy were found between both sampled margin cores. For example, anisotropy was 50 at the base of the ET4 margin peat core, with K_H (10^{-4} m s^{-1}; Fig. 4–3) considerably higher than well–humified basal peat measured elsewhere in the AOSR (Scarlett and Price, 2013; Wells et al., 2015a, 2017). Conversely, anisotropy was 0.94 at the base of the WT2 margin peat core. Considering these appreciable differences between the two cores, an averaged anisotropy was not applied to the field measured K_H data for the purpose of calculating vertical fluxes, and instead the original data were used alongside the laboratory–measured K_V data. It is acknowledged that K_{sat} is typically variable at the field scale (Hoag and Price, 1995; Fraser et al., 2001); however, the

sampling resolution in this study was not extensive enough to effectively capture this variability and determine an appropriate mean anisotropy.

Large differences were observed in the vertical groundwater flow patterns of margin versus fen areas. Contrary to fen areas, which functioned primarily as vertical groundwater discharge zones during wet periods, and were subject to flow reversals during dry periods (Fig. 4–5c; chapters 1 and 2), average vertical hydraulic gradients in lower and upper margin areas were consistently negative throughout the five–year pre–fire instrumental period. Therefore, margins operate primarily as vertical recharge windows to the underlying outwash aquifer (Fig. 4–5c). Recharge was also strongest during wet periods (Fig. 4–6), suggesting that recharge conditions are enhanced during years characterized by higher rainfall and shallower margin water tables. Greater absolute fluxes compared to fen areas were not only due to relatively strong negative (downward) vertical hydraulic gradients (Fig. 4–6b), but also due to the higher hydraulic conductivity, which creates a higher weighted harmonic mean of the peat–mineral flow path (mean = 4.0×10^{-7} m s^{-1}) relative to that of the fen (mean = 1.7×10^{-7} m s^{-1}) (Fig. 4–4). Although margins operate as large water sinks, the Poplar Fen watershed is underlain by a thick (~16 m) aquitard (see chapter 1), and therefore most recharge is retained within the outwash aquifer and directed to the toe of margins and to lower–lying fen areas. Thus, margins play an important role in recharging to the local flow systems that develop in uplands and discharge vertically from underneath the low–lying fen areas and help maintain fen water levels (see chapter 2).

Margins were shown to exhibit an important control on the lateral groundwater connectivity over the upland–fen ecotone. In chapter 2, the importance of a transmissivity feedback mechanism at Poplar Fen was described, whereby horizontal groundwater is discharged at relatively higher volumes from upland to fen during wet periods, due to two primary processes: (1) the hydraulic gradient between upland and fen becomes higher following a rainfall event; and (2) the higher water table exploits higher K_H layers, increasing the transmissivity of the upland to fen flow path. The results for this study help refine our understanding of the transmissivity feedback mechanism at Poplar Fen. High vertical recharge (Fig. 4–6) restricts margin water tables to greater depths (Fig. 4–5a), thus, reducing the mean K_{sat} of the flowpath from upland to fen. In addition, relatively larger horizontal fluxes of groundwater were discharged from upland to margin due to the greater head difference caused by vertical recharge in margin areas (Fig. 4–6).

Complete flow reversals from fen to margin, and from margin to upland, were also detected, but only intermittently during the summer and fall of 2015 (Fig. 4–5b), a particularly dry year. During certain dry periods in 2011 and 2012, convergent flow conditions occurred in the margins (Fig. 4–5b), where lateral groundwater flow from the upland to the margin converges with flow from the fen to the margin. Similar convergent flow conditions were witnessed in laggs between upland and peatland in the Bécancour region of Quebec (Ferlatte et al., 2015). However, due to decreases in K_H with depth (Clymo, 1978; Fraser et al., 2001), the transmissivity feedback mechanism also causes horizontal fluxes to remain low during lateral flow reversals, constricting drainage from fen and margin areas (Waddington et al., 2014).

The groundwater connection directing flows from upland to margin is reflected in the similarities in their pH, EC, and dissolved ion concentration (Fig. 4–9). Without this lateral groundwater connection, margins, which act as vertical recharge zones, would likely have lower water tables with sub–surface water more characteristic of rainfall, characterized by lower pH and base–cation concentrations. This dynamic lateral groundwater connection with the upland explains why margins host moderate–rich fen indicator species (specifically *T. nitens*; Chee and Vitt, 1989). Conversely, fen water chemistry comprised EC and cation and Cl^- concentrations between those measured in the margin peat porewater and the underlying outwash aquifer (Fig. 9), and therefore was influenced by both sources of groundwater. Thus, margins are also important transmitters of ion–rich groundwater to fen areas. Without this lateral connection between fen and margin, fen subsurface water chemistry would likely be more characteristic of rainfall, especially due to the vertical flow reversals observed during drier periods.

The results reported here are different from those reported on peatlands overlying clay plains and till moraines (Ferone and Devito, 2004), where margins have exhibited limited horizontal connectivity with uplands, which comprise finer–grained soils, and flow is typically directed towards the upland. The result of this hydrological connectivity allows margins at Poplar Fen to access ion–rich groundwater and host a unique vegetation community assemblage. However, given their susceptibility to water table drawdown under dry periods and their susceptibility to fire (Lukenbach et al., 2016), they remain particularly vulnerable and will continue to be so under a changing climate.

4.5.2 The effects of wildfire on the hydrologic function and ecology of margins

Following the fire on May of 2018, margin water tables at Poplar Fen behaved similarly to pre–fire levels (Fig. 4–5a), with little evidence of flooding during wet periods, or rapid drawdown during drier periods. Thus, these margins behave differently than those at URSA described by Lukenbach et al. (2017), which showed that margins connected to local rather than regional groundwater flow rather than regional flow systems were subject to extremes (flooding and drawdown) during wet and dry periods, respectively.

Trends in vertical and horizontal flow direction between 2016–17 were similar to similar wet years observed prior to the wildfire (Fig. 4–5). Following wildfire, margins continued to be significant sources of recharge to the underlying outwash aquifer, as well as receivers and transmitters of lateral groundwater throughflow between upland and fen (Fig. 4–6). However, contrary to other years of high rainfall (e.g. 2013), horizontal fluxes were relatively low in 2016 (Table. 4–1). This was likely due to the considerable moisture deficits that had accumulated between summer 2015 and the fire in May of 2016 at Poplar Fen (Elmes et al., 2018 (chapter 2)), which required greater rainfall for recharge. This ultimately reduced the margin water levels (Fig. 5a) and therefore the weighted arithmetic mean K_H of the effective peat column (see Fig. 4–4) minimizing the transmissivity feedback. However, as heavy rainfall persisted into the fall of 2016, moisture deficits were restored. This created relatively shallow margin water tables in early 2017, and despite rainfall comparable to 2015 (dry year) (Fig. 4–5a), resulted in appreciable fluxes to margin and fen areas (Fig. 4–6). This feedback was enhanced by a reduction in ET in fen, margin, and upland areas due to the decimation of living vegetation (Kettridge et al., 2014), and resulted in a net gain to the water balance.

The primarily groundwater function of margins at Poplar Fen appeared to have been maintained following wildfire, as they continued to be important transmitters of groundwater to fen areas and the underlying outwash aquifer. However, due to a different collection of nests being used for analyses in in 2016–2017 (i.e. following the fire), caution is required when interpreting average vertical and horizontal fluxes, as NT, WT and ET transects have shown to exhibit differences in strength of hydraulic gradients (chapter 2; Elmes et al., 2018 (chapter 3)). In addition, insufficient information and knowledge regarding the changes in the hydrophysical

properties of peat following wildfire will also likely result in errors to the calculated fluxes. Furthermore, interpretations may be limited by an insufficient knowledge regarding the effects of wildfire on the hydrophysical properties of the upland soils. Wildfire has been shown to often increase soil hydrophobicity (Krammes and Orborn, 1969; DeBano et al., 1979; DeBano, 1991), resulting in a reduction in infiltration capacity (Imeson et al., 1992), an increase in overland flow (Campbell et al., 1977; Burke et al., 2005), and reductions in soil moisture retention (Imerson et al., 1992). A better understanding of these effects will lead to a sounder understanding of the response of moderate–rich fens and adjacent margins in the AOSR to wildfire.

In chapter 3 (Elmes et al., 2018) significant degrees of burning were reported in margin areas, with depth of burn averaging 0.13 m, which removed the entire living layer of margin mosses. By the end of the first summer following the burn, certain species, particularly *Equisetum sylvaticum*, had returned, with little recovery of mosses (see Fig. 4–7). Given that the lateral connection between margin and upland was maintained, the conditions that favour the pre–fire community composition are present.

Over the past decade, there has been an increased concern that climate change may result in longer fire seasons (Wotton and Flannigan, 1993; Flannigan et al., 2013; Kirchmeier–Young et al., 2017), an increase in large high–intensity wildfires (Tymstra et al., 2007) and total burned area each year (Podur and Wotton, 2010) in Alberta. Given the susceptibility of peatland margins to wildfire (Bauer et al., 2009; Lukenbach et al., 2015; Hokanson et al., 2016), it is anticipated that these systems will become more vulnerable over time and will undergo more physical and chemical changes due to wildfire. As negative as these consequences may be, however, results suggest that the important groundwater hydrologic function of these systems is maintained following wildfire, assisting with the reestablishment of vegetation in fire–impacted fen areas (Benscoter and Vitt, 2008).

4.6 Conclusions

This seven–year study examined the hydrologic function of peatland margins, prior to, and following wildfire, within a moderate–rich fen watershed in the Athabasca Oil Sands Region of the Western Boreal Plain. Pre–fire results highlight that the margins at Poplar Fen act as large transmitters of lateral groundwater throughflow between upland and fen, as well as large vertical

recharge zones to the local flow systems which discharge from underneath low–lying fen areas. These groundwater patterns also provide these recharge features with circumneutral ion–rich upland groundwater, allowing them to host a specific assemblage of upland and moderate–rich fen indicator species.

Margins in the WBP have been shown to be particularly vulnerable to wildfire and deep combustion (Bauer et al., 2009; Lukenbach et al., 2015; Hokanson et al., 2016), and therefore are subject to ecological and hydrophysical changes. However, post–fire hydrological results indicate that the primary groundwater function of margin areas was maintained following wildfire. Margins continued to provide lateral throughflow to fen areas at Poplar Fen, while also providing a source of vertical recharge to the underlying outwash aquifer. Thus, margins will play an important role in helping provide the moisture conditions necessary for moss reestablishment in fen areas. Margins will likely return to a similar community composition over time, dominated primarily by feather mosses and *S. fuscum*, and certain moderate–rich fen indicator species.

4.7 Acknowledgements

The authors wish to thank D. Price and J. Asten for their assistance in the field. We gratefully acknowledge funding from a grant to Jonathan S. Price from the National Science and Engineering Research Council (NSERC) of the Canada Collaborative Research and Development Program, co–funded by Suncor Energy Inc., Imperial Oil Resources Limited, and Shell Canada Energy.

5 Changes to the hydrophysical properties of upland and riparian soils in a burned fen watershed in the Athabasca Oil Sands Region, northern Alberta, Canada

5.1 Introduction

Peatlands represent significant sinks for atmospheric carbon (Waddington and Roulet 1996, Alm et al. 1997) and account for roughly one third of the world's soil carbon pool (Gorham et al., 1991). In North America alone, northern peatlands store an estimated 180 Pg of carbon (Bridgham et al., 2006), with ~82% of this stock residing within Canada (Tarnocai, 2006). However, the terrestrial carbon stocks stored within peatlands in northern Canada are susceptible to degradation and carbon release due to a number of disturbances that are exacerbated by the increased severity and frequency of drought conditions attributed to climate change (Roulet et al., 1992; Petrone et al., 2005). This includes enhanced peat oxidation and subsequent decomposition from water table drawdown (Ise et al., 2008; Waddington et al., 2014), and enhanced soil moisture decline and subsequent peat combustion from wildfire (Weber and Flannigan, 1997; Tymstra et al., 2007; Flannigan et al., 2016; Elmes et al., 2018 (chapter 3)). Although susceptible to degradation, northern peatlands are regarded as resilient ecosystems, characterized by numerous negative feedbacks, which minimize water loss during extended drying periods (Waddington et al., 2014).

The sub–humid low–relief Western Boreal Plain (WBP) of northern Alberta comprises a mosaic of peatlands and forested uplands, which overlie a deep and generally heterogeneous surficial geology. In this region, hydrogeologic setting exhibits an important control on peatland–landscape connectivity (Devito et al 2005; 2012), which therefore results in a diverse array of peatland types, ranging from ombrogenous bogs to geogenous and/or saline fens (Vitt et al., 1995; Wells et al., 2015a). Numerous conceptual models have been constructed, which altogether outline the variability in hydrologic function of peatland systems in the WBP, as well as landscape connectivity (Ferone and Devito, 2004; Devito et al., 2005, 2012; Wells et al., 2015, 2017; chapter 2). For example, Ferone and Devito (2004) found minimal groundwater exchange between bogs in the Utikuma Region Study Area and the surrounding mineral landscape. Wells et al. (2017) measured runoff coefficients >20% in a poor–fen watershed located within a headwater catchment in the Stoney Mountains south of Fort McMurray. In chapter 2, the hydrological connectivity of uplands and a sand and gravel outwash aquifer with a moderate–rich fen in the Athabasca Oil

Sands Region (AOSR) of the WBP was discussed. Thus, given the variability in peatland form, function and landscape connectivity, the response of these peatland systems to disturbance will vary considerably, and will likely be site–specific (Devito et al., 2005, 2012).

The WBP is a fire–dominated landscape, where wildfire burns a variable, yet considerable area (~208 000 ha; 2006–2015), of Alberta annually (Government of Alberta, 2017), with the majority of wildfire occurring within the boreal forest (Tymstra et al., 2007). Recently, there has been concern over the impacts of climate change on wildfire behaviour in the western boreal forest, including longer fire seasons (Wotton and Flannigan, 1993; Flannigan et al., 2013; Kirchmeier–Young et al., 2017) and an increased potential for large high–intensity wildfires (Tymstra et al., 2007; Boulanger et al., 2014). The result is a mosaic of fire–influenced peatlands and forested uplands, which undergo numerous hydrophysical changes (Doerr et al., 2000), as well as enhanced ecological succession of Alberta's mixedwood and conifer forests to climatologically favourable aspen woodland and grassland (Stralberg et al., 2018).

In the WBP, several recent large–scale fires have occurred over the past two decades. For example, the 1998 Virginia Hills Fire (163,000), 2002 House River Fire (280,000 ha), 2011 Flat Top Complex (750,000 ha) and Richardson Fire (576,000 ha), and 2016 Horse River Wildfire (590,000 ha) have all challenged wildfire management and suppression efforts, leading to significant damage to large tracts of boreal mixedwood uplands and peatlands (Hirsch and de Groot, 1999; Tymstra et al., 2005; FTCWRC, 2012; MNP, 2017). Among these notable fires, several have occurred within the AOSR (Fig. 5–1), where peatlands, primarily as moderate–rich fens (Chee and Vitt, 1989), are a dominant peatland type. Moderate–rich fen systems have been shown to be hydrologically connected to uplands (chapter 2), relying on their discharge during periods of frequent rainfall. However, to date, no studies have addressed the hydrophysical changes to uplands following wildfire in the AOSR, let alone the WBP.

The influence of wildfire on the hydrology of forested uplands is well–documented. Studies have often attributed wildfire to increases in soil hydrophobicity (Krammes and Orborn, 1969; DeBano et al., 1979), which has been shown to lead to a reduction in infiltration capacity (Imeson et al., 1992), an increase in runoff (Campbell et al., 1977; Burke et al., 2005), preferential flow (Ritsema et al., 1993), and reductions in soil moisture retention and evapotranspiration (Imerson

et al., 1992). Ultimately, the induced changes from wildfire will be determined by several factors, which include, but may not be limited to, the natural (pre–fire) hydrophobicity of the soil, total forest biomass (fuel load), soil texture, functional groups produced (amphiphilic vs. aliphatic hydrocarbons), temperatures reached during the fire, soil moisture content, and climatic conditions (Doerr et al., 2000; Chanasyk et al., 2003). As a result, the effects of fire on hydrophobicity is typically site and region specific (Doerr et al., 2000).

In this study, an extensive hydrological knowledge of a moderate–rich fen watershed (Poplar Fen) was utilized, to explore how the hydrologic role of uplands will change following wildfire. The objectives of this study are to: 1) characterize the hydrophysical changes to upland soils at Poplar Fen following wildfire; and 2) explore the potential implications of these changes for post–fire peatland recovery. It is hypothesized that: 1) burned soils will exhibit higher hydrophobicity and lower infiltration rates and moisture retention; 2) which will lead to more surface water ponding and evaporative loss; and 3) will therefore lead to an overall decrease in upland recharge. These results will serve as a baseline for helping predict the fate of moderate–rich fen watersheds in the AOSR that are impacted by wildfire.

5.2 Methodology

5.2.1 Study site and research design

Our study was conducted in the AOSR in northeastern Alberta, located within the Central Mixedwood Subregion of the Boreal Plains Ecozone (Natural Regions Committee, 2006). Here, the climate is defined as sub–humid (Bothe and Abraham, 1993; Marshall et al., 1999), with annual PET exceeding precipitation (P) in most years (Devito et al., 2012). Average annual air temperature (1981–2010) is 1°C; average annual precipitation is 419 mm, with ~75% falling as rain (Environment Canada, 2017). Research was conducted primarily at ‘Poplar Fen’ (56°56′ N, 111°32′; ~320 m ASL), a 2.5 km^2 moderate–rich fen watershed (total relief: ~11 m), located ~25 km north of the town of Fort McMurray (Fig. 5–1) within the Dover Plain region of the AOSR, northern Alberta.

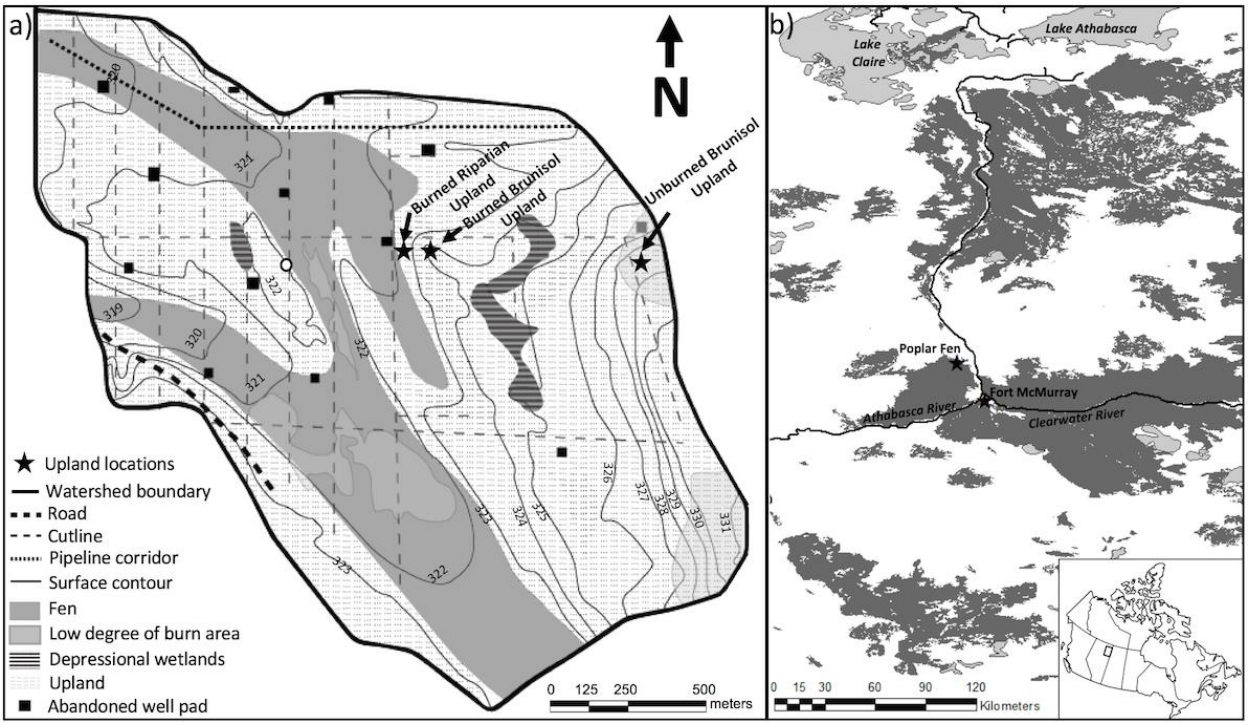

Figure 5–1. Map of the Poplar Fen watershed (**a**; 56°56′ N, 111°32′ W), with unburned areas highlighted in light grey. Included is an inset of the AOSR (**b**) showing total burned area from 1998–2017 (dark grey).

Poplar Fen watershed is characterized by low relief topography (~10 m), with undulating sand and gravel–dominated uplands. Drift is reported to be relatively thin (<20 m) in the study area (Andriashek and Atkinson, 2007) and is dominated by fine to coarse sand with heterogeneous deposits of boulders, gravel, silt, and clay. The site is situated within a ~10 km belt of meltwater channels extending northward to the southern portion of the Syncrude basemine. It was illustrated in chapter 2 that the watershed is underlain by the Cretaceous Clearwater formation, a well–known regional aquitard, as well as a silt–dominated till deposit. These substrates comprise a relatively thick (~16 m) aquitard, which constricts the hydrologic connectivity between the watershed and underlying regional flow systems (chapter 2). Groundwater flow at Poplar Fen is therefore confined to local flow systems which develop from precipitation–driven recharge to mixedwood uplands supplied groundwater to low–lying fen areas, via vertical flow from the underlying outwash aquifer to the base of the peat, and lateral flow from upland to fen. Furthermore, this connection was found to be strongest during periods of high rainfall and moisture availability, and subject to flow reversals during extended dry periods (chapter 2).

Dystric Brunisols have developed over the majority of the sand and gravel–dominated uplands, and are characterized by a relatively thin (<0.1 m) organic layer and a jack pine (*Pinus*

banksiana) and aspen (*Populus tremuloides*) mixedwood overstorey and mixed lichen and bare ground cover with typically low amounts of ground litter. At riparian uplands adjacent to peatland margins, upper soil horizons are characterized by a higher fraction of fine–grained material, as well as a thicker (~0.3 m depth), more well–developed organic layer with a black spruce (*Picea mariana*) overstorey and a feathermoss (*Pleurozium schreberi, Hylocomium splendens*, and *Dicranum polysetum*) dominated surface cover. These contrasting upland locations have been found to differ in their average water table depth as well as soil moisture content, with riparian areas having shallower water tables and higher soil moisture.

It was ultimately the accumulated moisture deficits that occurred between summer 2015 and spring 2016 that led to the burning of Poplar Fen watershed, as part of the greater Horse River Wildfire (Elmes et al., 2018 (chapter 3)). Fen areas experienced a variable degree of burning (moderate–high), with low depth of burn (mean = 2 cm; Elmes et al., 2018 (chapter 3, Table 3–4)), along with a small proportion of area (~7%) left virtually unburned (Fig. 5–1). Conversely, no margin areas were left unburned, and had a higher mean depth of burn (13 cm) relative to fen areas. All riparian uplands burned over, and only a small area of brunisol upland in the eastern portion of the watershed was left unburned (Fig. 5–1). To examine the hydrophysical changes to upland soils following wildfire, four locations were chosen for field and laboratory analyses, a burned and an unburned brunisol upland area, and a burned and an unburned riparian upland area (Fig. 5–1). However, due to the fact that all riparian areas were burned at Poplar Fen, a riparian upland was sampled within an extreme–rich fen watershed located ~2 km northeast of the field site (56°57′9.5” N, 111°31′47.5” W). This site was chosen based on similarities with the riparian uplands at Poplar Fen in their state prior to the fire, including canopy height and density, surface vegetation composition, organic layer thickness, and grain size distribution of the upper ~20 cm of mineral sediment. Prior to all analyses, the top organic layer was removed from the riparian upland until only 3 cm of organic material was left. This was done in order to compare similar substrate depths, due to the significant depth of burn that occurred at this upland location. The following analyses were conducted on all four upland locations to identify any differences between burned versus unburned brunisol and riparian upland locations.

5.2.2 Water droplet penetration time and molarity of ethanol droplet tests

Between 12–14 Sept., 2017, ten 24–cm deep soil cores were obtained from each of the four upland types, with samples typically comprising a ~3 cm thick organic layer with the remaining ~21 cm as mineral sediment. Once cores were obtained, they were wrapped, refrigerated, and shipped to the University of Waterloo Wetlands Hydrology laboratory where they were sectioned into 3–cm stratigraphic intervals. Special care was taken to ensure that the structure of each interval was left intact.

Water droplet penetration time (WDPT) experiments were used as a metric to identify the potential water repellency of field moist samples. WDPT measures the time it takes for a droplet of water to fully infiltrate into the soil surface. Droplets of deionized water (four tests per soil sample) were applied to each interval and WDPT was recorded to the nearest second. This provided 40 measurements of WDPT for each 3–cm stratigraphic interval for each upland type. Measurements were then organized into five different degrees of hydrophobicity based on the categories described by Dekker et al. (2000): hydrophilic (<5 s), slightly hydrophobic (5–60 s), highly hydrophobic (60–600 s), severely hydrophobic (600–3600 s), and extremely hydrophobic (>3600 s).

Following WDPT tests, molarity of ethanol droplet (MED) tests were conducted on all stratigraphic intervals as a supplementary measure of the severity of water repellency (Doerr, 1998). The MED test uses a number of aqueous solutions of varying ethanol concentrations ranging between 0% and 36% (Dekker et a., 2009), and determines the minimum ethanol concentration that can penetrate the soil within 5 s (Letey, 2001). Seven ethanol concentrations were used to classify the severity of water repellency, following the methods outlined in Doerr (1998): 0% (very hydrophilic), 3% (hydrophilic), 5% (slightly hydrophobic), 8.5% (moderately hydrophobic), 13% (strongly hydrophobic), 24% (very strongly hydrophobic), and 36% (extremely hydrophobic). Prior to the MED tests, all samples were oven dried at ~32°C to remove all moisture. The temperature was chosen specifically to not exceed air temperatures measured in the summer in the WBP, while also being low enough to prevent any potential heat–induced increases in hydrophobicity that may occur due to oven drying (Dekker et al., 1998; Doerr, 1998). Samples were then weighed to obtain measurements of field moisture content and bulk density (n

= 10 for each depth interval and upland type). A total of four MED tests were then conducted on all soil samples, yielding a sample size of 40 for each depth interval of each upland type.

5.2.3 Grain size analysis

Following air drying, particle size distribution was measured on a random subsample of soil intervals (excluding organic interval from 0–3 cm depth) from burned (n = 35) and unburned (n = 28) brunisol, and burned (n = 28) and unburned (n = 20) riparian upland samples. Results for each sample were then transformed into relative proportions of sand (0.06–2.0mm diameter), silt (<0.05–0.004 mm diameter) and clay (<0.004 mm diameter). Particle size analysis was conducted at Wilfrid Laurier University using a high-performance laser diffraction analyzer (Horiba LA–960). In order to help disperse the silt and clay fractions, a 0.1% sodium hexametaphosphate solution was used along with a 10 s ultrasonic treatment.

5.2.4 Infiltration tests

To explore the effect of wildfire on infiltration capacity, a series of infiltration tests were conducted between Sept. 12–14, 2017 on randomly–chosen burned (n = 50) and unburned (n = 40) brunisol, and burned (n = 50) and unburned (n = 36) riparian, upland locations, using a 7 cm inner-diameter single–ring infiltrometer. The hydrometeorological conditions during the time of testing were relatively dry, with the watershed only receiving ~7 mm of rainfall over the previous fourteen days, and thus were reflective of meteorological conditions frequently observed in the WBP.

5.2.5 Moisture retention

On the same days that infiltration tests were conducted, six randomly located, 3 cm thick, 7 cm diameter soil cores were extracted from both duff and underlying mineral substrates in the four upland locations (yielding 48 cores total). Cores were first extracted from the duff layer, and following retrieval, the upper mineral layer directly underneath was sampled. Samples were then wrapped, cooled, and shipped to the laboratory. Prior to retention analyses, WDPT experiments (four tests per core) were conducted on the surface of all duff cores, at field moisture, in order to obtain surface WDPT values (n = 24 for each upland type).

Moisture retention experiments were conducted on each soil core using saturated porous plates (Soilmoisture Equipment Corp.) with an air entry pressure of 0.5–bar. Measurements were made in a 5–bar pressure cell (Soilmoisture Equipment Corp.), where cores were subjected to a number of constant tension (ψ) steps (–10, –20, –30, –40, –60, –100, –300, and –500 cm). Following drainage to –500 cm, pressures were reversed to a series of constant steps (–300, –100, –80, –60, –40, –20, and –10 cm) to determine wetting hysteresis. Each pressure step was held for a minimum of 3 days or until equilibrium was reached. The volumetric moisture content (VMC) of each soil core at each pressure step was determined from its saturated weight and volume. Following all moisture retention measurements, soil cores were dried at 60°C for approximately two days to calculate dry bulk density. Saturated volumetric moisture content (θ_s) was assumed to be equal to porosity. MED tests (4 tests per core) were then conducted on the surface of the dried duff cores, yielding an n of 24 for each of the four upland categories.

Following retention experiments, retention data (drying only) from each soil core were modelled in the RET–C curve fitting program (van Genuchten et al., 1991) using the van Genuchten/Mualem (van Genuchten, 1980):

$$\theta = \theta_s\,[1 + (\alpha\psi)^n]^m, \qquad (5–1)$$

where α is related to the inverse of air entry tension (cm^{-1}), n is a measure of the pore size distribution, and m = 1–1/n. θ_r, the residual volumetric moisture content, is determined by using the fitting parameters to predict θ at –1500 cm, the permanent wilting point (van Genuchten, 1980).

5.2.6 Field Hydrological Data

Field hydrometeorological data were obtained in the summer of 2016, following the fire on May 17, 2016. Ground heat fluxes were measured in the burned and unburned brunisol upland locations by two replicate ground heat flux plates (HFP01; Huskeflux Thermal Sensors, Delft, Netherlands) placed 2 cm under the soil surface. Within the same locations, a Stevens Hydra Probe II was placed horizontally into the top 3 cm of upland soil. Precipitation was measured in two open upland areas with a logging Onset RG3–M tipping bucket rain gauge. Interception loss was measured in burned and unburned brunisol locations by measuring throughfall, which was routed through PVC rain gutters and into sealed containers (three replicates for burned and two for

unburned). Manual rain gauges were also installed in close proximity to these locations in an open portion of the upland. These data will be presented in the discussion section when addressing the implications of the changes to water repellency and the hydrophysical properties of upland soils to the hydrologic function of the watershed.

5.2.7 Numerical Analyses

To test for significant differences between burned and unburned uplands, a suite of statistical analyses were employed and conducted separately for brunisol and riparian upland samples. First, a chi–square goodness of fit test was conducted on particle size data, to identify whether there were significant differences in the average proportions of sand, silt, and clay between burned and unburned locations. For WDPT, a series of depth–specific Mann–Whitney–Wilcoxian tests were conducted to test for significant differences in WDPT between burned and unburned uplands. Tests were conducted separately for each depth interval (e.g. burned vs. unburned brunisol upland WDPT at 0–3 cm). Then, for the MED data, a series of chi–square goodness of fit tests were conducted to test for significant differences in the average proportion of MED classes between burned and unburned uplands, using the same depth interval–specific methods. For infiltration data, Mann–Whitney–Wilcoxian tests were conducted to test for significant differences in infiltration rates between burned and unburned uplands. Lastly, using the modeled retention data for each soil core, curve–fitting parameters θ_r, a, and n were tested for significant differences between burned and unburned locations using a series of *t*–tests. The *t*–tests were conducted separately for brunisol and riparian locations and for duff and mineral cores. *t*–tests were also employed to test for significant differences in bulk density between burned and unburned retention cores, and were tested individually for brunisol duff and mineral, and riparian duff and mineral, cores (4 tests total).

5.3 Results

5.3.1 Grain Size

Grain size distribution results indicate significantly (X^2 (4, N = 63) = Inf., $p < 0.05$) different proportions of sand, silt, and clay in burned (0.836, 0.162, and 0.002, respectively) and unburned (0.920, 0.080, and 0.000, respectively) brunisol upland soil samples; however, both locations were dominated primarily by sand (Fig. 5–2). The burned brunisol upland samples

ranged from a sand to sandy loam soil, and all unburned upland samples were characterized as sand, with the exception of one sample characterized as loamy sand. No clay was detected in any of the unburned brunisol upland samples, whereas 40% of burned brunisol upland samples had proportions of clay ranging from 0.1–1.4 %. Silt proportions were also ~2 times higher on average than that which was measured in the unburned brunisol upland samples (Fig. 5–2). For riparian upland areas, grain size distributions showed significantly different (X^2 (2, N = 48) = 99.7, p< 0.05) proportions of sand, silt, and clay in burned (0.556, 0.306, 0.138) and unburned (0.571, 0.366, 0.063) locations. Samples from both locations ranged from sandy loam to sandy clay loam, with one burned riparian upland sample characterized as clay loam. The majority of burned riparian upland samples had higher proportions of clay, with values 2.2 times greater on average. In general, riparian upland samples had higher proportions of silt and clay than brunisol upland samples (Fig. 5–2).

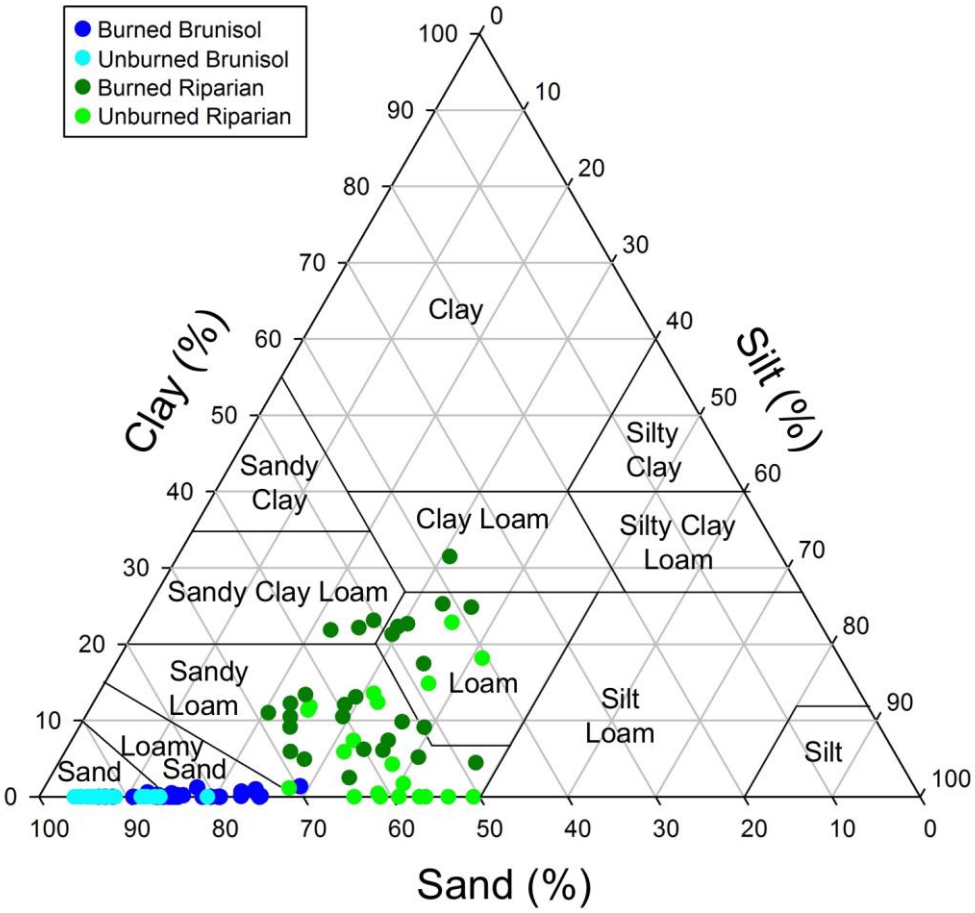

Figure. 5–2 Relative proportions of sand, silt, and clay for burned and unburned brunisol and riparian upland soil samples obtained at Poplar Fen. Samples are overlying a soil texture triangle with the 12 basic texture classes outlined by the USDA (Soil Science Division Staff, 2017).

5.3.2 Water Repellency

Water droplet penetration times differed significantly (p <0.05) for the majority of depth intervals between burned and unburned brunisol and riparian upland soil cores (Fig. 5–3a; see asterisks). A greater degree of water repellency was measured on the surface of the unburned rather than burned brunisol upland. Below the ground surface, burned brunisol uplands exhibited greater WDPT at all depth intervals, with burned and unburned differing significantly at all intervals except 0–3 cm and 12–15 cm below ground surface (b.g.s) (Fig. 5–3a). MED test results yielded significant differences between burned and unburned brunisol upland samples at all intervals (Fig. 3b). Corresponding closely to the results of the WDPT tests, MED was higher at the surface in unburned brunisol samples. Below the ground surface, MED was higher in burned brunisol upland samples at all intervals except 9–15 cm b.g.s. (Fig. 5–3b).

Compared to brunisol uplands, riparian upland samples exhibited greater differences in water repellency between burned and unburned samples. WDPT was significantly different at all depth intervals except 18–21 and 21–24 cm b.g.s, with WDPT lower in burned riparian upland samples at all intervals except 21–24 cm b.g.s. (Fig. 5–3a). The greatest differences were detected within the upper 12 cm. For example, unburned riparian upland samples within this range were characterized primarily as strongly to extremely hydrophobic, whereas burned samples were characterized more as hydrophilic to slightly hydrophobic (Fig. 5–3a). MED tests yielded results which corresponded closely to the WDPT results. However, depth intervals were classified entirely as very hydrophilic below 12 cm b.g.s. at unburned locations, and below 6 cm b.g.s. at burned locations. Significant differences in MED were detected between burned and unburned riparian upland samples from surface to 12 cm b.g.s. (Fig. 5–3b).

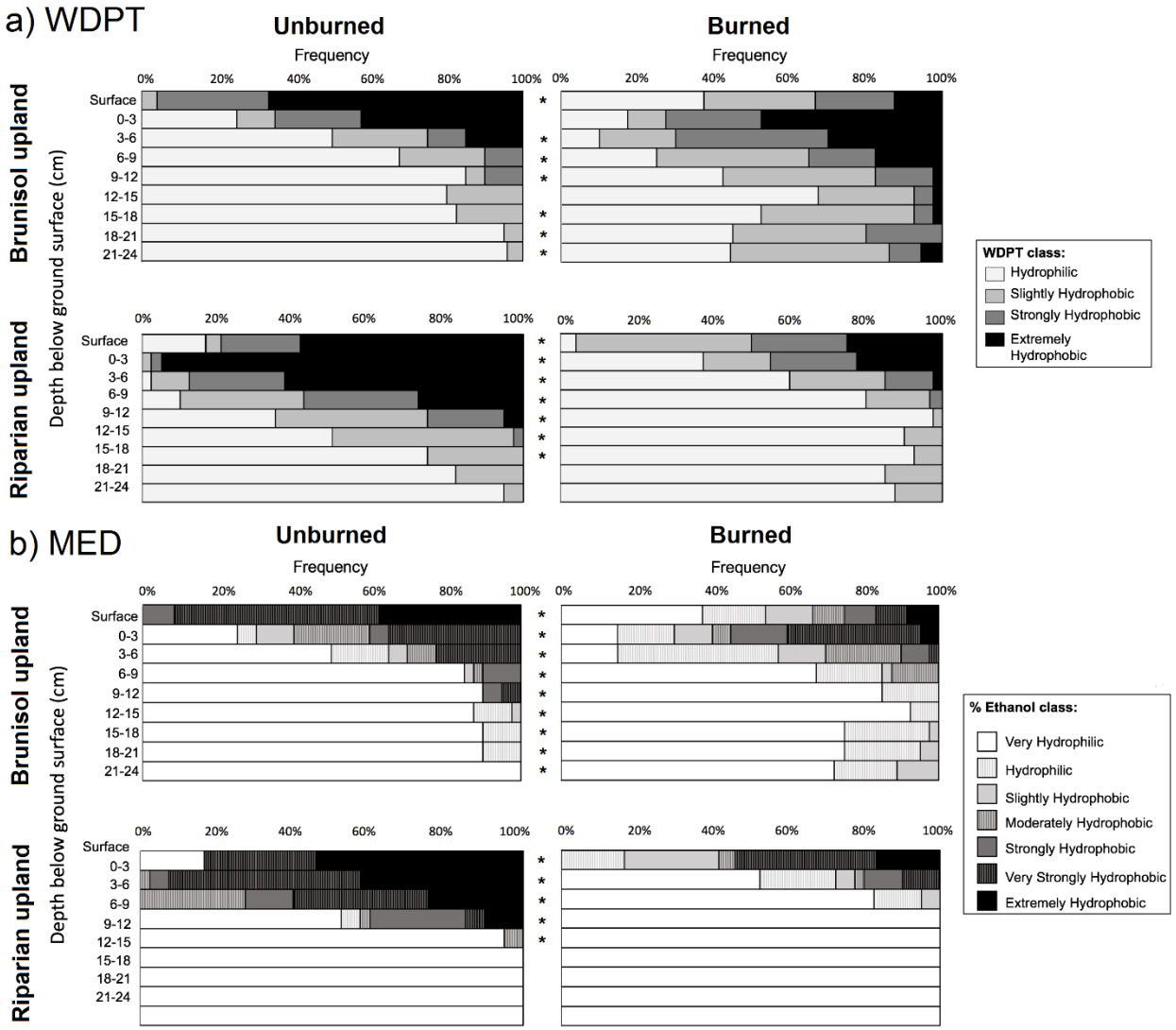

Figure. 5–3. Relative frequency of (**a**) WDPT and (**b**) MED results for surface (n = 24 at each location) and below ground surface (n = 40 for each depth interval at each location). Asterisks denote depth intervals where significant differences were detected between burned and unburned samples.

5.3.3 Organic layer bulk density

No significant differences ($t_{17.5}$ = 1.1; p = 0.28) were detected in the bulk density of the burned (mean = 1.7 ± 0.6 (SD) g cm^{-3}) and unburned (mean = 1.4 ± 0.7 (SD) g cm^{-3}) brunisol upland organic (0–3 cm) layer. However, significant differences ($t_{14.3}$ = 5.4; p = 0.0001) were detected in the bulk density of the burned (mean = 0.89 ± 0.3 (SD) g cm^{-3}) and unburned (mean = 0.37 ± 0.15 (SD) g cm^{-3}) riparian upland organic layer. Mean bulk density was higher in both burned uplands relative to the respective unburned locations.

5.3.4 Infiltration

Infiltration rates were higher in burned compared to unburned locations at both brunisol and riparian upland locations (Fig. 5–4). For brunisol uplands, average infiltration rates for burned and unburned locations were 1036 and 467 mm hr^{-1}, respectively, and their medians (burn = 327 mm hr^{-1}; unburned = 702 mm hr^{-1}) were significantly different from one another (W = 1386; p = 0.0006). For riparian uplands, average infiltration rates for burned and unburned locations were 1741 and 1011 mm hr^{-1}, respectively, and their medians (burn = 711 mm hr^{-1}; unburned = 1391 mm hr^{-1}) were also significantly different from one another (W = 1276; p = 0.0009). Burned locations also had more extreme outliers than their corresponding unburned locations, with rates reaching as high as 6200 and 6915 mm hr^{-1} for burned brunisol and riparian locations, respectively (Fig. 5–4).

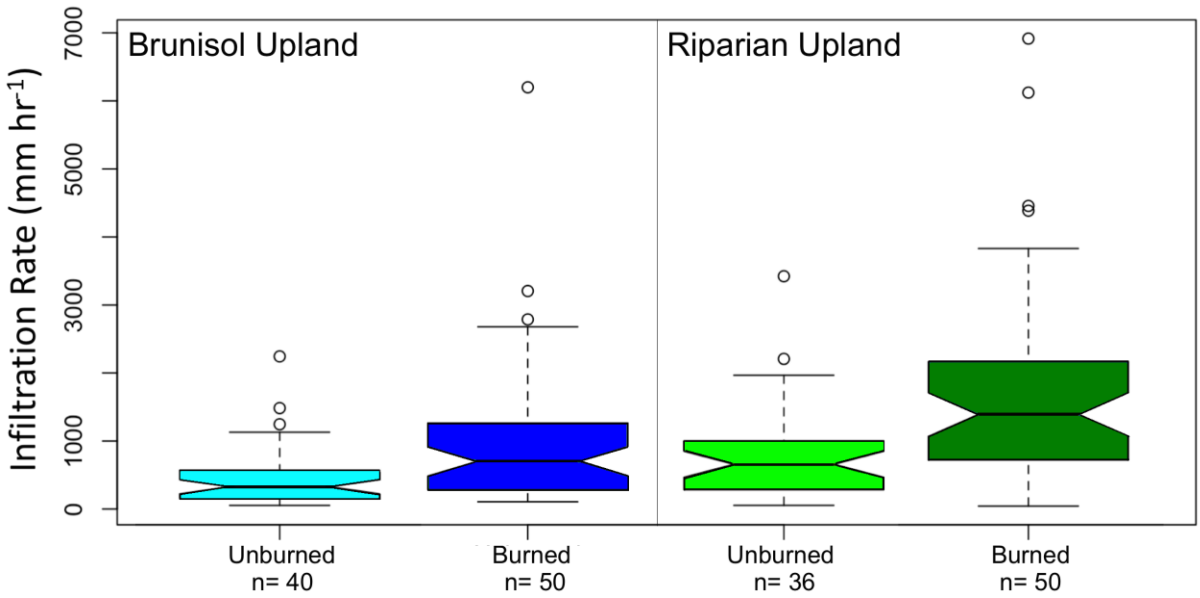

Figure 5–4. Notched boxplots of infiltration rate in burned and unburned brunisol and riparian upland locations.

5.3.5 Moisture Retention

Throughout the series of pressure steps, the measured volumetric moisture contents (VMC) from cores obtained from burned and unburned brunisol uplands exhibited little discernible differences in either duff or mineral cores (Fig. 5–5). Measured VMC at –500 cm was not significantly different for duff (mean: burned = 0.18; unburned = 0.18) or mineral (mean: burned = 0.13; unburned = 0.12) cores. There were also no significant differences for the modeled curve–

fitting parameters α (inverse of air entry pressure) *n* (pore size distribution), as well as θ_r for duff (mean θ_r: burned = 0.19; unburned = 0.20) and mineral (mean θ_r: burned = 0.15; unburned = 0.12) samples. On average, whether burned or unburned, duff soil cores obtained from brunisol uplands exhibited greater moisture retention than the underlying mineral soil cores. Following retention, the rewetting curves for all brunisol cores exhibited high hysteresis (Fig. 5–5), averaging 0.38 ± 0.06 (SD) at –10 cm.

Larger differences between burned and unburned retention were measured in the riparian upland duff and mineral cores, with the greatest differences in the duff cores (Fig. 5–5). For example, measured values of VMC at –500 cm were significantly different ($t_{8.3} = –3.8$; $p = 0.005$) between burned (mean = 0.27) and unburned (mean = 0.40) duff. No significant differences were detected between the modeled curve–fitting parameters α and *n*, however, values of θ_r were significantly different ($t_{9.1} = –3.5$; $p = 0.007$) between burned (mean = 0.24) and unburned (mean = 0.39) riparian upland duff samples. Despite notably different values of VMC at –500 cm between burned (mean = 0.19) and unburned (0.26) riparian upland mineral samples (Fig. 5–5), these differences were not significantly different from one another ($t_{8.0} = –2.2$; $p = 0.064$). No significant differences were detected in α and calculated θ_r (mean: burned = 0.20; unburned = 0.23); however, there were significant differences ($t_{5.3} = 2.6$; $p = 0.047$) in *n* between burned (mean = 2.9) and unburned (mean = 1.6) mineral cores. Following retention, the rewetting curves for all riparian cores exhibited high hysteresis (Fig. 5–5), with the difference in VWC between drying and wetting curves averaging 0.34 ± 0.08 (SD) at –10 cm.

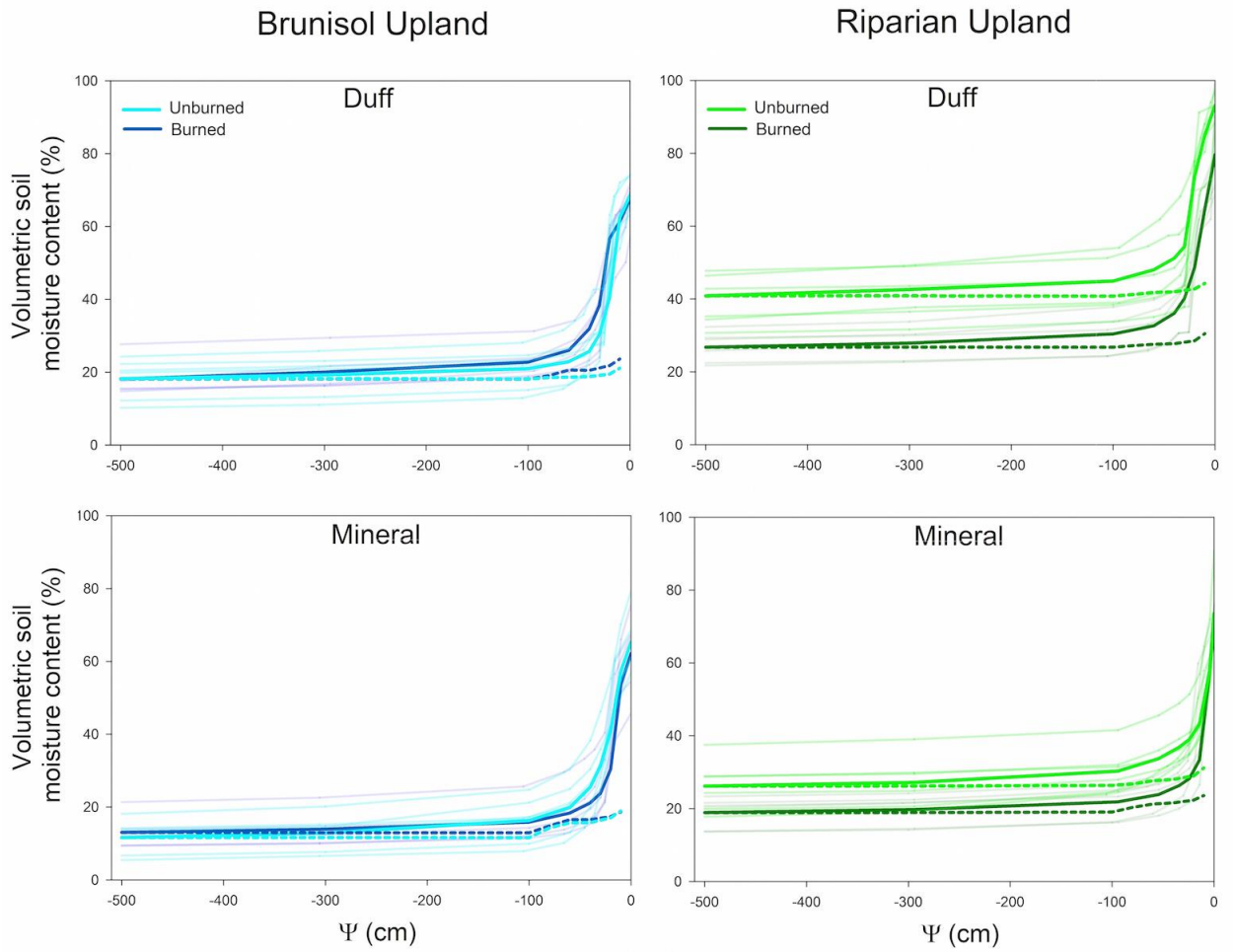

Figure 5–5. Measured soil–water retention, θ(ψ), for burned and unburned, brunisol and riparian, duff and mineral cores, along with average hysteresis (dash lines). All retention curves are plotted individually (see faint lines) and average wetting and drying curves are also plotted (bold lines).

5.4 Discussion

5.4.1 Changes to water–repellency following wildfire

Results from the WDPT and MED tests demonstrated differences in water repellency between burned and unburned uplands and with depth. For example, a stronger degree of water repellency was detected directly on the surface of unburned compared to burned brunisol upland soil cores (Fig. 5–3), and the 0–3 cm (organic) layer remained high in both cases (Fig. 5–3). These results suggest the organic layer, composed primarily of lichen and jack pine needles, contains a high degree of naturally occurring hydrophobic substances from a variety of sources (e.g. epicuticular waxes; Richardson and Hole, 1978). Lower water repellency at the surface of burned upland locations suggests that wildfire had destroyed a greater proportion of natural hydrophobic

substances than that was induced by the fire. Fire has not always been shown to enhance the hydrophobicity of a soil. For example, Doerr et al. (1996) did not find fire to enhance hydrophobicity on the surface of *Eucalyptus globulus* and *Pinus pinaster* forests in Portugal. Despite these measured differences, there are potential limitations involved in sampling unburned locations within close–proximity to a fire–affected area, given the potential for atmospheric transport and deposition of fire–induced hydrophobic substances onto nearby unburned areas.

Unlike in the organic layer, the mineral (3–24 cm b.g.s) intervals of the burned brunisol upland samples demonstrated higher water repellency. Higher water repellency at measured intervals suggests the potential for volatilisation of heated hydrophobic organic substances and subsequent downward migration along the temperature gradient (DeBano and Krammes, 1966., DeBano et al. 1970; DeBano, 2000). Wildfire has been shown to either increase or decrease the water repellency of sandy soils that are naturally hydrophilic or hydrophobic, respectively (DeBano and Krammes, 1966., DeBano et al. 1970). Thus, given the relatively low water repellency in the mineral layer prior to burn, an increase in hydrophobicity at depths below the organic layer would be expected.

For riparian upland locations characterized by finer–grained (loamy) soils (Fig. 5–2) and organic layers composed primarily of decomposed feathermosses, water repellency was significantly lower in burned samples at all depth intervals (including surface) above 18 cm (Fig. 5–3). These results did not conform to the initial hypotheses, and for duff cores were contrary to samples obtained from a feathermoss–dominated peatland ~270 km southwest of Poplar Fen, where a greater degree of water repellency was measured in burned than unburned feathermosses (Kettridge et al., 2014). The high degree of hydrophobicity in the unburned riparian upland location (Fig. 5–3) suggests that the organic layer exhibits a strong degree of natural hydrophobicity, which is likely enhanced by the low humidity (Burles and Boon, 2011) and soil moisture (Devito et al., 2012; Elmes et al., 2018 (chapter 3)) typically found in the WBP.

Similar to the organic layer, water repellency of the riparian upland mineral layer was significantly lower at all intervals above 18 cm b.g.s. This suggests that the relatively high degree of water repellency that existed naturally was compromised by the wildfire. Savage (1974) and DeBano et al. (1976) found that hydrophobic substances are destroyed above a certain threshold

temperature (270–300°C). Given the thickness of the organic layer and thus high fuel load and potential for exceeding the temperature threshold of repellency destruction relative to brunisol upland areas, there is greater potential for destruction of hydrophobic substances relative to the brunisol upland areas that are characterized by a thinner organic layer.

Between both burned locations, the brunisol upland exhibited a greater degree of water repellency at all depths below ground surface (Fig. 5–3). This would be expected given the observed differences in grain size between upland types (Fig. 5–2), and how hydrophobic substances typically impose a greater influence on water repellency in coarse–grained soils characterized by relatively low surface areas (DeBano et al., 1970; Roberts and Carbon, 1971). Conversely, a greater level of water repellency was measured in the upper 15 cm (excluding the surface) of unburned riparian soils compared to brunisol upland soil samples (Fig. 5–3). This was not expected, considering the proportion of silt and clay comprising riparian uplands (Fig. 5–2) and therefore greater surface area, decreasing the susceptibility of developing water repellency (DeBano et al., 1970; Cann and Lewis, 1994). It is likely that the relatively low clay content of the unburned riparian location (range = 0–23%; mean = 6±7(SD)%) compared to the more widespread fine–grained soils in the WBP (e.g. grey luvisols; Soil Classification Working Group, 1998) was not sufficiently large to significantly minimize the effect of leaching of naturally–derived hydrophobic substances from the relatively thick organic layer. It is anticipated that these ubiquitous riparian uplands in the AOSR will exhibit similar degrees of water repellency to that which was measured at Poplar Fen.

5.4.2 Changes to infiltration rates following wildfire

Contrary to the initial hypotheses, significantly higher infiltration rates were measured at the burned locations of both upland types (Fig. 5–4). Regardless of the pre–existing water repellency prior to the fire, an overall decrease in infiltration rates following fire would be expected, as runoff and erosion are typically mitigated by a plant and litter cover (Brock and DeBano, 1990). However, increased infiltration rates are consistent with the hydrophobicity results, which showed significantly lower water repellency at the surface of both burned upland locations, and either significantly lower or no detected differences within the organic layer (0–3 cm b.g.s.). And despite these differences, the lowest infiltration rates measured at these locations

(53–106 mm hr^{-1}) are sufficiently high to infiltrate the relatively mild and short duration convective cell precipitation events characteristic of the sub–humid WBP (Smerdon et al., 2005).

5.4.3 Changes to moisture retention and wettability following wildfire

Results suggest that wildfire had little effect on moisture retention of the upper mineral layer of both locations, and surprisingly, no detectable impact on the water retention capacity of the organic layer of brunisol uplands. Conversely, fire and subsequent combustion of riparian uplands transformed the relatively thicker (~30 cm) organic layer to an average post–fire thickness of ~3 cm. When compared to the bottom 3 cm of unburned riparian upland soils, significant differences in their retention were measured. This demonstrates that wildfire reduced their water holding capacity. Significantly higher bulk density was detected in the upper organic layer of burned versus unburned riparian uplands. Contrary to other unburned organic soils (i.e. peat), where retention is positively correlated with bulk density, the opposite was measured in the soil cores in this study. It is speculated that increases in bulk density were due primarily to the deposition of ash from overlying layers that were decimated by the fire, which may not exhibit a high water holding capacity.

Following retention, all cores exhibited extreme wetting hysteresis, suggesting that these uplands are likely to exhibit relatively poor retention and wettability under the typically dry conditions characteristic of the WBP (Burles and Boon, 2011).

5.4.4 Implications for the hydrologic functioning of Poplar Fen

Due to the regional position of Poplar Fen, situated within the relatively flat Dover Plains region of the AOSR (Andriashek, 2003), the undulating (0.5–1.5% slope) coarse–grained (Fig. 5–2) uplands have not been found to contribute surface runoff to fen areas during snow–free periods from 2011–2017. In chapter 2, the importance of precipitation–driven recharge to adjacent uplands was discussed, as a means of generating the lateral (upland to fen margin to fen) and vertical (underlying outwash to fen) local groundwater flow systems responsible for sustaining fen water tables and preventing water table drawdown. Moreover, between 2011–2015 (pre–fire), a transmissivity feedback mechanism was detected during periods when precipitation was sufficiently high to: 1) raise the fen water table to shallower layers characterized by a higher

specific yield and saturated hydraulic conductivity; and 2) elevate the upland water table and sustain strong horizontal hydraulic gradients between upland and fen (chapter 2). From the results of this study, it is proposed that reductions in surface water repellency and increases in infiltration rates due to wildfire will severely restrict surface water ponding and limit evaporative loss at both burned upland types. Although contrary to the initial hypotheses, these overall changes in water repellency and infiltration rates induced by the fire, combined with an 35% average decrease in interception loss measured throughout the 2016 growing season (appendix A.2), will likely enhance water table recharge at Poplar Fen.

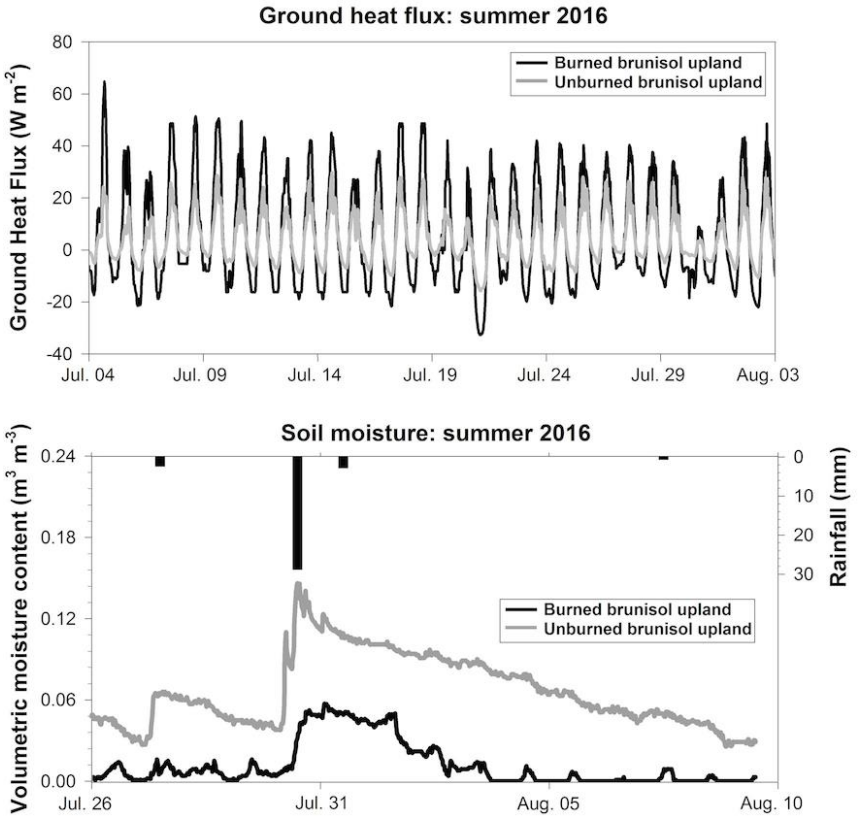

Figure 5–6. Measured ground heat flux (Q_G) and near surface (0–3 cm b.g.s.) volumetric moisture content in burned and unburned brunisol upland duff locations at Poplar Fen during the summer of 2016 following the fire (May. 17).

The uplands of Poplar Fen will also likely experience a net gain in groundwater recharge due to changes in evapotranspiration. For example, the decimation of upland vegetation will result in temporary decreases in transpiration until vegetation has regenerated. Rapid regeneration of aspen saplings was identified by the end of the 2016 growing season, which may continue to draw water from the upland and peatland margins via hydraulic lift (Depante et al., 2016). However, a

large proportion of brunisol upland areas dominated by jack pine were left completely devoid of regenerated aspen, and essentially unvegetated by the fall. Moreover, afternoon (15:00–16:00) Q_G was ~2.3 times higher on average in burned relative to unburned brunisol uplands (Fig. 5–6), due to the decimation of the canopy and reductions in albedo, leaf–area index, and radiation interception by the canopy (Amiro, 2001; Sass et al., 2006). These higher ground temperatures ultimately led to an enhanced drying of near–surface soil prior to rain events in burned brunisol upland locations (Fig. 6), and it is postulated that this would increase the water repellency and wetting hysteresis of the soil. Lower VMC (by 3–11%) was measured in the upper 3 cm of soil, prior to, and after a 29 mm rain event in late July, 2016, which then reduced to residual moisture content after 3 rain–free days (Fig. 5–6). Thus, the relatively high ground heat fluxes and low moisture contents reduced the wettability and therefore retention of the soil, reducing the amount of soil moisture available at the surface for evaporation.

5.5 Conclusions

Water repellency was found to be significantly reduced at the surface of burned versus unburned brunisol and riparian uplands. As a result, infiltration rates were significantly higher in both burned uplands relative to their respective unburned locations. Despite the relatively high degree of burning observed following the fire, no significant differences were detected in the moisture retention of burned and unburned brunisol upland duff cores, nor were they detected in the upper 3 cm of mineral soil in either brunisol or riparian uplands. However, due to the extreme hysteresis detected in these soils, combined with the higher ground heat fluxes and lower soil moisture, burned soils may exhibit a greater degree of water repellency during extended dry periods. Conversely, burned riparian upland duff cores exhibited lower water retention than unburned cores, likely due to the relatively high degree of burning (via greater fuel load), and subsequent destruction of the physical soil structure. Below the organic layer, brunisol uplands exhibited a significant increase in hydrophobicity; however, riparian uplands exhibited a significant decrease in hydrophobicity. These differences were likely attributed to a combination of site specific characteristics, including vegetation type, fuel load, pre–fire soil hydrophobicity, grain size, and fire duration and temperatures reached. Despite these differences, changes to the hydrophysical properties of upland soils are not expected to reduce water table recharge. This will

help in providing optimal recharge to the local flow systems which provide discharge to lower–lying fen areas and prevent fen water table drawdown, thus accelerating the moss recovery process.

5.6 Acknowledgments

The authors wish to thank C. Van Beest, O. Sutton, C. Cameron, T–L. Van Huizen, and B. Gharedaghloo for their work in the field or laboratory. We gratefully acknowledge funding from a grant to Jonathan S. Price from the National Science and Engineering Research Council (NSERC) of the Canada Collaborative Research and Development Program, co–funded by Suncor Energy Inc., Imperial Oil Resources Limited, and Shell Canada Energy

6 Summary and conclusions

The preceding thesis presented a comprehensive overview of the hydrologic setting and regime of a moderate–rich fen watershed in the AOSR of the WBP. The results will help refine the conceptual model of water movement in the WBP, specifically for base–rich fens overlying thin veneer–type (coarse over fine) glacial sediments. Contrary to bog and poor–fen systems studied throughout the WBP (Ferone and Devito, 2004; Scarlett and Price., 2013; Wells et al., 2017), the results presented in this thesis highlight the dynamic connection of moderate–rich channel fen areas, as well as margins, to local groundwater flow systems, which develop in adjacent topographic highs. Given the reliance of discharge function at Poplar Fen to diurnal trends in precipitation, these systems will likely become more vulnerable to flow reversals and water table drawdown under anticipated climate change scenarios, as increases in precipitation in northern regions will likely be insufficient to effectively offset increases in evapotranspiration (Collins et al., 2013).

A distinctly different response to climate change is expected for Poplar Fen compared to peatlands connected to deeper flow systems (Siegel and Glaser, 1987; Winter et al., 2003; Smerdon et al., 2005; Kløve et al., 2012), where water table drawdown is expected to be partially moderated by more consistent sources of groundwater discharge. Given that groundwater flow in and out of margins was strongest during wet periods, long–term changes to their hydrologic function are expected due to climate change. Specifically, these margins in the future will likely exhibit water table positions more similar to those observed during dry years (2011, 2015). Thus, margins will likely receive less groundwater from the upland, ultimately influencing transmissivity feedback to the channel fen, while also providing less vertical recharge to the local flow systems that discharge under the channel fen. Subsequently, channel fen areas are expected to undergo numerous changes, including lower average annual water tables similar to those observed in 2011 and 2015, as well as changes to peat porewater chemistry (e.g. lower pH and cation concentrations) due to reductions in groundwater discharge from upland and margin as well as from the underlying outwash aquifer. This will likely accelerate the general shift from rich to poor fen to bog, due to long–term changes to the hydrological processes (groundwater discharge) which mediate *Sphagnum* acidification (Kuhry et al., 1993).

The hydrological results reported in chapters 2 and 4 highlight the susceptibility of the Poplar Fen watershed to water table drawdown and subsequent drying over extended drought periods, and it was ultimately these dry conditions, which extended back to summer 2015, that rendered the watershed vulnerable to burning in May of 2016. These dry hydrometeorological conditions (outlined in chapter 3), however, are a regular occurrence in the sub–humid WBP, which helps explain why it is a wildfire–dominated region. And as these dry conditions are expected to be enhanced by climate change, watersheds similar to Poplar Fen may therefore become increasingly vulnerable to wildfire over time. As the watershed underwent a variable, yet considerable degree of burning, there was potential for wildfire to affect the hydrophysical properties of the upland soils, and therefore the overall connectivity of the watershed. The results of chapter 5 provide important insight for the implications of wildfire on the functioning of this watershed, which may serve as an analogue for other watersheds in the WBP with a similar hydrogeologic setting. Surprisingly, lower water repellency was measured in the organic layer of burned relative to unburned uplands at Poplar Fen, as well as higher infiltration rates. Therefore, a net gain in recharge to upland water tables is anticipated, and this feedback is expected to be further enhanced in riparian areas by the lower duff moisture retention that was measured in burned locations. Considering the importance of uplands for sustaining the local groundwater flow systems at Poplar Fen, the net gain in recharge will play an important role in optimizing lateral discharge from upland to margin to fen, and vertical discharge between the fen and underlying outwash aquifer. This important feedback will enhance the moisture conditions necessary for peatland moss recovery, and will become increasingly important under future anticipated climate change scenarios, as the WBP is expected to become more water–stressed over time.

Given that this was the first extensive hydrological study of a moderate–rich fen watershed in the AOSR, these findings may not apply to all associated fen systems in the region. Slight modifications in geologic setting parameters, including grain size, relief, topographic position, and parent material may result in large differences in the degree of connectivity between fen areas and groundwater flow systems of various scales (local, intermediate, and regional). For example, moderate–rich fens connected to larger groundwater flow systems may be more resilient to water table drawdown and acidification, as discharge may be sourced from groundwater characterized by much longer travel times (tens to hundreds of thousands of years), and can therefore partially offset reductions in precipitation and maintain base–richness. Moreover, fens which receive more

nutrient–poor (oligotrophic) groundwater may have a similar hydrologic function to Poplar Fen, but may function as poor–fens. Therefore, additional studies should be conducted on fens elsewhere throughout the AOSR and greater WBP, to better understand the range of natural variability in their hydrologic function. This will help in broadening our understanding of the susceptibility of these systems to present and future stressors.

6.1 Recommendations for fen reclamation

Considerable time, effort, and resources have been invested in oil sands wetland reclamation in recent years. Regulatory requirements require mined lands to be returned to the crown in a state of 'equivalent capability' (OSWWG, 2000), and reclamation has therefore focused on testing the feasibility of engineering fen peatlands (i.e. Nikanotee Fen watershed: Price et al., 2010; Ketcheson et al., 2016; 2017). Reclaimed watersheds must be engineered as 'closed' local systems to minimize hydrological connectivity with the regional water table (Price et al., 2010), at least during the period of mine operation. The results presented in this thesis suggest that the hydrologic function of natural fen systems (i.e. moderate–rich fens) in the AOSR can be replicated. The physiography of Poplar Fen, including coarse–grained drift, low relief, veer–type (coarse over fine) layering, and shallow depth to confining layer, are all conducive for generating local flow–systems in the sub–humid WBP. However, considering the susceptibility of fen watersheds with local flow systems to drying over WBP climate cycles, fen reclamation should focus on engineering landscapes to minimize vertical flow reversals, water loss, and susceptibility to carbon degradation from enhanced decomposition and/or wildfire. In addition, given the ubiquity of margins, and their importance as facilitators of groundwater recharge, consideration should be given regarding their inclusion on these engineered landscapes. However, given the similarities of margin porewater chemistry to uplands at Poplar Fen, special consideration will be needed for their design on constructed fen watersheds, to enhance vertical recharge, while reducing lateral flow, to avoid fens being subject to strong inflows from upland oil sands process–affected water.

7 References

Abatzoglou JT, Kolden CA. 2011. Relative importance of weather and climate on wildfire growth in interior Alaska. *International Journal of Wildland Fire*, **20**: 479–486, DOI: 10.1071/WF10046.

Adkinson AC, Syed KH, Flanagan LB. 2011. Contrasting responses of growing season ecosystem CO_2 exchange to variation in temperature and water table depth in two peatlands in northern Alberta, Canada. *Journal of Geophysical Research*, **116**: 17pp., DOI: 10.1029/2010JG001512.

Alberta Agriculture and Forestry. 2017. *Alberta Climate and Information Service*. Available at: http://agriculture.alberta.ca/acis (last access: 28 Aug. 2018).

Alberta Environment. 2014. *Guidelines for Wetlands Establishment on Reclaimed Oil Sands Leases, 3rd Edition*. Edited by West Hawk Associates for the Reclamation Working Group and the Aquatic Sub-Group and Wildlife Task Group of the Cumulative Environmental Management Association, Fort McMurray, AB.

Alexander ME. 1982. *Calculating spring Drought Code starting values in the Prairie Provinces and Northwest Territories*. Environment Canada, Canadian Forestry Service, Northern Forest Research Centre, Edmonton, Alberta, Edmonton, AB. For. Manag. Note 12, 4 pp., available at: https://cfs.nrcan.gc.ca/publications?id=11559 (last access: 28 Aug. 2018).

Alm J, Talanov A, Saarnio S, Silvola J, Ikkonen E, Aaltonen H, Nykänen H, Martikainen PJ. 1997. Reconstruction of the carbon balance for microsites in a boreal oligotrophic pine fen, Finland. *Oecologia*, **110**: 423–431, DOI: 10.1007/s004420050177.

Amiro BD. 2001. Paired–tower measurements of carbon and energy fluxes following disturbance in the boreal forest. *Global Change Biol*ogy, **7**(3): 253–268, DOI: 10.1046/j.1365-2486.2001.00398.x.

Amiro BD, Cantin A, Flannigan MD, de Groot WJ. 2009. Future emissions from Canadian boreal forest fires. *Canadian Journal of Forest Res*earch, **39**: 383–395, DOI: 10.1139/X08-154.

Andriashek LD. 2003. *Quaternary geological setting of the Athabasca oil sands (in situ) area, northeast Alberta*. EUB/AGS Geo-Note 2002-03, Alberta Energy and Utilities Board, Edmonton, Alberta, 295 pp.

Andriashek LD, Atkinson N. 2007. *Buried channels and glacial-drift aquifers in the Fort McMurray region, northeast Alberta*. Geol Surv Earth Sci Rep 01, Alberta Energy and Utilities Board, Edmonton, AB, 170 pp.

Bachu S, Underschultz BH, Hitchon B, Cotterill D. 1993. *Regional-Scale Subsurface Hydrogeology in Northeastern Alberta*. Alberta Geological Survey, Edmonton, AB, 49 pp., available at: https://ags.aer.ca/document/BUL/BUL_061.pdf (last access: 28 Aug. 2018).

Barr AG, van der Kamp G, Black TA, McCaughey JH, Nexic Z. 2012. Energy balance closure at the BERMS flux towers in relation to the water balance of the White Gull Creek watershed 1999–2009. *Agricultural and Forest Meteorology*, **153**: 3–13, DOI: 10.1016/j.agrformet.2011.05.017.

Bauer IE, Bhatti JS, Swanston C, Wieder RK, Preston CM. 2009. Organic Matter Accumulation and Community Change at the Peatland– Upland Interface: Inferences from ^{14}C and ^{210}Pb Dated Profiles. *Ecosystems,* **12**: 636–653, DOI: 10.1007/s10021-009-9248-2.

Benscoter BW, Wieder RK. 2003. Variability in organic matter lost by combustion in a boreal bog during the 2001 Chisholm fire. *Canadian Journal of Forest Res*earch, **33**: 2509–2513. DOI: 10.1139/x03-162.

Benscoter BW, Thompson DK, Waddington JM, Flannigan MD, Wotton BM, de Groot WJ, Turetsky MR. 2011. Interactive effects of vegetation, soil moisture and bulk density on depth of burning of thick organic soils. *International Journal of Wildland Fire,* **20**: 418–429, DOI: 10.1071/WF08183.

Benscoter BW, Vitt DH. 2008. Spatial Patterns and Temporal Trajectories of the Bog Ground Layer Along a Post-Fire Chronosequence. *Ecosystems*, **11**: 1054–1064, DOI: 10.1007/s10021-009-9178-4.

Beylea LR, Baird AJ. 2006. Beyond "The limits to peat bog growth": cross-scale feedback in peatland development. *Ecological Monographs*, **76**(3): 299–322, 2006, DOI: 10.1890/0012-9615(2006)076[0299:BTLTPB]2.0.CO;2

Bhatti JS, Errington RC, Bauer IE, Hurdle PA. 2006. Carbon stock trends along forested peatland margins in central Saskatchewan. *Canadian Journal of Soil Sci*ence, **86**: 321–333, DOI: 10.4141/S05-085.

Bishop KH. 1991. *Episodic increase in stream acidity, catchment flow pathways and hydrograph separation*. Doctoral Dissertation, University of Cambridge, 246 pp.

Bothe RA, Abraham C. 1993. Evaporation and evapotranspiration in Alberta 1986 to 1992 addendum, Surface Water Assessment Branch, Technical Services & Monitoring Division, Water Resources Services, Alberta Environmental Protection. Edmonton, available at: https://agriculture.alberta.ca/acis/docs/mortons/mortons-evaporation-estimates.pdf (last access: 5 May, 2018).

Boulanger Y, Gauthier S, Burton PJ. 2014. A refinement of models projecting future Canadian fire regimes using homogeneous fire regime zones. *Canadian Journal of Forest Research,* **44**: 365–376, DOI: 10.1139/cjfr-2013-0372.

Bridgham SD, Megonigal JP, Keller JK, Bliss NB, Trettin C. 2006. The carbon balance of North American wetlands. *Wetlands*, **264**: 889–916, DOI: 10.1672/0277-5212(2006)26[889:TCBONA]2.0.CO;2.

Brock JH, DeBano LF. 1990. Wettability of an Arizona chaparral soil influenced by prescribed burning. United States Department of Agriculture, Forest Service, General Technical Report, RM-191, 206–209.

Burke JM, Prepas EE, Pinder S. 2005. Runoff and phosphorus export patterns in large forested watersheds on the western Canadian Boreal Plain before and for 4 years after wildfire. *Journal of Environmental Engineering and Science*, **4**(5): 319–325, DOI: 10.1139/s04-072

Burles K. Boon S. 2011. Snowmelt energy balance in a burned forest plot: Crowsnest Pass, Alberta, Canada. *Hydrological Process*es, **25**, 3012–3029, DOI: 10.1002/hyp.8067.

Campbell RE, Baker MB, Folliot PF, Larson RF, Arvey CC. 1977. *Wildfire effects on a ponderosa pine ecosystem: an Arizona case study*. United States Department of Agriculture, Forest Service, Research Paper RM-191, Rocky Mountain Forest and Range Experimental Station, Fort Collins, Colorado, 21 pp.

Cann M, Lewis D. 1994. The use of dispersible sodic clay to overcome water repellence in sandy soils in the South East of South Australia. Proceedings of the 2nd National Water Repellency Workshop, 1–5 August, Perth, Western Australia. pp. 49–57.

CFRC (Chisholm Fire Review Committee). 2001. *Final Report*. Minister of Alberta Sustainable Resource Development, available at: https://open.alberta.ca/publications/2552904 (last access: 28 Aug. 2018).

Chanasyk DS, Whitson IR, Mapfumo E, Burke JM, Prepas EE. 2003. The impacts of forest harvest on wildfire on soils and hydrology in temperate forests: A baseline to develop hypotheses for the Boreal Plain. *Journal of Environmental Engineering Science*, **2**: S51–S62, DOI: 10.1139/s03-034.

Chee WL, Vitt DH. 1989. The vegetation, surface water chemistry and peat chemistry of moderate-rich fens in central Alberta, Canada. *Wetlands*, **9**(2): 227-261, DOI: 10.1007/BF03160747.

Clymo RS. 1978. *A model of peat bog growth*. In (eds). Production Ecology of British Moors and Montane Grasslands, Ecological Studies Series, Heal OW, Perkins DF, 27, Springer-Verlag: Berlin, Germany; 187–223.

Clymo, R.S., 1984. The Limits to Peat Bog Growth. *Sciences*, **303**(1117): 605–654, DOI: 10.1098/rstb.1984.0002.

Collins M, Knutti R, Arblaster J, Dufresne JL, Fichefet T, Friedlingstein P, Gao X, Gutowski WJ, Johns T, Krinner G, Shongwe M, Tebaldi C, Weaver AJ, Wehner M. 2013. *Long-term climate change: projections, commitments and irreversibility.* In: Climate Change 2013: The Physical Science Basis. Contribution of Working Group I to the Fifth Assessment Report of the Intergovernmental Panel on Climate Change, Stocker TF, Qin D, Plattner G-K, Tignor M, Allen SK, Boschung J, Nauels A, Xia Y, Bex V, Midgley PM (eds.). Cambridge University Press, Cambridge, United Kingdom and New York, NY, USA.

Connolly CA, Walter LM, Baadsgaard H, Longstaffe FJ. 1990. Origin and evolution of formation waters, Alberta Basin, Western Canada Sedimentary Basin. II. Isotope systematics and water mixing. *Applied Geochemistry*, **5**: 397–413, DOI: 10.1016/0883-2927(90)90017-Y.

Daly C, Price JS, Rezanezhad F, Pouliot R, Rochefort L, Graf M. 2012. *Initiatives in oil sand reclamation: Considerations for building a fen peatland in a post-mined oil sands landscape.* In: Restoration and Reclamation of Boreal Ecosystems - Attaining Sustainable Development. Vitt D, Bhatti JS (eds.) Cambridge University Press, pp: 179-201.

Dasgupta S, Siegel DI, Zhu C, Chanton JP, Glaser PH. 2015. Geochemical Mixing in Peatland Waters: The Role of Organic Acids. *Wetlands*, **35**(3): 567–575, DOI: 10.1007/s13157-015-0646-2.

de Groot WJ, Pritchard JM, Lynham TJ. 2009. Forest floor fuel consumption and carbon emissions in Canadian boreal forest fires. *Canadian Journal of Forest Research*, **39**: 367–382, DOI: 10.1139/X08-192.

DeBano LF, Krammes JS. 1966. Water repellent soils and their relation to wildfire temperatures. *International Bulletin of the Association of Hydrological Scientists*, **2**: 14–19, DOI: 10.1080/02626666609493457.

DeBano LF, Mann LD, Hamilton DA. 1970. Translocation of hydrophobic substances into soil by burning organic litter. *Proceedings of the Soil Science Society of America*, **34**: 130–133, DOI: 10.2136/sssaj1970.03615995003400010035x.

DeBano LF, Savage SM, Hamilton AD. 1976. The transfer of heat and hydrophobic substances during burning. Proceedings of the *Soil Science Society of America*, **40**: 779–782, DOI: 10.2136/sssaj1976.03615995004000050043x

DeBano LF, Rice RM, Conrad CE. 1979. *Soil heating in chaparral fires: effects on soil properties, plant nutrients, erosion and runoff*. United States Department of Agriculture, Forest Service, Research Paper PSW-145, Pacific Southwest Forest and Range Experimental Station, Berkeley, California, 21 pp.

DeBano, LF. 1991. *The effects of fire on soil properties.* United States Department of Agriculture, Forest Service, General Technical Report, INT-280, 151–156.

DeBano LF. 2000. The role of fire and soil heating on water repellency in wildland environments: a review. *Journal of Hydrol*ogy, **231–232**: 195–206, DOI: 10.1016/S0022-1694(00)00194-3.

Dekker LW, Ritsema CJ, Oostindie K, Boersma OH. 1998. Effect of drying temperature on the severity of soil water repellency. *Soil Science*, **163**(10): 780–796, DOI: 10.1097/00010694-199810000-00002

Dekker LW, Ritsema CJ, Oostindie K. 2000. Extent and significance of water repellency in dunes along the Dutch coast. *Journal of Hydrology*, **231–232**: 112–125, DOI: 10.1016/S0022-1694(00)00188-8.

Dekker LW, Ritsema CJ, Oostindie K, Moore D, Wesseling JG. 2009. Methods for determining soil water repellency. *Water Resources Research*, **45**: 6pp., DOI: 10.1029/2008WR007070.

Depante M. 2016. Nutrient and Hydrologic Conditions Post-Fire: Influences on Western Boreal Plain Aspen (*Populus trembloides* michx.) Re-establishment and Succession. M.Sc. thesis, University of Waterloo, Department of Geography and Environmental Management.

Devito K, Creed I, Gan T, Mendoza C, Petrone R, Silins U, Smerdon B. 2005. A framework for broad-scale classification of hydrologic response units on the Boreal Plain: is topography the last thing to consider? *Hydrological Process*es, **19**: 1705–1714, DOI: 10.1002/hyp.5881.

Devito KJ, Waddington JM, Branfireun BA. 1997. Flow reversals in peatlands influenced by local groundwater systems. *Hydrological Process*es, **11**: 103–110, DOI: 10.1002/(SICI)1099-1085(199701)11:1<103::AID-HYP417>3.0.CO;2-E.

Devito K, Mendoza C, Qualizza C. 2012. *Conceptualizing water movement in the Boreal Plains, Implications for watershed reconstruction*. Synthesis report prepared for the Canadian Oil Sands Network for Research and Development, Environmental and Reclamation Research Group, 164 pp., DOI: 10.7939/R32J4H.

Dimitrov DD, Bhatti JS, Grant RF. 2014. The transition zones (ecotone) between boreal forests and peatlands: modelling water table along a transition zone between upland black spruce forest and poor forested fen in central Saskatchewan. *Ecological Modeling*, **274**: 57–70, DOI: 10.1016/J.ecolmodel.2014.07.020.

Doerr SH, Shakesby RA, Walsh RPD. 1996. Soil water repellency variations with depth and particle size fraction in burned and unburned *Eucalyptus globulus* and *Pinus pinaster* forest terrain in the Agueda basin, Portugal. *Catena*, **27**(1): 25–47, DOI: 10.1016/0341-8162(96)00007-0.

Doerr SH. 1998. On standardizing the 'water drop penetration time' and the 'molarity of an ethanol droplet' techniques to classify soil hydrophobicity: a case study using medium textured soils. *Earth Surface Processes and Landforms*, **23**: 663–668, DOI: 10.1002/(SICI)1096-9837(199807)23:7<663::AID-ESP909>3.0.CO;2-6.

Doerr SH, Shakesby RA, Walsh RPD. 2000. Soil water repellency: its causes, characteristics and hydro-geomorphological significance. *Earth–Science Reviews*, 51: 33–65.

Domenico PA. 1972. *Concepts and models in groundwater hydrology*. McGraw-Hill, New York.

Ecoregions Working Group. 1989. *Ecoclimatic Regions of Canada*. Ecological Land Classification Series No. 23.

Elmes MC, Thompson DK, Sherwood JH, Price JS. 2017. *(NHESS) Data.zip*. DOI: 10.6084/m9.figshare.5346484 (last access: 28 Aug. 2018).

Elmes MC, Thompson DK, Sherwood JH, Price JS. 2018. Hydrometeorological conditions preceding wildfire, and the subsequent burning of a fen watershed in Fort McMurray, Alberta, Canada. *Natural Hazards and Earth System Sciences*, **18**: 157–170, 2018, DOI: 10.5194/nhess-18-157-2018.

Elmes MC, Price JS. Hydrologic function of a moderate-rich fen watershed in the Athabasca Oil Sands Region of the Western Boreal Plain, northern Alberta. Submitted to: *Journal of Hydrology*.

Environment Canada. 2017. *Canadian Climate Normals 1981–2010 Station Data*. Government of Canada, Ottawa, Available at http://climate.weather.gc.ca/climate_normals/ (last access: 28 Aug. 2018).

Environment and Climate Change Canada. 2018. *Fort McMurray Historical Total Precipitation*. Government of Canada. Available at https://fortmcmurray.weatherstats.ca/metrics/precipitation.html (last access: 28 Aug. 2018)

Ferlatte M, Quillet A, Larocque M, Cloutier V, Pellerin S, Paniconi C. 2015. Aquifer–peatland connectivity in southern Quebec (Canada). *Hydrological Proces*ses, **29**: 2600–2612, DOI: 10.1002/hyp.10390.

Ferone JM, Devito KJ. 2004. Shallow groundwater-surface water interactions in pond-peatland complexes along a Boreal Plain topographic gradient. *Journal of Hydrol*ogy, **292**, 75–95, DOI: 10.1016/j.jhydrol.2003.12.032.

Flannigan MD, Harrington JB. 1988. A Study of the Relation of Meteorological Variables to Monthly Provincial Area Burned by Wildfire in Canada (1953–80). *Journal of Applied Meteorol*ogy, **27**: 441–452, DOI: 10.1175/1520-0450(1988)027<0441:ASOTRO>2.0.CO;2.

Flannigan M, Cantin AS, de Groot WJ, Wotton M, Newbery A, Gowman LM. 2013. Global wildland fire season severity in the 21st century, *Forest Ecology and Manag*ement, **294**: 54–61, DOI: 10.1016/j.foreco.2012.10.022.

Flannigan MD, Wotton BM, Marshall GA, de Groot WJ, Johnson J, Jurko N, Cantin AS. 2016. Fuel moisture sensitivity to temperature and precipitation: climate change implications, *Climatic Change*, **134**: 59–71, DOI: 10.1007/s10584-015-1521-0.

Fraser CJD, Roulet NT, Moore TR. 2001. Hydrology and dissolved organic carbon biogeochemistry in an ombrotrophic bog. *Hydrological Processes*, **15**: 3151–3166. DOI: 10.1002/hyp.322.

Freeze RA, Cherry JA. 1979. *Groundwater*. Prentice-Hall, Englewood Cliffs, NJ.

Forestry Canada Fire Danger Group. 1992. *Development and structure of the Canadian Forest Fire Behaviour Prediction System*. Forestry Canada, Ottawa, Inf. Rep. ST-X-3, available at: https://cfs.nrcan.gc.ca/publications?id=10068 (last access: 28 Aug. 2018).

FTCWRC (Flat Top Complex Wildfire Review Committee). 2012. *Flat top complex*. Submitted to the Minister of Alberta Environment and Sustainable Resource Development, available at: https://wildfire.alberta.ca/resources/reviews/documents/FlatTopComplex-WildfireReviewCommittee-A-May18-2012.pdf (last access: 28 Aug. 2018).

Glaser PH, Siegel DI, Shen YP, Romanowicz EA. 1997. Regional linkages between raised bogs and the climate, groundwater, and landscape features of northwestern Minnesota. *Journal of Ecol*ogy, **85**: 3–16, DOI: 10.2307/2960623.

Goetz JD, Price JS. 2014. Role of morphological structure and layering of *Sphagnum* and *Tomenthypnum* mosses on moss productivity and evaporation rates. *Canadian Journal of Soil Science*, **95**: 109-124, DOI: 10.4141/cjss-2014-092.

Gorham E. 1953. Some early ideas concerning the nature, origin, and development of peat lands. *Journal of Ecology*, **41**: 257–274, DOI: 10.2307/2257040.

Gorham E. 1991. Northern Peatlands: role in the carbon cycle and probable responses to climatic warming. *Ecological Applications*, **1**: 182–195, DOI: 10.2307/1941811.

Government of Alberta. 2017. *Area Burned (2006–2015)*. Available at: http://wildfire.alberta.ca/resources/historical-data/documents/AreaBurned-Mar08-2017.pdf (last access: 28 Aug. 2018).

Grasby SE, Chen Z. 2005. Subglacial recharge into the Western Canada Sedimentary Basin: impact of Pleistocene glaciation on basin hydrodynamics. *Geological Society of America Bulletin*, **117**(3): 500–514, DOI: 10.1130/B25571.1.

Hayward PM, Clymo RS. 1983. The Growth of Sphagnum: Experiments on, and Simulations of, Some Effects of Light Flux and Water-Table Depth. *Journal of Ecology*, **71**: 845–863, DOI: 10.2307/2259597.

Hirsch KG, de Groot WJ. 1999. Integrating Fire and Forest Management: A report for Millar Western Industries. Canadian Forest Service, Northern Forestry Centre, Edmonton, Alberta, available at: http://www.cfs.nrcan.gc.ca/bookstore_pdfs/20421.pdf (last access: 28 Aug. 2018).

Hitchon B, Friedman I. 1969. Geochemistry and origin of formation waters in the Western Canada Sedimentary Basin - I. Stable isotopes of hydrogen and oxygen. *Geochimica et Cosmochimica Acta*, **33**: 1321–1349, DOI: 10.1016/0016-7037(69)90178-1.

Hoag RS, Price JS. 1995. A field-scale, natural gradient solute transport experiment in peat at a Newfoundland blanket bog. *Journal of Hydrology*, **172**: 171–184, DOI: 10.1016/0022-1694(95)02696-M.

Hokanson KJ, Lukenbach MC, Devito KJ, Kettridge N, Petrone RM, Waddington JM. 2016. Groundwater connectivity controls peat burn severity in the boreal plains. *Ecohydrology*, **9**: 574–584, DOI: 10.1002/eco.1657.

Howie SA, Meerveld IT-v. 2011. The essential role of the lagg in raised bog function and restoration: a review. *Wetlands*, **31**: 613–622, DOI: 10.1007/s13157-011-0168-5.

Hvorslev MJ. 1951. *Time Lag and Soil Permeability in Groundwater Observations*. Vol Waterways Experimental Station Bulletin 36. Vicksburg, Mississippi, US Army Corps of Engineers.

IBC (Insurance Bureau of Canada). 2016. Northern Alberta Wild- fire Costliest Insured Natural Disaster in Canadian History – Estimate of insured losses: $3.58 billion, available at: http://www.ibc.ca/bc/resources/media-centre/media-releases/ (last access: 5 May, 2018).

Ingram HAP. 1983. Hydrology, in: Ecosystems of the World 4A. Mires: Swamp, bog, fen and moor, edited by: Gore AJP, Elsevier, Amsterdam, 67–224.

Imeson AC, Verstraten JM, Van Mullingen EJ, Sevink J. 1992. The effects of fire and water repellency on infiltration and runoff under Mediterranean type forests. *Catena*, **19**: 345–361, DOI: 10.1016/0341-8162(92)90008-Y.

IPCC. 2013. Climate change 2013: the physical science basis. Contribution of Working Group I to the Fifth Assessment Report of the Intergovernmental Panel on Climate Change. Cambridge University Press, Cambridge.

Ireson AM, Barr AG, Johnstone JF, Mamet SD, van der Kamp G, DeBeer C, Chun KP, Nazemi A, Sagin J. 2015. The changing water cycle: the Boreal Plains ecozone of the Western Canada. *WIREs Water*, **2**: 17pp., DOI: 10.1002/wat2.1098.

Ise T, Dunn AL, Wofsy SC, Moorcroft PR. 2008. High sensitivity of peat decomposition to climate change through water-table feedback. *Nature Geoscience*, **1**: 763–766, DOI: 10.1038/ngeo331

Kane ES, Kasischke ES, Valentine DW, Turetsky MR, McGuire AD. 2007. Topographic influences on wildfire consumption of soil organic carbon in interior Alaska: Implications for black carbon accumulation. *Journal of Geophysical Research*, 112, 11 pp., DOI: 10.1029/2007JG000458.

Keith DM, Johnson EA, Valeo, C. 2010. Moisture cycles of the forest floor organic layer (F and H layers) during drying, *Water Resources Res*earch, **46**: 14 pp., DOI: 10.1029/2009WR007984.

Kendall C, Caldwell EA. 2006. Fundamentals of Isotope Geochemistry. In: Kendall C, McDonnell JJ. (Eds.), Isotope Tracers in Catchment Hydrology. Elsevier, Amsterdam, The Netherlands, pp. 51–86.

Ketcheson SJ, Price JS, Carey SK, Petrone RM, Mendoza CA, Devito KJ. 2016. Constructing fen peatlands in post-mining oil sands landscapes: Challenges and opportunities from a hydrological perspective. *Earth-Science Reviews*, **161**: 130–139, DOI: 10.1016/j.earscirev.2016.08.007.

Ketcheson SJ, Price JS, Sutton O, Sutherland G, Kessel E, Petrone RM. 2017. The hydrological functioning of a constructed fen wetland watershed. *Science of the Total Environment*, **603-604**: 593–605, DOI: 10.1016/j.scitotenv.2017.06.101.

Kettridge N, Humphrey RE, Smith JE, Lukenbach MC, Devito KJ, Petrone RM, Waddington JM. 2014. Burned and unburned peat water repellency: Implications for peatland evaporation following wildfire. *Journal of Hydrology*, **513**: 335–341, DOI: 10.1016/j.jhydrol.2014.03.019.

Kirchmeier-Young MC, Zwiers FW, Gillet NP, Cannon AJ. 2017. Attributing extreme fire risk in Western Canada to human emissions, *Climatic Change*, **144**: 365–379, DOI: 10.1007/s10584-017-2030-0.

Kløve, B., Ala-aho, P., Okkonen, J., Rossi, P. 2012. Possible Effects of Climate Change on Hydrogeological Systems: Results From Research on Esker Aquifers in Northern Finland, pp. 305–322. In: Treidel, H., Martin-Bordes, J.J., Gurdak, J.J., (Eds.), Climate Change Effects on Groundwater Resources: A Global Synthesis of Findings and Recommendations. International Association of Hydrogeologists (IAH) – International Contributions to Hydrogeology. Taylor & Francis Publishing, 414pp.

Krammes JS, Osborn J. 1969. Water-repellent soils and wetting agents as factors influencing erosion. Proceedings of the Symposium on Water-Repellent Soils, University of California, May 1968, pp. 177–187.

Kuhry P, Nicholson BJ, Gignac LD, Vitt DH, Bayley SE. 1993. Development of *Sphagnum*-dominated peatlands in boreal continental Canada. *Canadian Journal of Botany*, **71:** 10–22, DOI: 10.1139/b93-002.

Langlois MN, Price JS, Rochefort L. 2015. Landscape analysis of nutrient-enriched margins (lagg) in ombrotrophic peatlands, *Science of the Total Environment*, **505**: 573-586, DOI: 10.1016/j.scitotenv.2014.10.007.

Lawson BD, Armitage OB. 2008. Weather Guide for the Canadian Forest Fire Danger Rating System, Natural Resources Canada, Canadian Forest Service, Northern Forestry Centre, Edmonton, Alberta, 84 pp., available at: http://cfs.nrcan.gc.ca/pubwarehouse/pdfs/29152.pdf (last access: 5 May, 2018).

Lemay TG. 2002. Geochemical and isotope data for formation water from selected wells, Cretaceous to Quaternary succession, Athabasca Oil Sands (in situ) area, Alberta. EUB/AGS Geo-note 2002-02, Energy and Utilities Board, Edmonton, AB, 71 pp.

Letey J. 2001. Causes and consequences of fire-induced soil water repellency. *Hydrological Processes*, **15**: 2867–2875, DOI: 10.1002/hyp.378.

Locky DA, Bayley SE. 2010. Plant diversity in wooded moderate-rich fens across boreal

Western Canada: An ecoregional perspective. *Biodiversity and Conservation*, **19**: 3525–3543, DOI: 10.1007/s10531-010-9914-x.

Lukenbach MC, Hokanson KJ, Moore PA, Devito KJ, Kettridge N, Thompson DK, Wotton BM, Petrone RM, Waddington JM. 2015. Hydrological controls on deep burning in a northern forested peatland, *Hydrological Processes*, **29**: 4114–4124, DOI: 10.1002/hyp.10440.

Lukenbach MC, Hokanson KJ, Devito KJ, Kettridge N, Petrone RM, Mendoza CA, Granath G, Waddington JM. 2017. Post-fire ecohydrological conditions at peatland margins in different hydrogeological settings of the boreal plain. *Journal of Hydrology*, **548**: 741–753, DOI: 10.1016/j.jhydrol.2017.03.034.

Marshall IB, Schut P, Ballard M. 1999. A National Ecological Framework for Canada: Attribute Data. Environmental Quality Branch, Ecosystems Science Directorate, Environment Canada and Research Branch, Agriculture and Agri-Food Canada, Ottawa/Hull, available at http://sis.agr.gc.ca/cansis/nsdb/ecostrat/1999report/index.html (last access: 5 May, 2018).

McPherson RA, Kathol CP. 1977. Surficial geology of potential mining areas in the Athabasca Oil Sands region; unpublished report prepared for Alberta Research Council by Quaternary Geosciences Ltd., 177 p.

MNP. 2017. A Review of the 2016 Horse River Wildfire, Prepared for Forestry Division, Alberta Agriculture and Forestry, available at: https://www.alberta.ca/assets/documents/Wildfire-MNP-Report. pdf (last access: 5 May, 2018).

Natural Regions Committee. 2006. Natural regions and subregions of Alberta. Pub. no. T/582, Government of Alberta, Edmonton, AB, 264 pp.

Natural Resources Canada. 2018. Canadian Wildland Fire Information System, available at: http://cwfis.cfs.nrcan.gc.ca/datamart (last access: 5 May, 2018).

NWWG. 1997. The Canadian Wetland Classification System Warner BG, Rubec CDA (eds). National Wetland Working Group, University of Waterloo, Wetlands Research Centre; 68pp.

Oil Sands Wetlands Working Group (OSWWG). 2000. Guidelines for wetland establishment on reclaimed oil sands leases, N. Chymko, ed., Rep. ESD/LM/00-1, Alberta Environment, Environmental Services Publication No. T/517.

Petrone RM, Kaufman S, Devito KJ, Macrae ML, Waddington JM. 2005. Effect of drought on greenhouse gas emissions from pond/peatland systems with contrasting hydrologic regimes, Northern Alberta, Canada. In: Dynamics and Biogeochemistry of River Corridors and Wetlands (Proceedings of symposium S4 held during the Seventh IAHS Scientific Assembly at Foz do Iguaçu, Brazil, April 2005), IAHS Publ. 294.

Petrone RM, Silins U, Devito KJ. 2007. Dynamics of evapotranspiration from a riparian pond complex in the Western Boreal Forest, Alberta, Canada. *Hydrological Processes*, **21**: 1391-1401.

Pinno BD, Errington RC, Thompson D K. 2013. Young jack pine and high severity fire combine to create potentially expansive areas of understocked forest, *Forest Ecology and Management*, **310**: 517–522, DOI: 10.1016/j.foreco.2013.08.055.

Podur J, Wotton BM. 2010. Will climate change overwhelm fire management capacity? *Ecological Modelling*, **221**: 1301–1309, DOI: 10.1016/j.ecolmodel.2010.01.13.

Pomeroy JW, Gray DM, Shook KR, Tóth B, Essery RLH, Pietroniro A, Hedstrom N. 1998. An evaluation of snow processes for land surface modelling. *Hydrological Processes*, **12**: 2339–2367, DOI: 10.1002/(SICI)1099-1085(199812)12:15<2339::AID-HYP800>3.0.CO;2-L.

Price JS. 1983. The effect of hydrology on ground freezing in a watershed with organic terrain, in: Proc. Fourth Int. Conf. on Permafrost, Fairbanks, Alaska, National Academy Press, Washington, DC, 1009–1014.

Price JS, FitzGibbon JE. 1987. Groundwater storage-streamflow relations during winter in a subarctic wetland, Saskatchewan. *Canadian Journal of Earth Sciences*, **24**: 2047–2081, DOI: 10.1139/e87-196.

Price JS, Maloney DA. 1994. Hydrology of a patterned bog-fen complex in southeastern Labrador, Canada. *Nordic Hydrology*, **25**: 313-330.

Price JS, McLaren RG, Rudolph DL. 2010. Landscape restoration after oil sands mining: conceptual design and hydrological modelling for fen reconstruction. *International Journal of Mining Reclamation and Environment*, **24**: 109–123.

Quinton WL, Hayashi M, Chasmer LE. 2009. Peatland hydrology of discontinuous permafrost in the northwest territories: overview and synthesis. *Canadian Water Resources Journal*, **34**: 311–328, DOI: 10.4296/cwrj3404311.

Redding T, Devito K. 2011. Aspect and soil textural controls on snowmelt runoff on forested Boreal Plain Hillslopes, *Hydrology Research*, **42**: 250–267, DOI: 10.2166/nh.2011.162.

Reeve A, Siegel DI, Glaser PH. 2000. Simulating vertical flow in large peatlands. *Journal of Hydrology*, **227**(1-4): 207–217, DOI: 10.1016/S0022-1694(99)00183-3.

Richardson JL, Hole FD. 1978. Influence of vegetation on water-repellency in selected western Wisconsin soils. *Journal of the Soil Science Society of America*, **42**: 465–467, DOI: 10.2136/sssaj1978.03615995004200030018x.

Riddell J. 2008. Assessment of surface water-groundwater interaction at perched boreal wetlands, north-central Alberta. M.Sc. Thesis, Earth and Atmospheric Sciences, University of Alberta.

Ritsema CJ, Dekker LW, Hendrickx JMH, Hamminga W. 1993. Preferential flow mechanism in a water repellent sandy soil. *Water Resources Research*, **29**: 2183–2193, DOI: 10.1029/93WR00394.

Roberts FJ, Carbon BA. 1971, Water repellence in sandy soils of south-western Australia. I. Some studies related to field occurrence: Field Station Record, CSIRO Division of Plant Industries (Australia), v.10, p. 13-20.

Rooney RC, Bayley SE, Schindler DW. 2012. Oil sands mining and reclamation cause massive loss of peatland and stored carbon. *Proceedings of the National Academy of Sciences*, **109**: 4933–4937, DOI: 10.1073/pnas.1117693108.

Roulet NT, Woo, MK. 1986. Hydrology of a wetland in the continuous permafrost region. *Journal of Hydrology*, **89**: 73–91, DOI: 10.1016/0022-1694(86)90144-7.

Roulet NT, Moore TIM, Bubier J, Lafleur P. 1992. Northern fens: methane flux and climatic change. *Tellus B*, **44**: 100–105, DOI: 10.1034/j.1600-0889.1992.t01-1-00002.x.

Roulet NT, Lafleur PM, Richard PJH, Moore TR, Humphreys ER, Bubier JL. 2007. Contemporary carbon balance and late Holocene carbon accumulation in a northern peatland, *Global Change Biology*, **13**: 397–411, DOI: 10.1111/j.1365-2486.2006.01292.x

Sass AP, Amiro BD, Orchansky AL. 2006. Surface energy balances of Canadian boreal forests following fire. Pages P.1.2-P.1.5 in Proceedings: 27th Conference on Agricultural and Forest Meteorology. May 22-25, 2006, San Diego, California, USA. American Meteorological Society, Boston, Massachusetts, USA.

Savage SM. 1974. Mechanism of fire-induced water repellency in soils. *Proceedings of the Soil Science Society of America*, **38**: 652–657, DOI: 10.2136/sssaj1974.03615995003800040033x.

Scarlett SJ, Price JS. 2013. The hydrological and geochemical isolation of a freshwater bog within a saline fen in north-eastern Alberta. *Mires and Peat*, **12**(4): 12pp.

Siegel DI. 1983. Ground water and evolution of patterned mires, Glacial Lake Agassiz Peatlands, Northern Minnesota. *Journal of Ecology*, **71**: 913–921, DOI: 10.2307/2259601.

Siegel DI, Glaser PH. 1987. Groundwater flow in a bog–fen complex, Lost River peatland, Northern Minnesota. *Journal of Ecology*, **75**: 743–754, DOI: 10.2307/2260203.

Sjörs H. 1950. On the relation between vegetation and electrolytes in north Sweden mire waters. *Oikos*, **2**: 241–257, DOI: 10.2307/3564795.

Smerdon BD, Kevito KJ, Mendoza CA. 2005. Interaction of groundwater and shallow lakes on outwash sediments in the sub-humid Boreal Plains of Canada. *Journal of Hydrology*, **314**(1): 246–262, DOI: 10.1016/j.jhydrol.2005.04.001.

Smerdon BD, Mendoza CA, Devito KJ. 2008. Influence of subhumid climate and water table depth on groundwater recharge in shallow outwash aquifers, *Water Resources Research*, **44**: 15pp., DOI: 10.1029/2007WR005950.

Soil Classification Working Group. 1998. The Canadian System of Soil Classification (Third Edition). Ottawa, ON, Agriculture and Agri-Food Canada.

Soil Science Division Staff. 2017. Soil survey manual. C. Ditzler, K. Scheffe, and H.C. Monger (eds.). USDA Handbook 18. Government Printing Office, Washington, D.C.

Soilmoisture Equipment Corp. 2015. 1500F2 15 Bar Pressure Plate Extractor Operating Instructions. Available at: https://www.soilmoisture.com/pdfs/Resource_Instructions_0898-1500F2_15%20Bar%20Pressure%20Plate%20Extractor.pdf (last access: 5 May, 2018).

Stralberg D, Wang X, Parisien M-A, Robinne F-N, Sólymos P, Mahon CL, Nielsen SE, Bayne EM. 2018. Wildfire-mediated vegetation change in boreal forests of Alberta, Canada, *Ecosphere*, 9(3) 23pp., DOI: 10.1002/ecs2.2156.

Tarnocai C. 2006. The effect of climate change on carbon in Canadian peatlands. *Global and Planetary Change*, **53**: 222–232. DOI: 10.1016/j.gloplacha.2006.03.012.

Thormann MN, Bayley SE. 1997. Decomposition along A moderate-rich fen-marsh peatland gradient in boreal Alberta, Canada. *Wetlands*, **17**(1): 123–137, DOI: 10.1007/BF03160724.

Tóth J. 1999. Groundwater as a geologic agent: An overview of the causes, processes, and manifestations. *Hydrogeology Journal*, **7**: 14 pp., DOI: 10.1007/s100400050176.

Turetsky MR, Amiro BD, Bosch E, Bhatti JS. 2004. Historical burn area in western Canadian

peatlands and its relationship to fire weather indices, *Global Biogeochemical Cycles*, **18**: 9 pp., DOI: 10.1029/2004GB002222.

Turetsky MR, Wieder RK, Halsey L, Vitt DH. 2002. Current disturbance and the diminishing peatland carbon sink, *Geophysical Research Letters*, **29**: 4 pp., DOI: 10.1029/2001GL014000.

Turetsky MR, Kane ES, Harden JW, Ottmar RD, Manies KL, Hoy E, Kasischke ES. 2011. Recent acceleration of biomass burning and carbon losses in Alaskan forests and peatlands, *Nature Geoscience*, **4**: 27–31, DOI: 10.1038/ngeo1027.

Turner JA. 1972. The drought code component of the Canadian forest fire behavior system, Environment Canada, Canadian Forestry Service, Ottawa, Ont. Publication No. 1316, available at: https: //cfs.nrcan.gc.ca/publications?id=28538 (last access 5 May 2018).

Tymstra C, Wang D, Rogeau M-P. 2005. Alberta wildfire regime analysis: Wildfire Science and Technology Report PFFC-01-5, Alberta Sustainable Resource Development, Forest Protection Division, Edmonton, AB, 178 pp.

Tymstra C, Flannigan MD, Armitage OB, Logan K. 2007. Impact of climate change on area burned in Alberta's boreal forest. *International Journal of Wildland Fire*, **16**: 153–160, DOI: 10.1071/WF06084.

Van Genuchten MT. 1980. A closed-form equation for predicting the hydraulic conductivity of unsaturated soils. *Soil Science Society of America Journal*, **44**: 892–898, DOI: 10.2136/sssaj1980.03615995004400050002x.

Van Genuchten MT, Leij FJ, Yates SR. 1991. *The RETC Code for Quantifying the Hydraulic Functions of Unsaturated Soils*. EPA Report 600/2-91/065, US Salinity Laboratory, USDA, ARS: Riverside, CA, USA.

Van Wagner CE. 1977. Conditions for the start and spread of crown fire, *Can. J. Forest Res.*, **7**: 23–34, DOI: 10.1139/x77-004.

Van Wagner CE. 1987. Development and structure of the Canadian Forest Fire Weather Index System, Canadian Forestry Service, Ottawa, Ont., 46 pp., available at: https://cfs.nrcan.gc.ca/publications?id=19927 (last access: 5 May, 2018), 1987.

Vitt, D. H, Bayley, S. E., and Jin, T-L. 1995. Seasonal variation in water chemistry over a bog-rich fen gradient in Continental Western Canada. *Canadian Journal of Fisheries and Aquatic Sciences*, **52**: 587–606, DOI: 10.1139/f95-059.

Vitt DH, Chee W-L. 1990. The relationships of vegetation to surface water chemistry and peat chemistry in fens of Alberta, Canada. *Vegetatio*, **89**(2): 87–106, DOI: 10.1007/BF00032163

Vitt D, Halsey L, Thormann M, Martin T. 1996. Peatland Inventory of Alberta. Phase 1: Overview of Peatland Resources in the Natural Regions and Subregions of the Province. University of Alberta, Edmonton.

Waddington JM, Roulet NT. 1996. Atmosphere–wetland carbon exchanges: scale dependency of CO2 and CH4 exchange on the developmental topography of a peatland. *Global Biogeochemical Cycles*, **10**: 233–245, DOI: 10.1029/95GB03871.

Waddington JM, Morris PJ, Kettridge N, Granath G, Thompson DK, Moore PA. 2014. Hydrological feedbacks in northern peatlands, *Ecohydrology*, **8**(1), 113–127, DOI: 10.1002/eco.1493

Waddington JM, Thompson DK, Wotton M, Quinton WL, Flannigan MD, Benscoter BW, Baisley SA, Turetsky MR. 2012. Examining the utility of the Canadian Forest Fire Weather Index System in boreal peatlands. *Canadian Journal of Forest Research*, **42**: 47–58, DOI: 10.1139/X11-162.

Weber MG, Flannigan MD. 1997. Canadian Boreal Forest Ecosystem structure and function in a changing climate: impact on fire regimes. *Environmental Reviews*, **5**: 145–166, DOI: 10.1139/er-5-3-4-145.

Wells CM, Price JS. 2015a. A hydrologic assessment of a saline spring fen in the Athabasca oil sands region, Alberta, Canada – a potential analogue for oil sands reclamation, *Hydrological Processes*, **29**: 4533–4548, DOI: 10.1002/hyp.10518.

Wells CM, Price JS. 2015b. The hydrogeologic connectivity of a low-flow saline-spring fen peatland within the Athabasca oil sands region, Canada, *Hydrogeology Journal*, **23**: 1799–1816, DOI: 10.1007/s10040-015-1301-y.

Wells CM, Ketcheson S, Price J. 2017. Hydrology of a wetland-dominated headwater basin in the Boreal Plain, Alberta, Canada, *Journal of Hydrology*, **547**: 168–183, DOI: 10.1016/j.jhydrol.2017.01.052.

Westerling AL, Hidalgo HG, Cayan DR, Swetnam TW. 2006. Warming and earlier spring increase western US forest wildfire activity. *Science*, **313**: 940–943, DOI: 10.1126/science.1128834.

Whittington PN, Price JS. 2006. The effects of water table draw-down (as a surrogate for climate change) on the hydrology of a fen peatland, Canada. *Hydrological Processes*, **20**: 3589–3600, DOI: 10.1002/hyp.6376.

Winter TC. 1999. Relation of streams, lakes, and wetlands to groundwater flow systems. *Hydrogeology Journal*, **7**: 28–45, DOI: 10.1007/s100400050178.

Winter TC, Rosenberry DO, Buso DC, Merk DA. 2001. Water source to four U.S. wetlands: implications for wetland management. *Wetlands*, **21**(4): 462–473, DOI: 10.1672/0277-5212(2001)021[0462:WSTFUS]2.0.CO;2.

Winter TC, Rosenberry DO, LaBaugh JW. 2003. Where does the ground water in small watersheds come from? *Groundwater* **41**(7): 989–1000.

Wotton BM, Flannigan MD. 1993. Length of the fire sea- son in a changing climate. *Forestry Chronicle*, **69**: 187–192, DOI: 10.5558/tfc69187-2.

Wotton BM, Stocks BJ, Martell DL. 2005. An index for tracking sheltered forest floor moisture within the Canadian Forest Fire Weather Index System. *International Journal of Wildland Fire*, **14**: 169–182, DOI: 10.1071/WF04038.

Zha T, Barr AG, van der Kamp G, Black TA, McCaughey JH, Flanagan LB. 2010. Interannual variation of evapotranspiration from forest and grassland ecosystems in western Canada in relation to drought. Agricultural and Forest Meteorology, **150**:1476–1484, DOI: 10.1016/j.agrformet.2010.08.003

A.1 Appendix 1: Average community composition, reported as absolute cover (%), for vegetation plots measured along WT2 (left) and ET4 (right) (refer to Fig. 1 and 2).

WT2

Name	Upland	Upper Margin	Lower Margin	Fen transition	True fen
Hylacomium Splendins	**32.65**	**4.88**	**1.06**	**0.00**	**0.00**
Pleurozium schreberi	**46.55**	**25.10**	**41.86**	**0.00**	**0.00**
Dicranum polysetum	**4.50**	**0.00**	**0.00**	**0.00**	**0.00**
Ptilium crista-castrensis	**0.55**	**0.00**	**0.00**	**0.00**	**0.00**
leaf lichen	**0.23**	**1.17**	**1.00**	**0.00**	**0.00**
Rosa acicularis	**4.37**	**0.00**	**0.00**	**0.00**	**0.00**
Vaccinium myrtilloides	**1.09**	**0.37**	**0.00**	**0.00**	**0.00**
Cornus canadensis	**0.45**	**0.00**	**0.00**	**0.00**	**0.00**
Equisetum arvense	**0.00**	**0.77**	**6.23**	**0.00**	**0.00**
Carex aquatilis	**0.00**	**0.98**	**8.58**	**4.13**	**17.95**
Equisetum sylvaticum	**0.00**	**1.71**	**5.26**	**0.00**	**0.00**
Ledum Groenlandicum	**4.52**	**28.31**	**7.21**	**4.03**	**0.00**
Picea mariana	**5.08**	**20.26**	**1.75**	**0.00**	**0.00**
Sphagnum fuscum	**0.00**	**3.84**	**15.97**	**0.34**	**0.00**
Polytrichum strictum	**0.00**	**0.14**	**0.00**	**0.00**	**0.00**
Aulacomnium palustre	**0.00**	**0.14**	**0.96**	**1.85**	**4.42**
Vaccinium vitis-idaea	**0.00**	**8.73**	**6.19**	**0.00**	**0.00**
Smilacina trifolia	**0.00**	**0.98**	**0.35**	**3.43**	**2.29**
Oxycoccus microcarpus	**0.00**	**0.57**	**1.33**	**3.98**	**0.00**
Drosera rotundifolia	**0.00**	**0.07**	**0.16**	**0.08**	**0.00**
Larix laricina	**0.00**	**1.96**	**0.65**	**5.52**	**3.81**
Sphagnum warnstorfii	**0.00**	**0.00**	**0.35**	**14.05**	**0.78**
Equisetum fluvial	**0.00**	**0.00**	**0.16**	**0.45**	**0.17**
Carex leptalea	**0.00**	**0.00**	**0.62**	**0.00**	**0.00**
Salix planifolia	**0.00**	**0.00**	**0.31**	**0.58**	**0.00**
Tomenthypnum nitens	**0.00**	**0.00**	**0.00**	**37.67**	**17.34**
Drepanocladus aduncus	**0.00**	**0.00**	**0.00**	**0.51**	**13.88**
Helodium blandowii	**0.00**	**0.00**	**0.00**	**0.34**	**0.19**
Potentilla palustre	**0.00**	**0.00**	**0.00**	**1.46**	**0.00**
Stellaria longifolia	**0.00**	**0.00**	**0.00**	**0.60**	**0.19**
Carex gynocrates	**0.00**	**0.00**	**0.00**	**3.49**	**0.00**
Carex disperma	**0.00**	**0.00**	**0.00**	**0.36**	**0.00**
Carex tenuiflora	**0.00**	**0.00**	**0.00**	**1.81**	**0.00**
Carex pauciflora	**0.00**	**0.00**	**0.00**	**0.95**	**0.00**
Betula pumila	**0.00**	**0.00**	**0.00**	**5.91**	**20.87**
Salix pedicellaris	**0.00**	**0.00**	**0.00**	**8.47**	**1.81**
Campyllium stellatum	**0.00**	**0.00**	**0.00**	**0.00**	**6.03**
Bryum pseudotriquetrum	**0.00**	**0.00**	**0.00**	**0.00**	**1.79**
Calliergon giganteum	**0.00**	**0.00**	**0.00**	**0.00**	**2.51**
Mnium stellare	**0.00**	**0.00**	**0.00**	**0.00**	**0.56**
Caltha palustris	**0.00**	**0.00**	**0.00**	**0.00**	**0.83**
Galium triflorum	**0.00**	**0.00**	**0.00**	**0.00**	**0.48**
Carex diandra	**0.00**	**0.00**	**0.00**	**0.00**	**4.11**

ET4

Name	Upland	Margin	Fen transition	True fen
Hylacomium Splendins	**6.42**	**19.96**	**0.00**	**0.87**
Pleurozium schreberi	**54.99**	**26.03**	**0.00**	**0.43**
Dicranum polysetum	**0.58**	**0.66**	**0.00**	**0.00**
Viola canadensis	**2.00**	**0.00**	**0.00**	**0.00**
Viola renifolia	**0.60**	**0.00**	**0.00**	**0.00**
Archillea millefolium	**0.40**	**0.00**	**0.00**	**0.00**
Rosa acicularis	**4.77**	**0.00**	**0.00**	**0.00**
Vaccinium myrtilloides	**1.80**	**0.00**	**0.00**	**0.00**
Vaccinium vitis-idaea	**11.71**	**11.93**	**0.00**	**0.00**
Galium Boreale	**0.60**	**0.00**	**0.00**	**0.00**
Potentilla fruticosa	**0.60**	**0.00**	**0.00**	**0.00**
Equisetum Scirpoides	**1.17**	**0.33**	**0.00**	**0.00**
Equisetum arvense	**0.38**	**2.94**	**0.00**	**0.00**
Ledum Groenlandicum	**11.59**	**16.30**	**0.00**	**0.00**
Picea mariana	**0.40**	**2.75**	**12.39**	**1.01**
Populus balsamifera	**2.00**	**0.00**	**0.00**	**0.00**
Sphagnum fuscum	**0.00**	**0.33**	**0.00**	**0.00**
Polytrichum strictum	**0.00**	**0.16**	**1.77**	**0.00**
Aulacomnium palustre	**0.00**	**1.01**	**1.57**	**5.25**
Tomenthypnum nitens	**0.00**	**0.50**	**27.35**	**13.60**
Smilacina trifolia	**0.00**	**3.93**	**16.07**	**9.09**
Oxycoccus microcarpus	**0.00**	**0.34**	**1.26**	**0.00**
Carex aquatilis	**0.00**	**1.30**	**2.03**	**0.27**
Larix laricina	**0.00**	**9.66**	**19.12**	**32.46**
Salix planifolia	**0.00**	**0.33**	**0.00**	**0.00**
Salix pedicellaris	**0.00**	**1.56**	**0.93**	**0.00**
Sphagnum warnstorfii	**0.00**	**0.00**	**0.72**	**4.02**
Drepanocladus aduncus	**0.00**	**0.00**	**0.12**	**0.00**
Helodium blandowii	**0.00**	**0.00**	**0.92**	**4.27**
Campyllium stellatum	**0.00**	**0.00**	**1.47**	**0.00**
Bryum pseudotriquetrum	**0.00**	**0.00**	**0.24**	**0.00**
Calliergon giganteum	**0.00**	**0.00**	**0.37**	**0.00**
Dicranum undulatum	**0.00**	**0.00**	**0.36**	**0.58**
Mnium stellare	**0.00**	**0.00**	**1.83**	**3.68**
leaf lichen	**0.00**	**0.00**	**0.24**	**0.00**
Drosera rotundifolia	**0.00**	**0.00**	**0.12**	**0.00**
Potentilla palustre	**0.00**	**0.00**	**0.37**	**0.00**
Pyrola asarifolia	**0.00**	**0.00**	**0.36**	**1.52**
Equisetum fluvial	**0.00**	**0.00**	**0.46**	**1.13**
Carex leptalea	**0.00**	**0.00**	**0.16**	**0.00**
Carex gynocrates	**0.00**	**0.00**	**2.89**	**1.40**
Carex disperma	**0.00**	**0.00**	**0.16**	**0.41**
Carex diandra	**0.00**	**0.00**	**2.89**	**4.20**
Carex pairaei	**0.00**	**0.00**	**0.36**	**0.00**
Salix candida	**0.00**	**0.00**	**1.77**	**0.14**
Betula pumila	**0.00**	**0.00**	**1.70**	**2.76**
Sphagnum squarrosum	**0.00**	**0.00**	**0.00**	**0.71**
Sphagnum angustifolium	**0.00**	**0.00**	**0.00**	**9.18**
Stellaria longifolia	**0.00**	**0.00**	**0.00**	**0.42**
Caltha palustris	**0.00**	**0.00**	**0.00**	**1.50**
Carex paupercula	**0.00**	**0.00**	**0.00**	**1.09**

A.2 Appendix 2: Interception loss for burned and unburned brunisol upland locations measured in the summer of 2016.

Date	2016-07-05	2016-07-07	2016-07-14	2016-07-23	2017-08-01
Measured Precipitation (mm)	4.99	6.24	1.78	10.31	42.65
Interception Loss (%)					
Unburned 1	42	31	90	56	46
Unburned 2	41	23	87	40	40
Burned 1	41	39	36	40	25
Burned 2	39	33	35	36	30
Burned 3	41	20	12	27	27